Modeling power failures in deep-level mines to assist with emergency dewatering planning

D Tamine

orcid.org/0000-0003-4012-3577

Dissertation accepted in fulfilment of the requirements for the degree *Master of Engineering in Mechanical Engineering* at the North-West University

Supervisor:	Dr JH Marais
Mentor:	Mr I Mathews
Graduation:	June 2023
Student number:	28492307

ACKNOWLEDGEMENTS

I would like to give my sincere and warmest thanks to ETA Operations (Pty) Ltd. and Enermanage (Pty) Ltd. for granting me the opportunity to embark on this research project and providing the resources and guidance to complete it. Without them, this study would not have been possible.

Thank you to my supervisor, Dr Johan Marais, and mentor, Ian Mathews, for your continued guidance, criticism, and input throughout the study. Your efforts are greatly appreciated.

To my fiancé, Martinique Weideman, thank you for believing in me and always keeping me motivated. Your love and support were major contributing factors to the progress made.

Thank you to my parents, Michelle, and Colin Tamine, as well as my sister, Colby Tamine, for your continuous support throughout my academic career thus far. I would not be where I am today without your sacrifices and constant willingness to put my needs above your own.

Finally, I would like to give thanks to my Lord and Saviour. I have experienced your guidance and grace day by day for which I am eternally grateful.

ABSTRACT

Title: Modeling power failures in deep-level mines to assist with emergency dewatering planning

Author: D Tamine

Supervisor: Dr JH Marais

Mentor: Mr I Mathews

Degree: Mater of Engineering in Mechanical Engineering

Keywords: Deep-level mining, integrated, dynamic, simulation, emergency planning, flooding, dewatering

A mining complex's intricate dewatering system removes water that enters the shaft through various means. This system comprises a series of water pumps that require a constant power supply to avoid flooding key areas of the mine. Due to the instability of Eskom's infrastructure and power supply, mines need to plan for unforeseen power failures.

The problem addressed in the study is that mines are unsure of how the dewatering system will respond to a total power failure. It is further not feasible to conduct a real-life test on the system's response as human lives and expensive equipment will be put at risk.

To address the problem, a three-dimensional thermohydraulic simulation tool, namely Process Toolbox, was used to model an integrated dewatering system with dynamic boundaries. The simulation was developed to challenge the existing industry method that excludes dynamic boundaries and only assesses components individually; therefore, it does not integrate a holistic system.

A verified, integrated, and dynamic dewatering system was developed in Process Toolbox to replicate Mine A's operating conditions. The dewatering simulation model was built and calibrated using data obtained during physical investigations (pump tests and ultrasonic flow meter readings) and digital investigations (data) to ensure the simulation components could replicate real-world operating conditions to within a mean absolute error of 5%.

Mine A determined that a 48-hour period would be sufficient for restoring power or implementing alternative plans to avoid flooding. Therefore, a 48-hour requirement with no pumping after a power failure had to be achieved. Critically, the results of the integrated dynamic simulation tool indicated that the lowest pumping level would flood after 22 hours. This opposed the existing method's result of 67 hours, which was a cause for concern given that the industry method's error is 67% when compared with the simulation method.

The results further illustrated the importance of accurate simulation methodologies. The mine would have lost equipment and put lives in danger if the 67-hour calculation time was supported and an incident occurred.

The modelling environment provided a platform for testing contingency planning hypotheses through scenario simulations. Four scenarios were developed through 200 simulations and iterations. Each scenario built on previous scenarios until the 48-hour requirement was met. This type of scenario testing is not possible with the current method.

The study objective was met by providing verified, dynamic, and integrated simulation-backed results based on semi-empirical data. The solution provided a reliable platform to aid decision-making, scenario investigations, and process predictions – factors the industry method could not provide.

TABLE OF CONTENTS

LIST OF FIGURES

LIST OF TABLES

NOMENCLATURE

Symbol	Unit	Description
η	[%]	Efficiency
μ	[mPa·s]	Absolute viscosity
$\dot{m}$	[kg/s]	Mass flow rate
ρ	[kg/m^3]	Fluid density
A	[m^2]	Area
d	[m]	Distance
D	[m]	Hydraulic diameter
f_d	[–]	Darcy friction factor
F_p	[Pa]	Pipe friction loss
g	[m/s^2]	Gravitational acceleration
h	[m]	Height
L	[m]	Length
p	[kPa]	Pressure
P	[kW]	Power
Q	[m^3/s]	Volumetric flow rate
r^2	[–]	Coefficient of determination
Re	[–]	Reynold's number
t	[s]	Time
T	[°C]	Temperature
ν	[mm^2/s]	Kinematic viscosity
V	[m/s]	Velocity

LIST OF ABBREVIATIONS

1#	Shaft 1
2#	Shaft 2
FEFLOW	Finite Element Subsurface FLOW
GIS	geographic information systems
L	Level (for example, 5L for Level 5)
MAE	mean absolute error
MHSA	Mine Health and Safety Act No. 29 of 1996
MPSO	modified particle swarm optimisation
MSE	mean square error
OHSA	Occupational Health and Safety Act No. 85 of 1993
PI	proportional-integral
PTB	Process Toolbox
SCADA	supervisory control and data acquisition

1. INTRODUCTION AND LITERATURE

1.1. Background

The mining industry uses complex and integrated engineering systems for maximising production [1]. Figure 1 indicates typical systems and processes in an underground mine. These processes include exploration and development, drilling, blasting, mechanical excavation, loading, hauling, crushing, grinding, classifying, separating, dewatering, and storage or disposal [1].

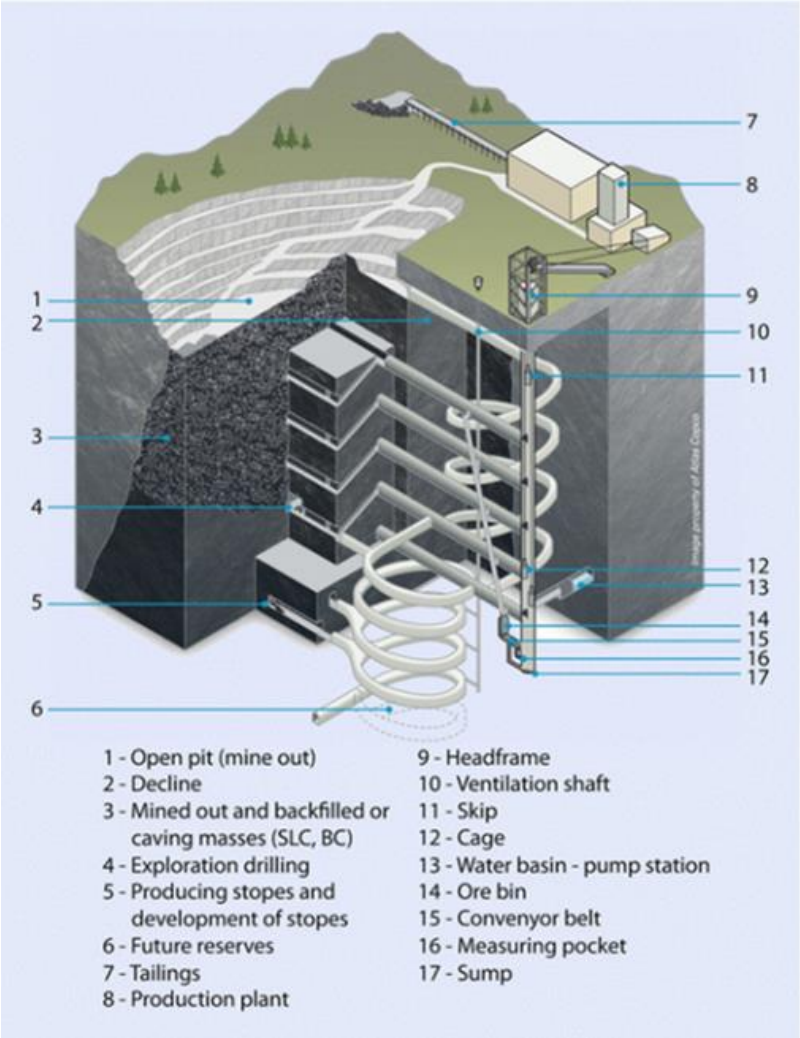

Figure 1: Underground mining systems [2]

The engineering systems developed to aid the mining processes include ventilation, water reticulation (see Figure 2), and compressed air networks. These systems ensure safe working environments and ease the process of extracting ore from extreme depths [1], [3].

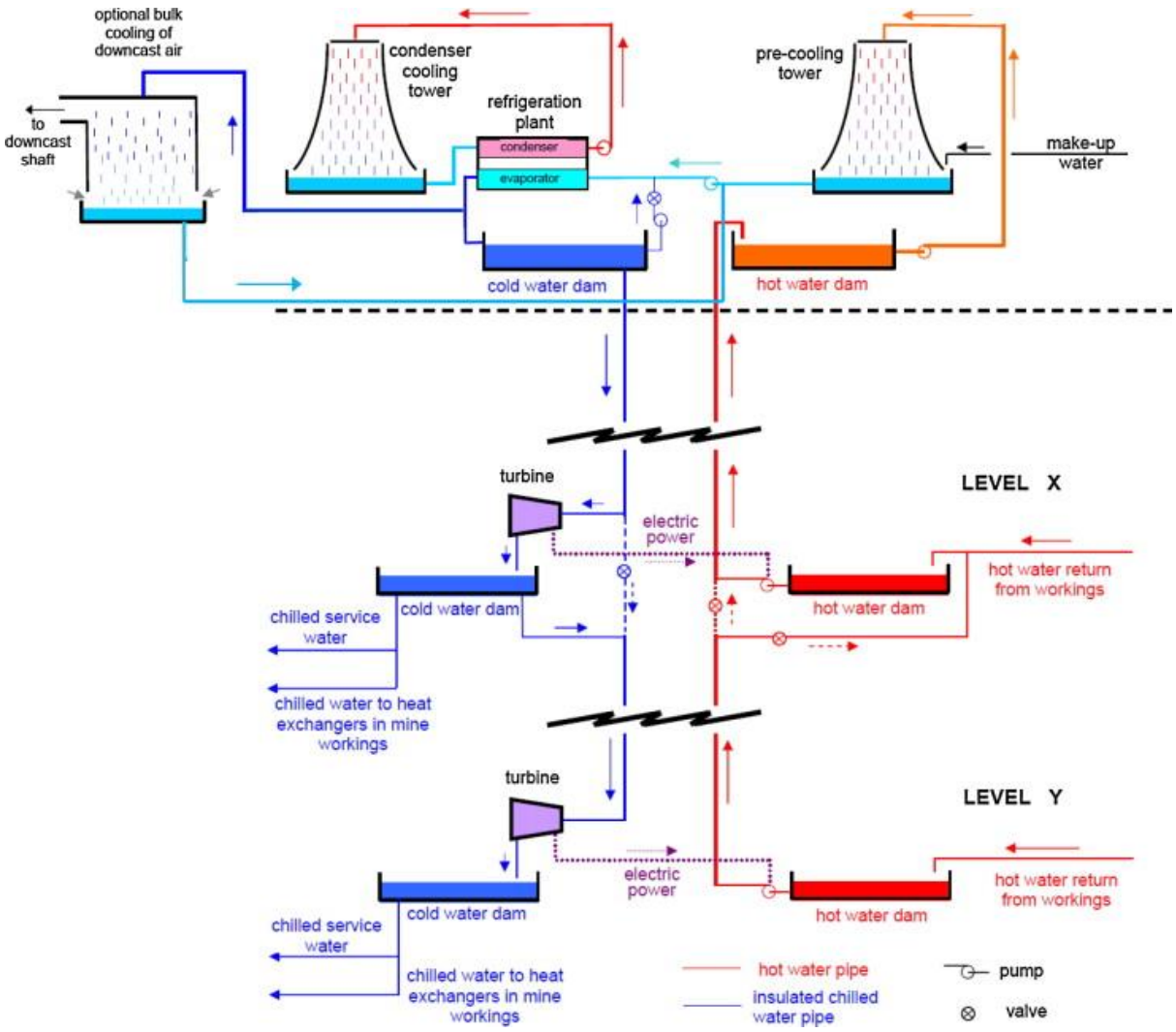

Figure 2: Water reticulation system [4]

The water reticulation system, illustrated in Figure 2, extracts hot water from the mine, cools it down, and returns it underground for various uses. The chilled water sent underground is used for cooling, drilling, cleaning, and dust suppression. Other mine water sources are primarily groundwater seepage, meteorological precipitation, and potable water [5]–[11].

Usually, water is drained to the lowest level of the mine where is it purified and then pumped up to surface [6], [9]–[11]. Dewatering can thus be defined as “the collection of water from an underground operation to prevent flooding or loss of ground stability” [12].

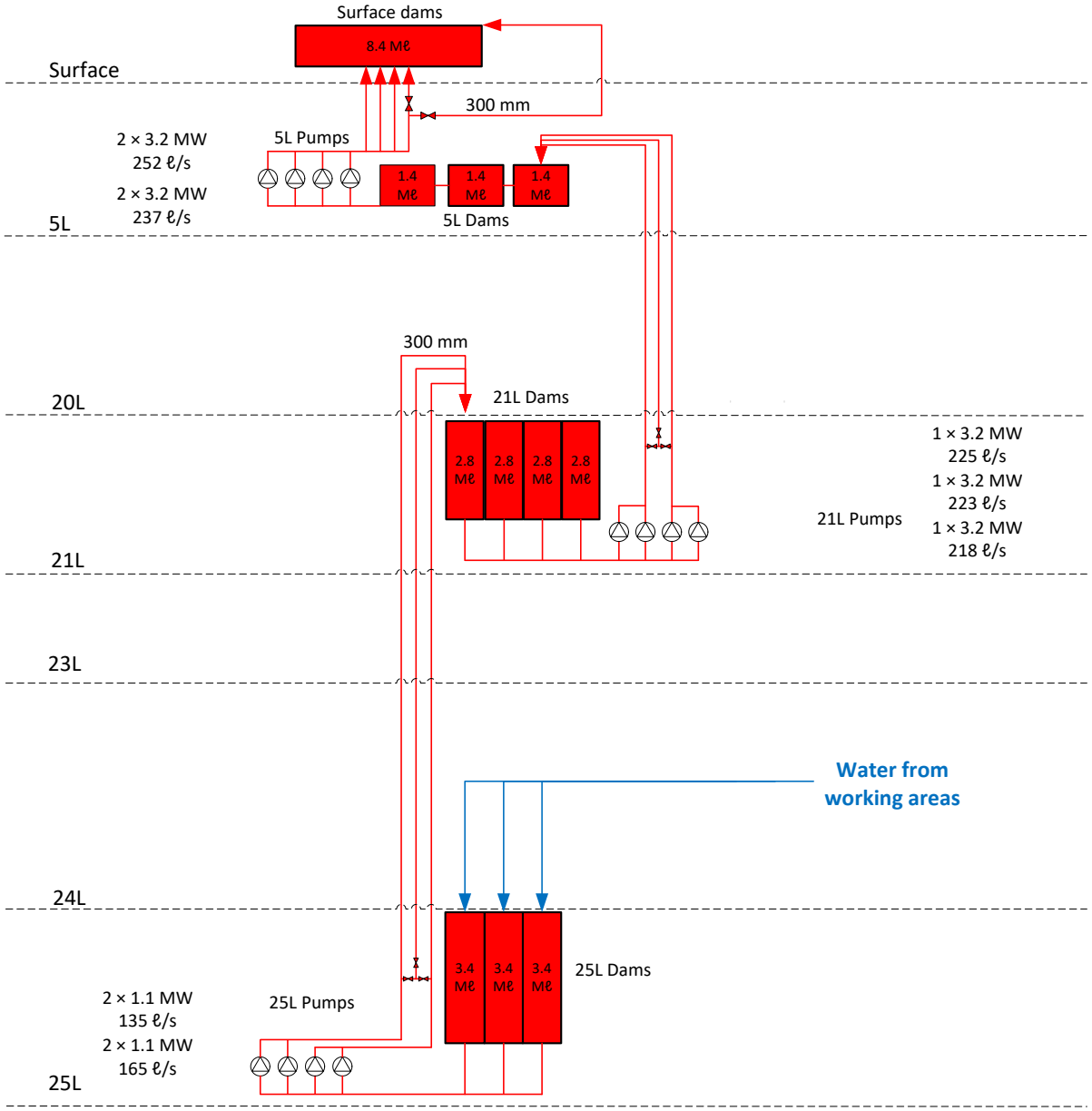

Figure 3: Deep-level mine dewatering system with three lifting stages adapted from [8]

Botha estimates water usage to vary between 1.25 kℓ and 4.15 kℓ per ton of rock mined [13], [14]. Most deep-level mines can have over 200 ℓ/s of water in circulation at any given time [4], [6], [13]. Therefore, dewatering becomes an essential mining system for assuring safe operating conditions. Pumping heads, costs, and system complexity increase exponentially as a mine's working depth increases [5]–[8], [11], [15]. The increase in working depths may require mines to have a series of lifting stages, each with catchment dams and water pumps [8], [11], [15]. Figure 3 depicts this process while the components of the system are defined in Appendix A: Dewatering System Components Breakdown.

Mavhura [16] identified that dewatering is essential in deep-level mines for improving the safety of mining personnel. The statement was supported by Yang et al. [17] who observed the positive effect of dewatering on the safety of the mine and its benefit in decreasing the groundwater levels to a desired point.

Venburg [5] and Mudd [14] supported the statement above and further noted the following benefits of an efficient dewatering system:

- Improved slope stability.
- Less wear and tear on equipment.
- Elimination of caving and upheaval.
- Reduction of hydrostatic pressure.
- Proper alignment of diversion channels with minimal infiltration of water into mining slopes.
- Reduction in the number of sump pumps, water treatment equipment and other facilities.

Venburg [5] and Mudd [14] specifically alluded to the significance of devising methods to control groundwater during the mine planning stage to avoid the adverse effect it could have on the operation.

1.2. Infrastructure instability

The South African mining industry finds itself in a threatening situation due to economic uncertainty, tough operating conditions, depleting mineral reserves, and financial pressure [18]. To ensure that mineshafts stay operational, mining companies have opted to delve deeper. AngloGold's Mponeng is the world's deepest mine as it extracts gold from over 3.9 km

below surface. This increases the risk on all factors and puts equipment under severe stress and strain [9].[1, 2]

Dewatering pumps are required to pump heads exceeding 800 m in these exploits, exposing the pumps to extreme operating conditions [9], [19]. Increased mining depths significantly increase humidity and temperature, which decrease the water quality substantially [19]. The corrosive water and presence of suspended solids along with the harsh environmental conditions greatly deteriorate the pumps [19].[3]

As with any system, the success thereof relies on the infrastructure's stability. This is particularly difficult to ensure in underground mining with the equipment eventually succumbing to the myriad of problems presented [6], [9], [19].[3]

Therefore, the mining industry has adopted various technologies and developments to mitigate equipment breakdown. Physical sensors, anti-wicking cable entries, silicon-carbide mechanical seals, high chrome impellers are examples of upgrades available on the market.[1, 3] However, these measures are preventative and reactive which, according to Jacobs, Mathews and Kleingeld [19], induces failure creep that leads to random failures and unplanned downtime. An alternative approach, namely a predictive strategy, was presented and found that a quadratic relationship exists between the characteristic life and operating depth of a dewatering pump [19]. This is illustrated in Figure 4.

---

[1] Oreflow Australia, "A closer look at the biggest maintenance challenges in the mining industry," 2020. https://oreflow.com.au/a-closer-look-at-the-biggest-maintenance-challenges-in-the-mining-industry/ (accessed 20 Oct. 2021).

[2] K. Crowley, "Deeper gets deadlier in South Africa's aging gold mines," *Bloomberg*, 08 Sept. 2016. https://www.bloombergquint.com/onweb/deeper-gets-deadly-for-workers-in-aging-south-africa-gold-mines (accessed 20 Oct. 2021).

[3] Tsurumi Pump, "6 common threats to pumps in mining applications," 2016. https://www.tsurumi-global.com/article/detail/201612_1793.php (accessed 16 Sept. 16).

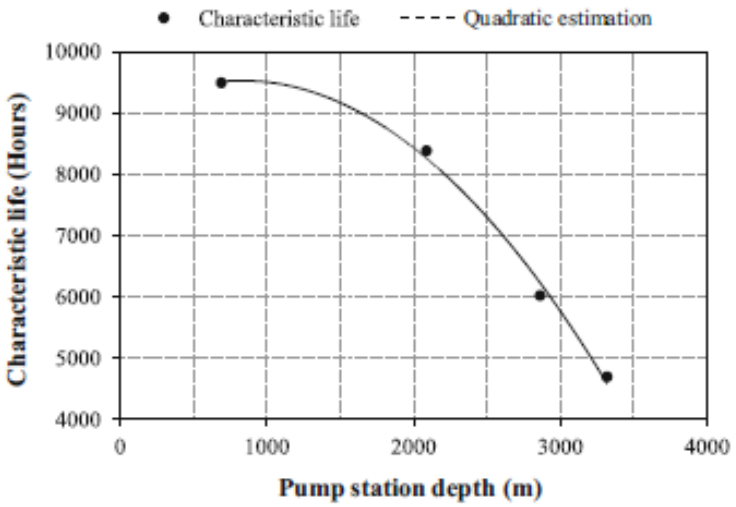

Figure 4: Characteristic life of a dewatering pump vs operating depth [19]

The available strategies can be implemented to reduce equipment downtime greatly and assist with implementing contingency plans.[2] However, the strategies do not take a total power outage into account. A dewatering system can account for 25–50% of a mine's total energy usage [4]. This indicates the system's reliance on a power supply – a power supply that is becoming increasingly unreliable.[4,5] Figure 5 depicts Eskom load-shedding as provided by the CSIR from 2007 till 2021.

[4] CSIR, "Load shedding statistics," 01 Dec. 2021. https://www.csir.co.za/load-shedding-statistics (accessed 02 May 2022).

[5] T. Creamer, "2021 confirmed as most intensive load-shedding year yet as Eskom's EAF continues to fall," *Creamer Media's Engineering News*, 07 Jun. 2022. https://www.engineeringnews.co.za/article/2021-confirmed-as-most-intensive-load-shedding-year-yet-as-eskoms-eaf-continues-to-fall-2022-06-07/rep_id:4136 (accessed 20 Jul. 2022).

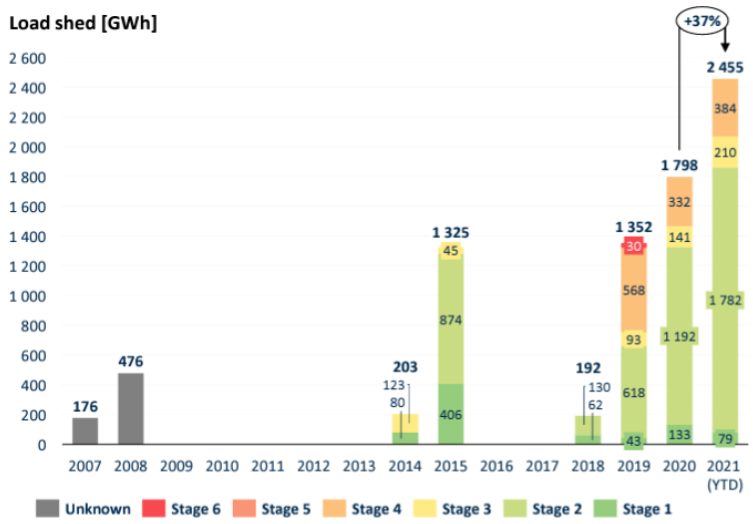

Year	Duration of outages (hours)	Energy shed (GWh)
2007	-	176
2008	-	476
....	....	....
2014	121	203
2015	852	1325
2016	-	-
2017	-	-
2018	127	192
2019	530	1352
2020	859	1798
2021 (YTD)	1136	2455

Figure 5: Eskom load-shedding from 2007 till 2021[4]

The trend from 2018 to 2021 paints an alarming picture for the future. Eskom's energy availability factor has dropped from 71.9% in 2018 to 61.8% in 2021, indicating that 38.2% of Eskom's power generation capacity is unavailable due to breakdowns and maintenance. The ever-declining energy availability factor indicates that load-shedding will endure, which is detrimental to all electrical equipment infrastructure.[6]

The Mine Health and Safety Council details regulations in the Mine Health and Safety Act No. 29 of 1996 (MHSA) that a mine must have two fully independent sources of electricity [20]. This is a mitigation strategy to ensure employees can be evacuated safely if the primary electricity supply is lost. Sibanye Stillwater is compliant with these regulations and provides each shaft with emergency diesel generators [21]. However, as mentioned previously, power surges do negatively affect electrical equipment, which is fundamental to a mining operation.

In 2018, Eskom's main and backup power lines were destroyed by a storm causing a total power failure at Sibanye Stillwater's Beatrix mining complex. At the time, 1 291 employees were underground across three shafts and major technical equipment was damaged [21]. The backup power at Beatrix 4 shaft was restored quickly, allowing 272 employees to evacuate

[6] E. van Zyl, "The impact of load shedding on electrical equipment," *Electrical Contractors' Association*, 13 Mar. 2020. https://ecasa.co.za/technical/the-impact-of-load-shedding-on-electrical-equipment/ (accessed 20 Jul. 2022).

safely. Emergency generators were used to hoist a further 64 employees to surface at Beatrix 1 shaft. The power surge did, however, damage the emergency generator and the software to the winder at Beatrix 3 shaft [21].

Although there are emergency escape routes throughout any mine, employees have to travel large distances and climb steep inclines. The risk of fatigue was too great, and the 955 employees were instructed to remain in a safe and well-ventilated area of 3 shaft. After 30 hours, Eskom was able to restore the system providing sufficient power to reboot the winder software and evacuate the employees [21].

While the decision to wait for power to be restored was correct for that scenario, total power failures can evidently be considered a major hazard in underground mining. Visagie [22] detailed the dangers of a total power failure on compressed air and ventilation systems. What was overlooked though, are the dangers that a total power failure will pose to a dewatering system.

Mining is intimately linked with groundwater as mineral extraction leads to an inflow of groundwater to the mine [23]–[25]. Excess water poses a major risk to the shaft's integrity and flooded areas are extreme risks for mining personnel and equipment [23]–[25]. It is therefore essential that mines plan for unforeseen failures – in this case, a total power failure is the most detrimental hazard – as the dewatering system should always be operational [23]–[28]. This requires extensive emergency planning procedures and adequate infrastructure [26]–[28].

1.3. Emergency procedures and requirements

The MHSA defines an emergency as "a situation, event or set of circumstances at a mine that could threaten the health or safety of persons at or off the mine, and which requires immediate remedial action, such as the evacuation, rescue or recovery of persons, to prevent serious injury or harm, or further serious injury or harm, to persons" [20].

Mavhura [16] and Onifade [27] identified several hazards underground such as dust, noise, and noxious gases. However, only the following hazards require immediate action:

- Fires.
- Fall of ground.
- Inundation of gas or water.
- Explosions.

As is evident from the above list, the mining industry has extensive health and safety risks. Nonetheless, with the introduction of safety legislations and protocols, along with advances in safety equipment and training, the fatality rate has slowly decreased over time.[2] The Occupational Health and Safety Act No. 85 of 1993 (OHSA) along with the MHSA formalise the regulations for safety in the South African mining industry [20], [29]. The MHSA governs health and safety regulations for miners in South Africa, whereas the OHSA governs the regulations pertaining primarily to factories in South Africa [20], [29]. The mining industry does, however, refer to the OHSA for areas not defined or clearly governed by the MHSA [22].

The implementation of these regulations saw a 91% reduction in fatalities and a 79% reduction in injuries across all mining sectors between 1995 and 2020. However, the first increase in mining-related fatalities in 10 years took place in 2017.[7] This realisation sparked a radical change in how safety in mines was perceived resulting in the development of the Khumbul'ekhaya strategy. This strategy aims to eliminate all mining-related fatalities through an improved safety culture.[8]

Mavhura [16] and Onifade [27] attribute the severity of an incident to the attitude, behaviour, and preparedness of the personnel involved. The crux of the matter is understanding the environment and being aware of the surroundings [16]. The Khumbul'ekhaya strategy promotes a safety-first philosophy throughout the mine [16], [22].

Onifade [27] and Kowalski-Trakofler et al. [30] support the concept that preparedness includes having a well-rehearsed and comprehensive emergency plan. They agree that

[7] Minerals Council South Africa, "Safety in mining fact sheet," January 2020. https://www.mineralscouncil.org.za/industry-news/publications/fact-sheets (accessed 09 May 2022).

[8] Department of Mineral Resources and Energy, "Mine accidents and disasters." https://www.dmr.gov.za/mine-health-and-safety/mine-accidents-and-disasters (accessed 09 May 2022).

emergency planning for mines should follow a continual and dynamic cycle. The research suggests that the mining environment is dynamic and requires continuous evaluation due to time constraints and multiple feedback loops. With mining emergencies having the potential to cause serious harm to any employee, immediate and timely response is crucial [27], [30]. There is, however, always a delay – the detection phase. Figure 6 indicates a timeline for the phases of an underground emergency.

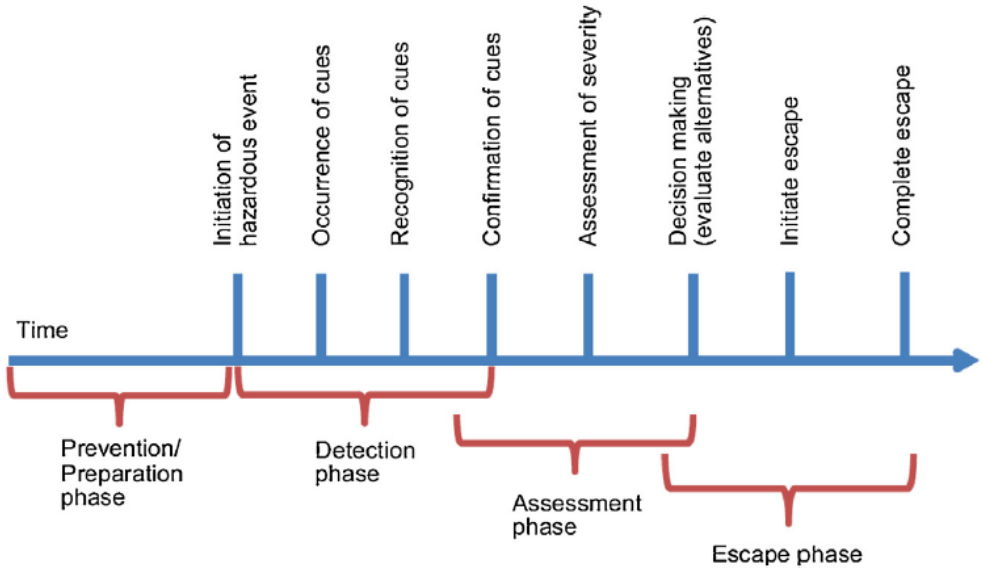

Figure 6: Timeline indicating the phases of an underground emergency [27]

As is evident by the MHSA and the OHSA, emergency planning on mines are required on a national level. According to Onifade [27], an effective strategy is to focus on two aspects, namely prevention and preparation. The main objective is to limit the hazard from spreading and reducing its adverse effects [27].

Mavhura [16] and Kowalski-Trakofler et al. [30] found that suitable planning and preparation of mine emergencies enhance disaster prevention, awareness, response and recovery. In turn, this allows mine operators to successfully deal with the emergency, protect workers, and return operation to production [16], [30].

Emergency planning, as defined by Alexander [31], is the process of systematically preparing for future contingencies. This should be an exploratory process that is updated periodically to the ever-changing mining environment circumstances. An effective emergency plan makes

provisions for managing anticipated hazards while offering generic protocols for managing unanticipated hazards.

1.4. Simulations

Owing to the development of the computer industry, software has become a widely used tool by various industries to investigate the future, optimise daily operations, and aid planning [22], [32]. Figure 7 indicates a simple simulation process flow.

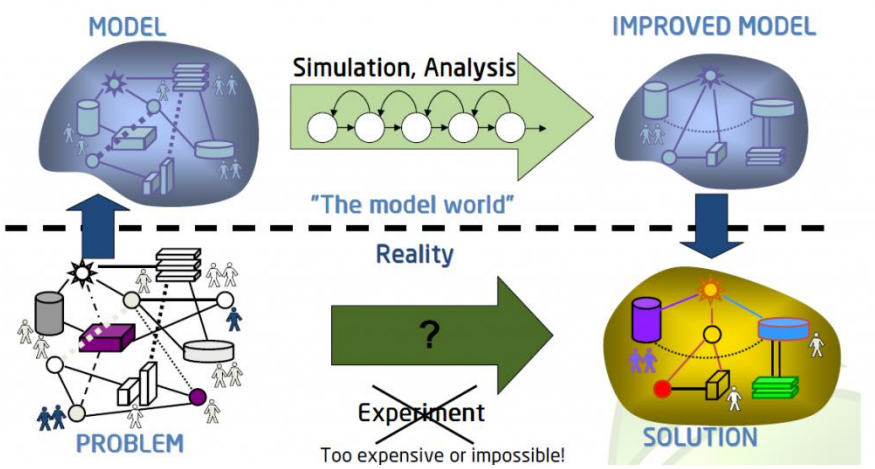

Figure 7: Simulation flow[9]

Advantages of using simulations include [22], [32]:[10]

- The behaviour of a system can be assessed without building it.
- Several days of an activity can be viewed for analysis by compressing time.
- Deep analysis can be done on one minute's data over several hours by expanding time.
- The effect of small changes on a complex system can be identified.
- Different scenarios can be investigated without disrupting the actual system.
- Complex systems can be simplified.

[9] Focus Group, "Simulation model as a decision support tool." https://focus-grp.com/simulation-modeling/ (accessed 06 Mar. 2022).

[10] X. Meng, "Advantages and disadvantages," Bucknell University, 2002. https://www.eg.bucknell.edu/~xmeng/Course/CS6337/Note/master/node3.htMℓ (accessed 19 Sep. 2021).

There are, however, disadvantages associated with simulations [22], [32]:[10] [21], [30]

- Simulations may be used incorrectly – an analytical solution may be better suited to the problem.
- Simulations are resource- and time-intensive.
- Simulation results may be difficult to interpret.
- Special training is required.

According to Alexander [31], the simulation exercise should[29] be designed with clear and well-formulated objectives and treated as a learning process. The evolution of the simulations should be monitored carefully so any change in scope or improvements can be detected [31].

1.4.1. Emergency planning

Alexander [31] identified that modern emergency responses are reliant on information and communications technology. Information technology, especially, is playing an increasing role in planning, particularly in the form of geographic information systems (GIS). GIS has become an integral part of several emergency plans where it is used to depict hazards, vulnerabilities, and patterns of emergency response [31]. Alexander [31], however, have not considered the challenges and applicability of using GIS systems for underground operations. Satellite imagery and similar systems are not available underground, and these constraints will be evaluated in the development of the solution to follow.

Zavila et al. [33], on the other hand, analysed the use of mathematical modelling for emergency planning purposes through statistical and dynamic models. Statistical models, such as ALOHA, include semi-empirical relations between coefficients based on data from field sets. Dynamic models, for example ANSYS, Fluidyn PANACHE and FLACS, are based on the numerical solution of systems of partial differential equations [33]. The conclusion of the study revealed that statistical models focus on the adverse consequences of emergencies. This is due to the models being limited to few parameters and their subsequent degrading reliability outside the set parameters. Dynamic models, in contrast, are more time-consuming and expensive but provide an accurate platform for solving spatiotemporal problems [33].

Alexander [31] went further to suggest that scenarios are a vital tool for emergency planning. This concept is supported by D'Uffizi et al. [34] who identifies that through what-if analyses, simulations permit the study of the dynamicity of relief operations. The research showed that a model could be developed to simulate emergency situations with both static and dynamic procedures. The model accounted for the severity of each event and the chronological time of the occurrences [34].

D'Uffizi et al. [34] acknowledged that the standard procedures applied in rescue operations do fail. The authors aimed to study different mechanisms that would provide more flexibility to emergency procedures and their effectiveness. Through discrete event simulation, several scenarios with different initial hypotheses were combined to create a generalised and flexible procedure. This could be applied to different situations and supported the notion of using simulations as a decision support tool for planning emergency and risk situations [34].

Samany, Sheybani and Zlatanova [35] determined that predicting safe areas before a flood is essential for the evacuation process. The authors proposed a GIS-based, multicriteria decision analysis and a particle swarm optimisation-based algorithm. The flood risk map obtained used an analytical hierarchical process and a weighted linear combination technique. Thereafter, a modified particle swarm optimisation (MPSO) with local search MPSO algorithm determined the optimal locations for evacuation stations [35].

Ant colony optimisation, simulated annealing, generic algorithms and fuzzy-rules-based methods were acceptable in location-allocation flood management problems. However, the comparison of results justified the efficiency of the proposed algorithm. The local search MPSO had three distinct advantages [35]:

- It converged to minimum cost quickly.
- It was less sensitive to local minima.
- It found a balance in the distribution of optimum locations so that all persons could benefit with suitable accessibility until evacuation.

Rahman et al. [36] used FLO 2D, a hydrodynamic model, in conjunction with a machine learning algorithm, namely scaled conjugate gradient neural network, to develop a flood

hazard map. The FLO 2D model computed the static or dynamic flood while the neural networks derived intricate links between the causal flood factors [36]. Generally, flood hazard mapping identified where floods were expected to occur. The proposed approach attempted to additionally provide hydrological information such as flood depth and velocity. The model was able to quantify the necessary disaster relief based on the hydrological output data by incorporating the hydrodynamic machine learning algorithm model into a GIS platform [36]. The authors concluded that flood hazard mapping is key to alleviating flood risks. Effective interventions can be designed to decrease the impact of floods and aid humanitarian responses in the pre- and post-flood activities [36].

The previously identified studies aim at assisting the preparation, response and recovery components of the flood management cycle, as illustrated in Figure 8. Mitigation is, however, another important factor that ties in closely with the study area. Mitigating a flood scenario, particularly in an underground mine environment, is vital as response activities are difficult to implement and require extensive recovery.

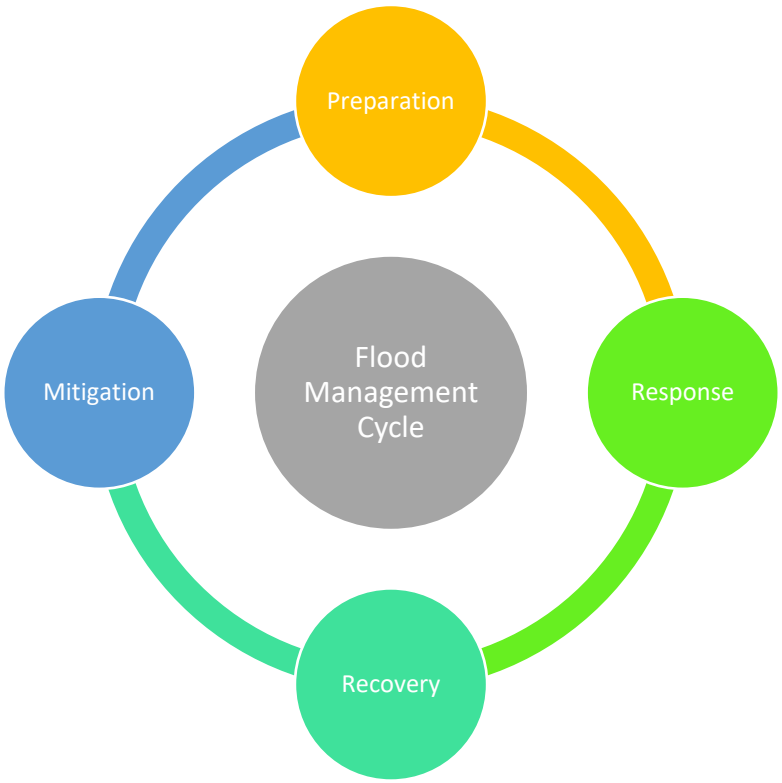

Figure 8: Flood management cycle, adapted from [35]

Lyu et al. [37] presented four approaches to assess the flood risk of metro systems, namely: statistical methods, multicriteria analysis, GIS and/or remote sensing analysis, and scenario-based analysis.

- Statistical methods are based on historical records. The method presumes that historical floods can be used to predict future floods [35].
- Multicriteria analyses use an index system to assess risk where flood risk is the object layer. Hazard, exposure and vulnerability make up the index layer, and the sub-index layer includes factors that induce a flood event [37].
- GIS- and remote-sensing-based techniques provide technical support. A GIS platform maps the spatial distribution of a flood risk while a remote sensing platform reflects the characteristics of an area's topography [35].
- Scenario-based analysis can be used to predict flood risk before it occurs by changing the spatial domain. Valuable information is gathered through this analysis, which is used to implement risk mitigation strategies [37].

Considering the four approaches, Lyu et al. [37] indicated that the following perspectives in Figure 9 provide a strong platform for flood mitigation. An analytical hierarchical risk evaluation process provides a qualitative assessment of risk. Early warning systems are recommended, particularly in sections with high risk. Scenario-based prediction provides an accurate and quantitative assessment upon which the countermeasures can be based [37].

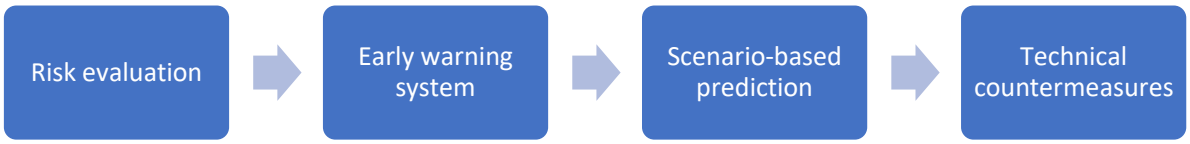

Figure 9: Perspectives for flood mitigation [37]

Dazzi et al. [38] assessed the efficacy of numerical modelling as a support tool for flood hazard analyses associated with levee breach. Moreover, they integrated the models into forecasting systems and precalculated scenarios to create a database of plausible flooding scenarios to mitigate negative consequences. A PARFLOOD code (two-dimensional model) was used to

predict the inundation dynamics (area, depths and arrival time) and identify countermeasures in advance [38].

These forms of analyses are crucial to the study as they highlight the importance of pre-emptive planning. The results of the studies conducted by Lyu et al. [37] and Dazzi et al. [38] were used for contingency planning purposes and assisted in developing emergency operations in case of an actual flood event. The expected flood arrival times at different locations proved successful in averting an inundation event as the countermeasures were implemented in time. Although the emergency activities are case-dependent, the model is adaptable for case-by-case analyses [38].

1.4.2. Dewatering systems

Excavation activities below the water table require groundwater extraction to ensure an acceptable working environment [39]. Pujades et al. [40] found that the success of these excavation activities lies in the stability of the excavation bottom, the effects of dewatering on surrounding systems, and/or the state of the enclosure. The characterisation and design of the dewatering system must therefore be considered carefully.

Dewatering influences groundwater levels, flow patterns, and soil movements [39]. Chen et al. [41] identified possible geological hazards associated with these influences:

- Quicksand.
- Piping.
- Flooding the excavation floor.
- Groundwater drawdown:
    - Foundation collapse.
    - Uneven ground subsistence.
    - Wasting of groundwater resources.

According to Brunetti et al. [39], the dewatering process consists of an extensive system of sumps and pump stations. There are various techniques for excavating under the water table. Pujades et al. [40] deemed the optimal approach to be dependent on the characteristics of

the soil and the hydrogeology of the site. Pujades et al. [40] emphasised the importance of applying procedures that ensure the safety of excavation activities when groundwater is present. To that extent, Shen et al. [42] proposed an automatic pumping recharging system to maintain the groundwater balance during the dewatering of metro tunnel construction sites.

Brunetti et al. [39] and Zeng [43] supported the notion by Pujades et al. [40] and identified that numerical models capable of simulating three-dimensional steady-state and transient groundwater flow could facilitate the engineering design of dewatering systems. To develop a sustainable dewatering system, a thorough understanding of the complex hydrogeological system is required [39]. Although this is often a demanding task, numerical simulations provide a solution to complex systems with limited data [41]. Chen et al. [41] evaluated that the only way to mitigate geological hazards was to predict the system's behaviour accurately.

Chen et al. [41] did identify that empirical formulas and analogy methods often encounter insurmountable difficulties in providing definitive solutions. Table 1 summarises the sources that proposed numerical simulation solutions to support the design and optimisation of dewatering schemes.

Table 1: Summary of dewatering systems' numerical analyses

Source	Simulation platform(s)	Outcome
[39]	• FEFLOW • Grid Builder • ArcView • ArcMap	Compute and assess the impacts of dewatering on groundwater flow, flow patterns, and subsequent land subsistence.
[40]	• TRANSIN-IV • CODE_BRIGHT	Detect excavation site defects through an integrated analysis of field data and numerical modelling to assist with the dewatering system design.
[41]	• MODFLOW-USG	Aid the construction and design of dewatering schemes in deep foundation pits under intricate hydrogeological environments to minimise environmental impacts.
[43]	• ABAQUS	Simulates a practical pumping test to evaluate the distributions of groundwater settlement and groundwater drawdown under different pumping conditions.
[44]	• TRANSINIV • VISUAL TRANSIN	Numerically analyse the groundwater's response to pumping as a means of evaluating the condition of non-linear underground enclosures.

Source	Simulation platform(s)	Outcome
[45]	• Visual Fortran 90 • PIV 3.0	Provide a methodology based on the control of land subsistence to design and optimise deep foundation pit dewatering systems.

Although the abovementioned sources executed separate objectives, the numerical modelling aided the development of effective intervention and remediation strategies. The overall goal was first to assess the past and then predict the future. Numerous scenarios were simulated in each case to determine the best dewatering system design.

These strategies closely relate to the study because, as it has already been pointed out, dewatering is vital to underground mining. The development of scenario-based decision-making also ties into what was identified in Section 1.4.1 and will be considered in the methodology to follow.

The boundary conditions of the numerical models proposed in Table 1 were vastly simplified, which resulted in decreased efficiencies. Each numerical model developed required additional GIS packages to assist with georeferencing operations and spatial analysis. This will be challenged in the development to provide an alternative solution.

1.4.3. Deep-level mine dewatering

The sources from Table 1 and those mentioned in Section 1.4.1 provide keen insight into pre-emptive planning to mitigate disasters and how simulations can be used for dewatering systems. These models are, however, based on surface or shallow-foundation environments. The analysis of mining water reticulation systems is more intricate owing to the multifaceted distribution system and the number of possible operating conditions [9], [10]. Therefore, the risk of the hazards mentioned by Chen et al. [41] increases ten-fold when deep-level mining is considered due to intense working conditions and difficulty in performing rescue operations [46].

The dewatering system is designed according to specified requirements relating to water flow rate and head [8]–[10], [47]. Mine water contains solid particles and dissolved chemicals which, along with inflow uncertainty and times of operation, rapidly increase the complexity

of the dewatering system [8], [47]. A suitable settling and decantation capacity is required to filter the water to preserve the components of the system upstream [8]–[10], [47]. Furthermore, the water is collected in sumps/dams where it is pumped to surface or an intermediate level depending on the number of lift stages [8]. Pumping plants comprise a series of pumps, valves, by-passes and filters to comply with the correct set-up, operation, and maintenance [8]–[10], [47].

There is, however, no assurance that the designed dewatering systems will remain optimal over time. Consequently, Romero et al. [8] implemented a predictive model control strategy to optimise the dewatering system design and adaptively maintain the system's optimality during operations. A predictive model control manages the system constraints (such as pump capacity and reservoir limits) and operational uncertainties common in mining [8]. The framework incorporates models that do not require high levels of precision and complexity but still yield sufficient results in designing and optimising dewatering systems [8]. The system's adaptability is the crux of the matter, which will be considered in the methodology so that an adaptable solution can be developed.

Yang et al. [17] used a similarity model to predict the effects of a dewatering system on an aquifer's hydraulic pressure. Aquifer dewatering reduces the water content in the sand layer, static reserves, and hydrostatic pressure on the roof. These reductions ensure that the hydraulic head decreases to below the head required to blow out the water [17]. The authors adopted the Terzaghi formula with borehole data and soil tests to calculate the critical hydraulic gradient. Thereafter, a scaled dewatering scheme was designed and tested, and a visible effect was observed on the water level [17]. This approach is, however, only practical on newly developed mines before intense mining has started to allow for changes to be made if need be.

Simulations, much like what was developed is Section 1.4.2, can also be developed for the optimal design and hydraulic analysis of the systems [6], [9]. Stephenson [6] identified that simulation platforms can be used to assess the following aspects of the underground water distribution system [6]:

- Optimisation of pipe sizes.

- Optimisation of water reticulation systems.
- Water quality deterioration.
- Water hammering.

Dewatering is a crucial element in ensuring geologically safe and efficient mining conditions [9], [48]. Hu et al. [48] found that analytical solutions and models are not sufficient for hydrogeologically complex conditions and intricate systems. Hence, numerical models are constructed to analyse, design, and optimise dewatering systems [48].

Yuan, Gai-ling and Guo-yong [49] implemented a dewatering strategy on a mine using the Finite Element Subsurface FLOW (FEFLOW) system and the Kriging finite element method. The three-dimensional hydrogeologic numerical model successfully predicted the dynamic variations of the groundwater levels as a result of dewatering conditions [49]. The outcomes support the notion made by Yang et al. [17] that dewatering can reduce the groundwater level and thus create a safe mining environment. By analysing mining accidents, Yuan et al. [49] established that dewatering aquifers before mining can prevent unexpected water inrush. To that extent, modelling groundwater flow was proposed as an effective strategy for planning, designing, and optimising dewatering systems [46], [48], [50].

In most cases, groundwater flow is three-dimensional [46]. Therefore, for a numerical model to be a reliable predictive tool, the groundwater flow model must be based on three-dimensional data. This approach is proposed by Martínez and Ugorets [46] as it allows for the groundwater system to be characterised fully. The authors demonstrated the advantages of modelling groundwater with complex hydrogeological conditions through three-dimensional numerical analysis for mine dewatering projects. Martínez and Ugorets [46] suggested Visual MODFLOW with MODFLOW-SURFACT or FEFLOW for these analyses as they are commercially available, have good modelling features for simulating mines, and are accepted by regulatory agencies.

Hu et al. [48] applied FEFLOW and MODFLOW-USG to their analysis of groundwater flow in deep-level mines. Eight scenarios of well designs were subsequently established following the modelling of dewatering capacity requirements. The authors coupled these results with a

geological model, namely GeoModeller, to address the uncertainties of the aquifer's geometry.

Mengistu et al. [50] executed the groundwater model on the Groundwater Modelling System (GMS 9.2). This user interface has numerical modelling codes such as MODFLOW and MT3DMS to investigate every phase of groundwater simulation, namely characterisation, model development, calibration, post-processing, and visualisation [50]. The authors highlighted the importance of integrating various data sets before developing and calibrating the models to improve reliability and accuracy [50]. Their goal was to avoid expensive dewatering schemes by developing a sustainable water management system based on the groundwater characteristics [50]. Therefore, various chemical data was used to characterise the flow sources, flow directions, and the mineral makeup of the water so that the dewatering system could be designed optimally [50].

The analysis from [46], [48], [50] correlates well with the research done for shallow pit dewatering. It is evident that combining numerical flow models with geological models improves the accuracy due to the improved spatial data. The models can be used for sensitivity analysis, various forms of planning, and prediction scenarios that minimise the risks associated with deep-level mining [46], [48], [50]. These forms of analyses are vital to the study and will be considered when developing a solution to address the problem statement.

Nell [9] and Wagner [10] used a three-dimensional thermohydraulic simulation platform, namely Process Toolbox (PTB), to develop dewatering simulations for deep-level mines. Nell [9] used a simulation model of a mine dewatering system to develop control strategies while Wagner [10] used a model to assist with planning and avoiding overexpenditure. Although their final objectives varied, both authors followed similar approaches in developing the dewatering models, which will be carefully evaluated and considered in this research's method.

1.4.4. Mine flooding simulations

As the depth of mining increases – an already established fact in South African gold mines – factors such as water pressure, geostress, and mining disturbances increase exponentially

[51]. This adds strain on the dewatering system that increases the risk of an underground mine flooding. Consequently, mitigative and preventative measures become increasingly important to ensure mine safety [51].

Water has the potential to cause major damage in the mining sector if not managed correctly. Whether it be on surface or underground, mining incidents have been attributed to water's destructive capacity [26]. On 21 January 2008, Amandelbult mine experienced the worst flood in its operating history when the water levels water levels topped the 1:150-year flood line for a "once in 200-year event" [26]. The abnormal rainfall exceeded the dewatering capacity and flooded the pump station and shaft bottom at a rate of more than 1 000 ℓ/s [26]. A task team established a dewatering strategy to incrementally dewater the shaft through interlevel pump stations and dams. During this time, production was halted with an estimated shortfall of between 1 400 kg and 2 000 kg of refined platinum. Full production resumed on 6 May 2008 and the recovery of production losses was estimated to be between three and six months [26].

Although the shaft personnel were evacuated safely, Meyer reported that a fitter assistant was injured fatally. The man was lowered into the shaft with the service winder and died on impact after hitting water that had accumulated in the shaft. Determining the exact levels of possible flooding areas, flooding flow paths, and flooding times are, therefore, crucial in emergency water planning [26].

Hundreds, if not thousands, of people need to be removed from the mine in the event of an emergency. Heavy equipment needs to be restarted and personnel need to be retrained as mistakes can be made in this process, which increases the risk of further incidents. The flooding of a mine has the potential to cause substantial loss. Along with the extensive evacuation procedures, equipment can be destroyed and there is always the potential for loss of life.[2]

The Department of Mineral Resources and Energy has the authority to shut down an entire mine following an incident to investigate and/or deem sections safe.[2] According to Crowley,[2] AngloGold and Sibanye Gold Ltd forwent approximately R1.9 billion of precious metals in the first half of 2016 due to closures. Safety and production are heavily correlated – a well-run

operation is generally a safe one. Considering the losses associated with production stoppage, emergency planning should be prioritised, and the mine water management plan should place considerable emphasis on water issues [14].[2]

Significant progress has been made in understanding the causal factors of water inrush and the prediction thereof through numerical modelling [51]. Li et al. [51] deemed it essential to develop models that can aid water inrush contingency planning. The authors proposed a three-dimensional spatiotemporal, dynamic model framework. The model aimed to dynamically express the flow-spread process development on underground roadways over time during a water inrush incident [51]. The spatiotemporal changes of water inrush spread on a roadway are influenced by the following factors [51]:

- The location of the inrush points.
- The level and yield of the water sources.
- The spatial aspects of the underground construction.
- The mine's dewatering and drainage capacity.

From the inrush locations, water pours onto the roadways and flows towards the shaft [51]. The water level continues to rise along the roadways until equilibrium is reached. To simulate this, the model must account for the water spreading along the roadways, the water level rising, and the dewatering system's effects on the incident [51].

A spatial representation of the mining roadways was developed through a roadway space network system in which the paths resolve for the water inrush spread process. The temporal-dynamic expression was generated from the hydraulic characteristics of the water current along with calculations for the velocity and time components of the inrush spread [51]. The extent of the water inrush spreading over a timeline, the spatial scope of the roadways, and the degree of impact can be viewed and analysed through the three-dimensional visual representation provided by the model [51].

The proposed approach is relative to this study as the results can be used to formulate contingency plans to plan for and avoid water disasters while assisting emergency rescuers

with possible real-time data. The following points identify advantages of the model proposed by Li et al. [51] that are applicable to the research and will be considered in the methodology:

- The model provides a three-dimensional space plus time description of the scenario.
- The model provides a flexible platform for developing plans that can assist with rescue operations and preventing underground mining water disasters.
- Due to the adjustable timescale, the model can be used to predict future scenarios.
- The model simulates the following accurately:
    - The head position of the water inrush.
    - The extent of the water disaster over a given timeline.
    - The time in which water will spread to certain locations.

The dynamic equilibrium of the model and the success of the mine's ability to deal with the inrush ultimately depend on the dewatering system's capabilities. Designing a dewatering system is, again, evidently vital to a mine's safety and operations. These statements are supported by the sources in Section 1.4.3 that highlight the importance thereof. There is an agreement that dewatering is crucial to avoid flooding and can be used to decrease the impacts of water inrush. But what happens if the system fails or stops operating?

Flooding is inevitable if a mine dewatering system is not in operation [52]. Álvarez et al. [52] likened an abandoned/closed mine to a reservoir and numerically modelled the flooding process of a closed mine to avoid unexpected and unwanted discharge at surface. Although mining stopped, the fractured rock mass it leaves in its wake facilitates water infiltration. Infiltration gradually floods the mine voids – a process known as groundwater rebound [52].

The infiltration flow rate and void volume are determining factors to the flood time [52]. The void storage capacity was estimated at 8 million m^3 by assessing the mining history and interconnections. A void is further not a homogenous or isotropic system; the water may move quickly through certain sections and be restricted in others. Therefore, the authors proposed numerical modelling. FEFLOW and GRAM (Groundwater Rebound in Abandoned Mineworkings) were used to model the flooding of a mine to aid pre-emptive and preventative planning [52].

The approach to decommissioned/closed mines indicates the importance of forward thinking and the benefit of simulating scenarios for preparing for the different scenarios presented in the mining industry. What is not considered is what would happen if an operational mine were to lose its pumping capacity. Mines do have control philosophies and instrumentation that provide semi-real-time feedback on their systems [22]. However, these systems fail at times which, along with the infrastructure instability highlighted in Section 1.2, increases the risks of impending disasters [22].

Burritt and Christ [53] suggested the need for an improved water accounting information system. The authors identified that intelligent systems could aid informed decision-making and emergency planning [53]. The authors indicated that simulations are a means of facilitating improved water risk data, which subsequently improves water risk management [53]. Dynamic risk management necessitates real-time spatial and temporal data to implement adequate emergency plans. Burritt and Christ [53] found process simulations to be a plausible solution. Process simulations provide a platform for understanding complex systems and analyse the effects of changes to a network on end users and the environment [53]. Thus, this proposal is ideal for the mining industry.

1.4.5. Process simulations

For an accurate model of a mine dewatering network, the software package must correctly simulate dynamic water pumps and the fluid dynamics of water through a large integrated network. The package must be capable of simulating transient-state scenarios as mines seldomly operate as steady-state systems and be based on empirical data to closely reflect day-to-day operations [22].

KYPipe is a one-dimensional isothermal flow simulation package capable of solving varying ideal and non-ideal fluid applications [22]. It uses Darcy–Weisbach equations and the ideal gas law in its solving functions [22]. Although it is generally limited to steady-state conditions, there are transient-state applications. However, the package is incapable of accurately

incorporating multiple components and a vast network in a transient-state solution.[11] The package is, therefore, not ideal for simulating a mine dewatering system.

Flownex is another thermal fluid package that was considered. The software uses a node-like structure ideal for network systems [22]. It has been used previously for designing reticulation systems, optimising pipe sizing, aiding compressor selections, developing energy optimisation strategies, and sizing heat exchangers.[12] The simulation tool does, however, require a high level of empirical data that is not always available in the South African mining industry [22].

To obtain the required data quality, manual measurements on every component of the system are required through high-tech equipment [22]. Although this is possible, it is highly impractical and time-consuming. The disadvantage of using Flownex is that the error associated with simulations resulting from insufficient/inaccurate data is too high for consideration in high-risk management decision-making [22]. The package is, therefore, not ideal for simulating a mine dewatering system in this instance.

A plausible simulation software package may be PTB, which was developed by ETA Operations and also uses a node-like structure. PTB is capable of simulating transient thermohydraulic systems to aid in the design, analysis, and optimisation of intricate systems. PTB has been proven by [3], [9], [10], [22], [54], [55] to simulate complex, integrated and dynamic systems based on empirical data to accuracies of 95% or better.

The following features and capabilities are included in PTB [3], [9], [10], [22], [54], [55]:

- Pipes and pressure nodes create flow paths for the system.
- Pressure drops are calculated in the pipe components.
- Thermohydraulic properties are calculated in the pressure node components.
- The gas flow solver is a semi-implicit, compressible quasi-steady-state solver.
- The energy solver is a transient explicit solver.

[11] KYPipe, “Pipe2020: Surge feature list.” https://kypipe.com/surgefeatures/ (accessed 28 Jun. 2022).

[12] Flownex Simulation Environment, “Precise 1D simulation.” https://flownex.com/ (accessed Jun. 28, 2022).

- Steady-state and/or transient systems can be simulated for any number of time periods and period size.
- The system component inputs, outputs, optimisation constraints, and optimisation variables automatically expand to match the specified number of time periods.

Thus, PTB meets the minimum requirements for simulating a mine dewatering system.

Friedenstein et al. [3] proposed a methodology on compressed air simulations that yielded simulation errors of between 1.36% and 3.00% on three different case studies. Visagie [22] applied the same methodology to determine the changes of compressed air during a power outage in refuge chambers, which also yielded accurate results capable of supplementing emergency planning.

Nell [9] and A. Wagner [10] both used PTB for their deep-level mine dewatering simulations. As mentioned in Section 1.4.3, Nell [9] used the simulation model of a mine dewatering system to develop control strategies while Wagner [10] used the model to assist with planning and avoiding over expenditure. While their objectives differed, both dewatering simulations yielded accuracies over 95%.

The studies showed that PTB is more than capable of accurately simulating complex networks. Therefore, the methodologies proposed by [3], [9], [10], [22], [54], [55] will be considered in the next section and altered according to the requirements of the research. They provide an accepted and proven strategy for accurately simulating complex thermohydraulic and transient-state networks.

1.5. Motivating the study

Meyer [26] correctly noted that high-consequence, low-probability events still require adequate planning and risk analyses. The Amandelbult disaster in South Africa pressed a move for revising risk analysis and emergency planning aimed at continually improving the process [26].

Google Scholar, ScienceDirect and Scopus were used as research engines to find information relating to the study. Table 2 provides a matrix of the 28 research studies identified above

that relate to the research topic and compares them in five key areas: emergency planning, simulation, dewatering, flooding, and deep-level mining. Simulation is further divided into three categories, namely empirical, dynamic, and integrated simulations.

Table 2: Breakdown of the relevant studies based on the criteria of this study

Reference	Emergency planning	Empirical simulation	Dynamic simulation	Integrated simulation	Dewatering	Flooding	Deep-level mine
[3], [54]		X	X	X			X
[8]		X	X	X	X		
[9]		X	X	X	X	X	X
[10]		X	X	X	X		X
[17]					X		
[22]	X	X	X	X			X
[26]						X	X
[35], [53]	X					X	
[33]	X	X	X				
[34]	X		X	X			
[36], [38]	X		X	X		X	
[37]	X	X	X	X		X	
[39]–[41], [43]–[45]		X	X	X	X		
[49]		X	X				
[46], [48], [50]		X	X	X	X		X
[51]	X	X	X			X	X
[52]		X	X			X	X
[55]		X	X	X			

Legend	
X	
Included in the scope of study	Not included in the scope of study

The purpose of the matrix is to clearly indicate the gaps in the literature pertaining to the use of process simulations for emergency planning on deep-level mine dewatering systems.

Need for the study

Evidently, a need exists to determine a dewatering system's response to a complete loss in pumping capacity. Empirical data will be crucial in developing a model with the capacity to simulate a dynamic and integrated mine dewatering system.

1.6. Research aim and objectives

The aim of this study is to develop a method for modelling a total power failure scenario in deep-level mines for emergency planning on the dewatering system. This can be achieved through the following objectives:

a) Develop a simulation-based method to model a mine dewatering system.
b) Calibrate the dynamic and integrated simulation-based model for the system using empirical data from a case mine.
c) Validate and/or verify the model's degree of accuracy.
d) Use the model to simulate a total power failure for the case mine to determine the current infrastructure's capabilities.
e) If applicable, develop contingency plans using the model to ensure requirements are met.
f) Evaluate the feasibility of the proposed contingencies and advise on what should be implemented.

2. DEVELOPMENT OF SOLUTION

2.1. Preamble

Chapter 2 focusses on describing the process followed in developing a solution to the problem statement defined in Chapter 1. The 28 relevant sources assessed provided various methods for addressing problems in the form of simulation models, which ultimately provided the foundation of the solution relevant to this study. Figure 10 depicts a high-level overview of this process and Chapter 3 will focus on applying this process to a real-world case study.

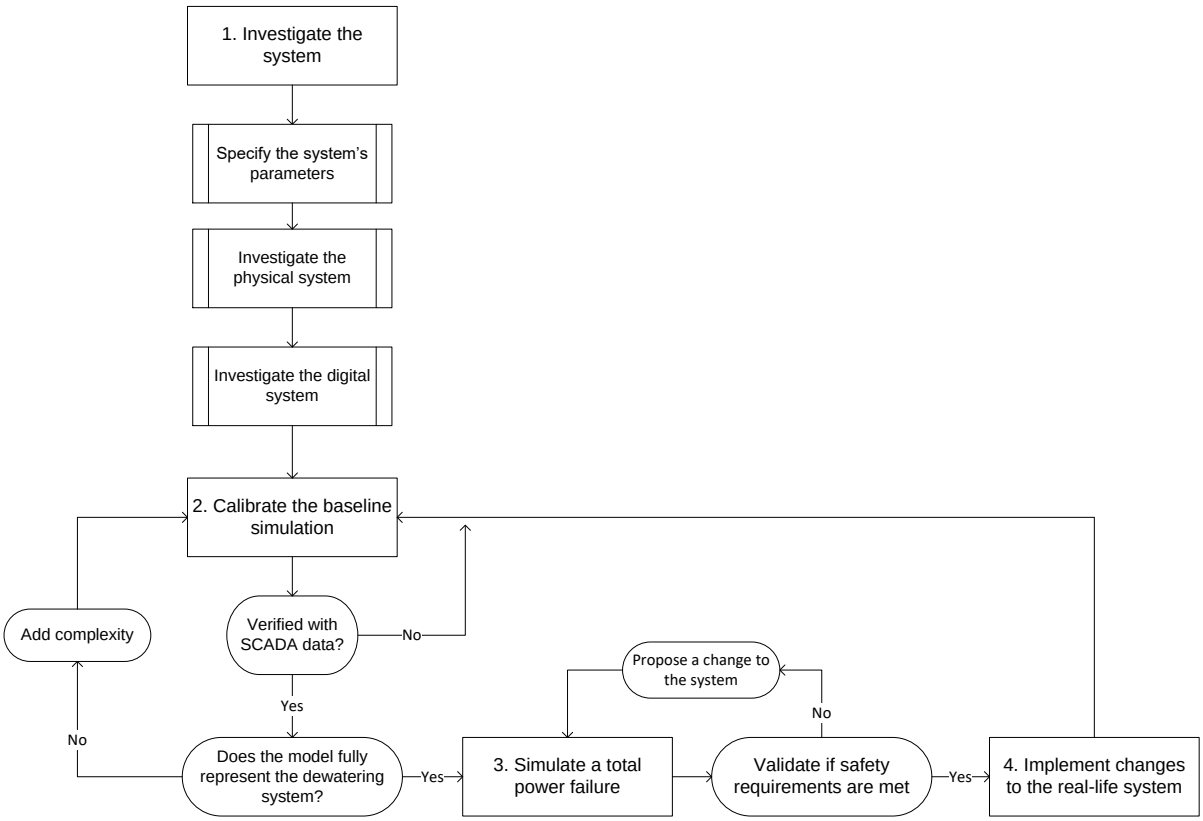

Figure 10: Flow diagram of the proposed method adapted from [3], [9], [10], [22], [54], [55]

The four basic steps detailed in Figure 10 are as follows:

1. **Investigate the system:** The system needs to be understood thoroughly before it can be simulated [3], [9], [10], [22], [54], [55]. In this case, the mine dewatering system must be investigated so that an accurate digital representation can be built.
2. **Calibrate the baseline simulation:** A basic simulation model is created to depict the mine dewatering system layout [3], [9], [10], [22], [54], [55]. This model is built and verified according to the real-life data provided by the mine's supervisory control and data acquisition (SCADA) system [3], [9], [10], [22], [54], [55]. More detail and complexity are added to the verified model in a recurring cycle until it accurately represents the real-life system [3], [9], [10], [22], [54], [55].
3. **Simulate a total power failure:** Thereafter, the verified simulation model is capable of performing various simulations for different applications [3], [9], [10], [22], [54], [55]. The simulations applicable to this research are to determine the system's response to a total power failure.
4. **Implement the system:** Finally, any proposed changes identified through the simulation investigations are implemented in the real-life system [3], [22], [55]. Once these changes have been made, the simulation is recalibrated and updated to match the new baseline system [22].

2.2. System investigation

The system needs to be understood thoroughly before it can be simulated [3], [9], [10], [22], [54], [55]. The system relating to this study is a mine dewatering system, which must first be wholly investigated to gain the required level of understanding. Only then can the system be transposed to a simulation platform to provide an accurate digital representation. The system investigation process is split into three main categories, namely: specify the system parameters, conduct the physical investigation, and conduct the digital investigation. These categories are closely related and should be carried out in parallel.

2.2.1. Specify system parameters

As previously mentioned, mining systems are complex and multifaceted [5]–[11]. Specifying the system's parameters pertains to defining the conditions/environment that will be investigated, such as the boundary conditions, required input parameters, and desired output parameters. This ensures that only the necessary components are identified to simplify the next two steps [3], [9], [10], [22], [54], [55].

A mine dewatering system is grouped into surface and underground systems. The following components and services are on the surface [4], [9]–[11]:

- Service/chilled water supply: Service/chilled water is typically supplied by a surface refrigeration system. Hot water from underground is cooled and sent underground for the different services before being dewatered.
- Potable water supply: Potable water is usually supplied by the local municipality.
- Hot dam(s): The hot dam(s) is the surface outlet of the underground dewatering system.

The underground components are as follows [4], [9]–[11]:

- Dams.
- Spindle pumps.
- Dewatering pumps.
- Annex and drain holes.
- Water pipes and valves.
- Water drains.
- Settlers.

More information pertaining to the underground components can be found in Appendix A: Dewatering System Components Breakdown.

Figure 11 illustrates an example of specified parameters pertaining to a mine. The information is initially gathered from the mine's planning and engineering personnel. As the physical and

digital investigation phases are carried out, the specifications become more detailed and representative of the real-life system.

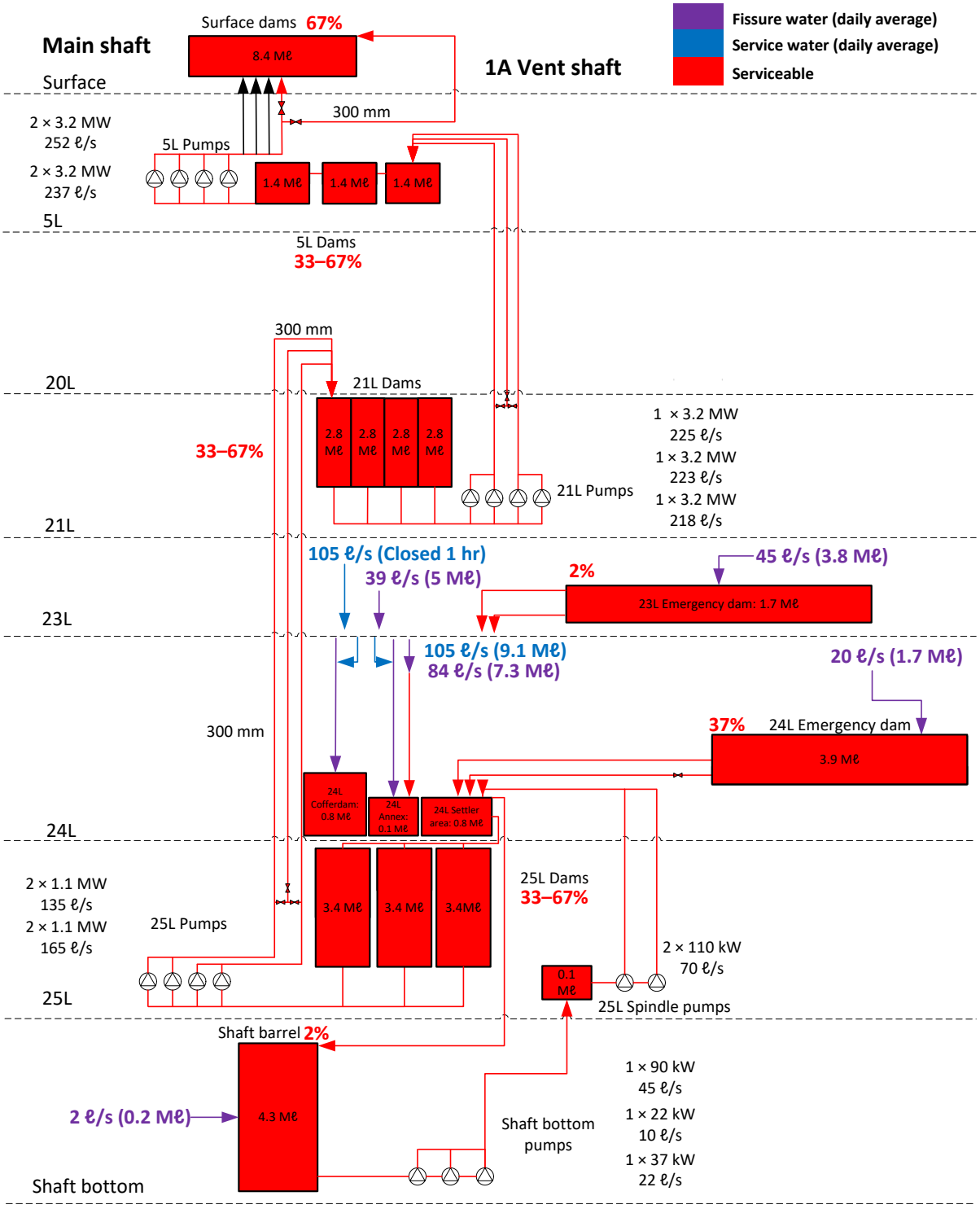

Figure 11: Specified parameters of a mine

From Figure 11, the following parameters were defined:

- Three lift stages (dewatering levels), each with four dewatering pumps located at the base of clear water dams.
- All the dam capacities are of voids that are available for use at all times.
- The shaft bottom pumps and the spindle pumps on 25L aid the dewatering of shaft bottom.
- Service water and potable water are grouped together and labelled ‘service water’ in this instance.
- Only 24L has settlers.
- The service water flow rate has been allocated below all of the working levels; i.e. starting from 23L as this is the first level where all the water arrives after it has been used.
- The fissure water flow rate is distributed according to the fissure water sources underground.
- The water flow rates are illustrated as daily averages.
- The dam levels on the dewatering levels (5L, 21L, 25L) are not to exceed 67% or go below 33% during operation.
- The surface dam is the outlet boundary condition.

2.2.2. Conduct physical investigation

Once the system parameters have been specified, a physical investigation can be conducted on the identified components. The physical investigation requires that the actual layout and components of the dewatering system be investigated [9], [10], [22]. Physically investigating the system confirms that empirical data and information are collected, which ensures that the simulation represents the real-life system [9], [10], [22], [55]. The exact location, layout, elevation, and specifications of the equipment are imperative to ensure the simulation’s accuracy. The observations and measurements made during this phase further allow for the design parameters to be verified.

The details regarding the specifications of the components in the system can be obtained by consulting the manufacturers of the equipment and the mine's planning office personnel. It is, however, important to note that drawings and information gathered can be outdated or untrue due to the ever-changing mining environment. Physical verifications, in the form of audits, should always be performed [22]. A detailed underground audit is defined in Appendix B: Detailed Underground Audit.

A physical investigation allows for the defined parameters to be verified and challenged. If observations and measurements made during the physical investigation challenge the defined system parameters, these need to be re-evaluated and redefined to ensure the system will be modelled correctly.

2.2.3. Conduct digital investigation

A detailed digital investigation of the system is required in conjunction with the first two processes [22]. Most mines have SCADA systems that log and monitor measured apparatus in the mining system [9], [10], [22]. The data obtained from investigating the SCADA system will be used to calibrate the simulation. A detailed SCADA data extraction procedure is defined in Appendix C: SCADA Data Extraction Process.

This, once again, ensures that empirical data is used and not design specifications so that the real-world system can be mimicked in the simulation environment. Studies, including [9], [10], [17], [22], [38], [46], [54], [55], all used historically measured data for simulation calibration, and Visagie [22] attributed an increased simulation accuracy as a result thereof.

The digital data required is as follows:

- Service water flow rate.
- Potable water flow rate.
- Total dewatering flow rate.
- Pump power or amperage.
- Number of columns used for dewatering pumping.
- Dam levels.

The extracted SCADA data further provides the foundation for a dynamic simulation. The dynamic profiles of aspects such as water flow rates and dam levels are used as input functions for the model. Figure 12 illustrates the graphical representation of SCADA data for a column's water flow rate.

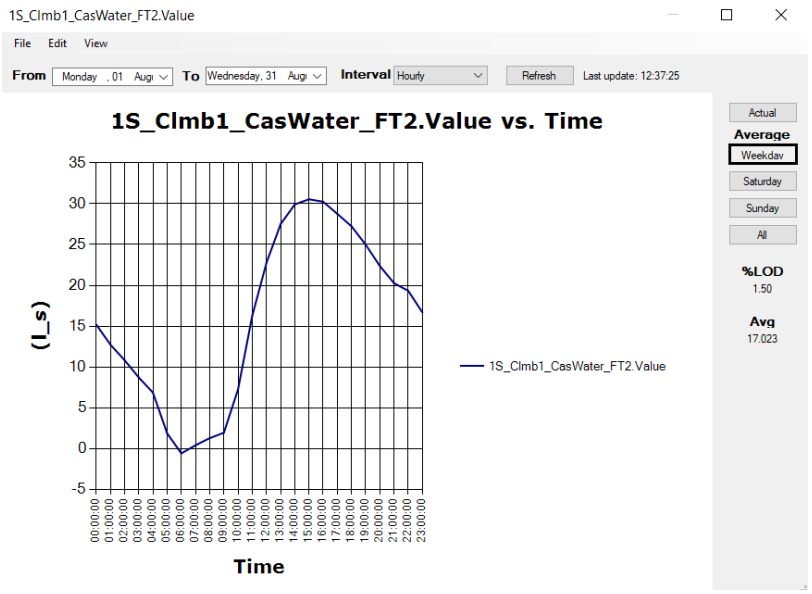

Figure 12: SCADA data for water flow rate

Data loss and quality are limiting factors of the SCADA system and may negatively affect the simulation's accuracy. Visagie [22] attributed the following factors to data loss and quality:

- Abnormal data readings.
- Damaged measuring equipment.
- Unit of measurement conversion errors.
- The methods used to collect and store data.
- Traceability associated with the measurement sources.

The required data can be acquired through manual measurements if the data has been lost or is defective. Hence, the physical and digital investigations should occur concurrently and should supplement the process of specifying the system's parameters. The manual measurements can be used to supplement missing data and to verify the logged SCADA data. Several studies used manual data acquisitions to supplement missing data, verify existing

data, and calibrate simulations [9], [10], [22], [39]–[41], [43]–[45]. In the unlikely event of data being completely unavailable, the model can simulate the missing values as used in [22].

Another crucially important investigation to conduct is a system mass balance [9]–[11]. For this research purpose, all the water entering the system needs to exit the system via dewatering and thus a mass balance will assist in accounting for all the water sources. If any discrepancies are observed, further audits and investigation will be required.

2.3. Baseline simulation calibration

After the investigation phase, a baseline simulation is developed. The baseline simulation represents the mine dewatering system as it operates to date. This serves as the control against which the impact of changes on the system is compared [9], [10], [22].

The model aims to simulate a fully integrated dewatering system and not only specific elements such as dewatering pumps, dam capacities, and water flow rates. This form of simulation has distinct advantages over segregated simulations, namely [55]:

- The impact of changes to an individual component on the entire system can be assessed.
- Multiple changes on various components in the system can be carried out and assessed.
- The platform allows for the system and its performance to be inspected visually, thus integrating numerical solutions with visual illustrations.
- This improves the accuracy and compatibility of the model against real-life performance as the components in the simulation influence one another as in reality.

PTB has the capacity to simulate a fully integrated and dynamic environment accurately based on empirical data as proven by [3], [9], [10], [22], [54], [55]. This capability, supplemented by the information provided in Section 1.4.5, supports the use of PTB as opposed to another simulation platform for the study.

PTB's software is component-based and uses a drag-and-drop interface. The platform allows the user to link components using links or connections through which each component transfers information to the next. Although PTB has a range of categories, only the water category will be explored for the research purpose. Table 3 lists the common components in PTB that will be used in the dewatering simulation models. Mathews' [55] thesis provides additional information on PTB's components for different simulating categories and their breakdowns. Additional information regarding detailed PTB inputs and outputs is provided in Appendix D: Detailed PTB Water Component Inputs and Outputs.

Table 3: PTB dewatering components

Component name	**PTB's component representation**	**Component's detail**
Water node		The point of calculation and measurement for the water network. ($T, p, h, -, -$)
Water pipe		Enables the flow of water between water nodes. ($\dot{m}$)
Water pressure boundary		Acts as a control volume boundary. ($T, p, -, -$)
Water pump	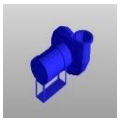	Increases the potential energy and pressure of water. ($\dot{m}, P, p, -, -$)
Water dam		Water storage. ($m^3, \Delta h, -$)
Controller		Takes an input and outputs a control variable to reach a user-specified set point.

2.3.1. The basic cycle

A structured and planned combination of the components identified above can provide a configuration to a system that represents a mine dewatering system – keeping in mind that each mine has a unique system. The system is built sequentially in PTB, starting with the basic cycle and then adding increasing levels of detail specific to the system in question. This process occurs concurrently with the calibration and verification processes to ensure the end product is an accurate representation of the actual system in question.

Figure 13 illustrates a simple water pipe connection configuration in PTB. Different valve configurations can also be specified. The image depicts a butterfly valve on the bottom pipe, a check valve on the left-most pipe, and no valve on the right-most pipe.

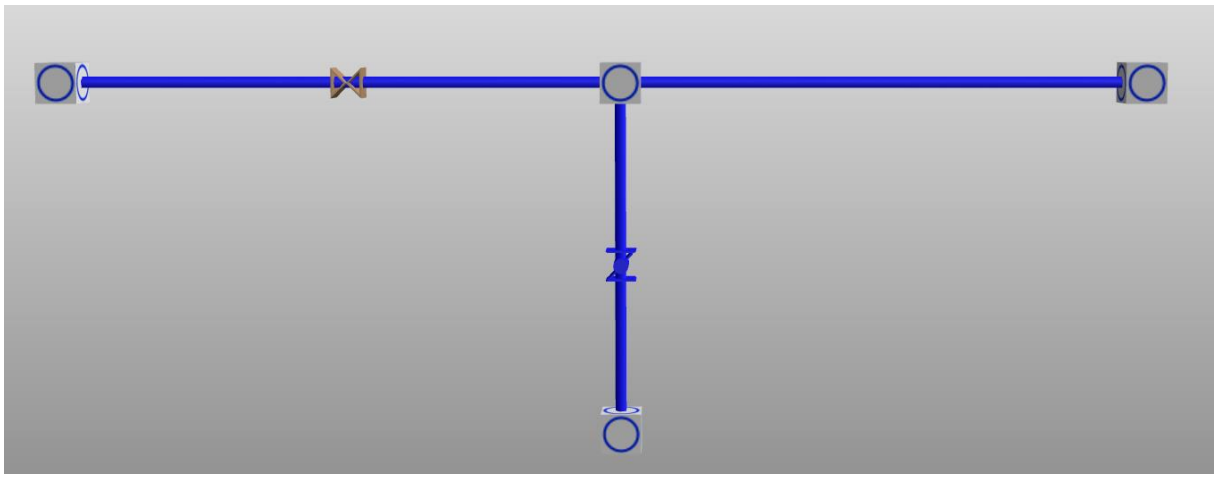

Figure 13: Basic water pipe – water node connection

The following steps were followed in specifying and linking the components:

1. Drag-and-drop the components to the desired locations.
2. Double-click on the components to specify their parameters individually.
3. Link the components: Right-click on a component and drag the cursor to the component it should be linked to.

Specifying and linking different components, as done in Figure 13, can be applied to a larger system. A simplified controlled pumping system is illustrated in Figure 14. A proportional-integral (PI) controller is used to control the water mass flow through a pipe from a boundary source to a dam. Thereafter, the step controller controls a calibrated pump to keep the dam's level between a defined interval (40–80%, for example). The water is pumped to an outlet boundary condition.

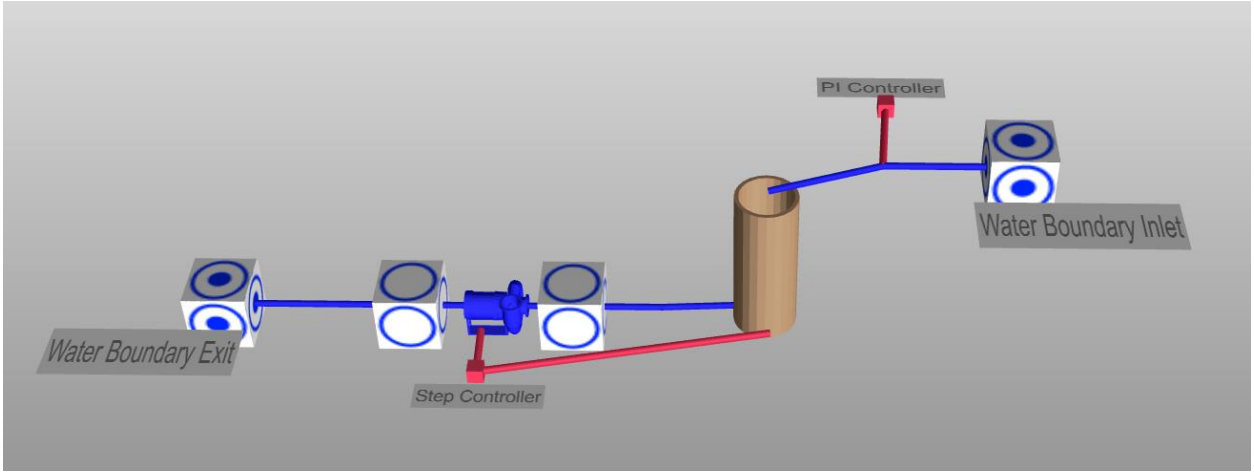

Figure 14: Controlled pumping system

A similar approach – illustrated in Figure 13 and Figure 14 – can be implemented on a larger scale. Figure 15 illustrates the component configuration for a basic mine dewatering system. In the figure, a single water mass flow, calibrated to account for all the water in the system, is configured to flow into two of the six available settlers. Thereafter, the water flows through the settlers and into two of the three available dams from where it is pumped to surface. The surface conditions are defined through a water pressure boundary component.

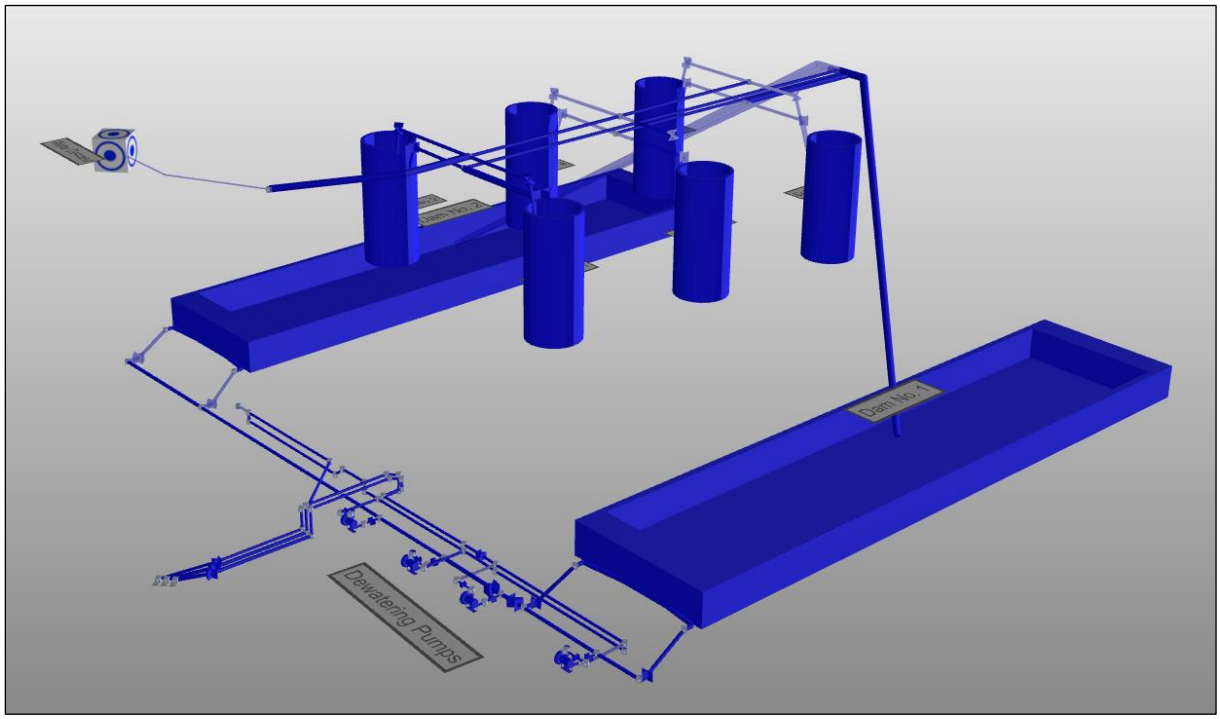

Figure 15: Basic dewatering configuration in PTB

The model simulated in Figure 15 only accounts for a high-level mine dewatering system and is therefore vastly simplified. However, a basic calibrated model does provide an adequate foundation upon which the complexity can be improved. The level of complexity increases during the calibration and verification processes during which the boundary conditions and simulating environment are expanded to wholly account for the real-life system.

Complexity is increased by evolving the model to entail more detailed configurations of the system's components and adding them to the basic model. For example, distributing the water mass flows into the respective sections/levels; controlling pumps and valves as they are controlled in reality; and adding dynamic boundaries to the system.

A more detailed breakdown of the components and the respective PTB interface is provided in Appendix D: Detailed PTB Water Component Inputs and Outputs.

2.3.2. Simulation calibration

The calibration process is adapted from [9], [10], [22], [55] and comprise the following steps:

1. Calibrate: Start by calibrating components individually according to the data obtained in the system investigation.
2. Achieve steady state: Ensure the simulation solver converges.
3. Ensure accuracy: The calibration accuracy need to be within a specified target.
    a. For this study, the target is 5%.
    b. Mathews deemed 5% simulation accuracy as sufficient as instrumentation and measurement accuracy can deviate by as much as 5% [55].
4. Increase complexity: Introduce more components to the system and then restart the process until the model accurately represents the real-life system.

The process, depicted in Figure 16, is iterative and occurs concurrently with the basic cycle development and verification processes. The defined system parameters also affect this cycle as it outlines the boundaries in which the cycle needs to be developed.

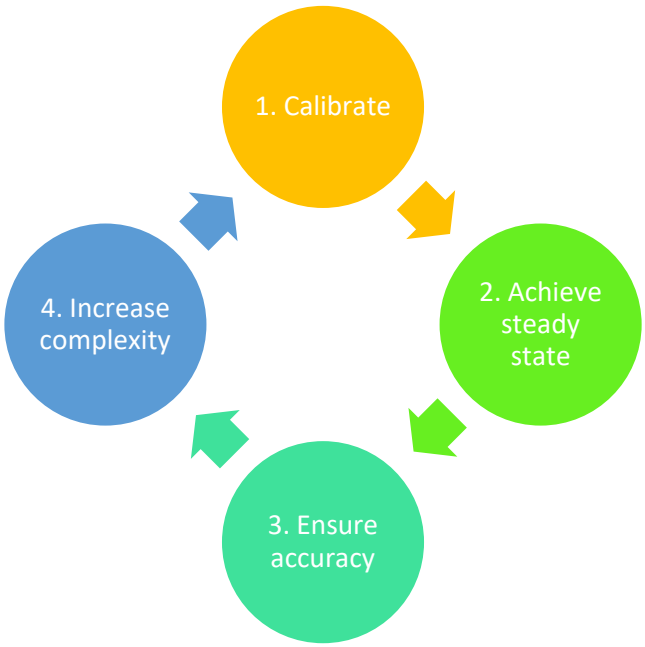

Figure 16: Calibration cycle

The data acquired during the system investigation phase is used to calibrate the components, for example: water mass flows are used to calibrate the flow through a pipe section, and pumping specs and tests are used to calibrate the pump. An average day's data is used as the

input data. The data should ideally represent a day during which no data loss or unusual events occurred. This data is used to reduce the error of the simulation's output.

Table 4 identifies the components that do not require calibration. However, their input data still needs to be a realistic representation of the system to ensure simulation accuracy.

Table 4: PTB components that do not require calibration

PTB component	Use	Important input parameters
Water pipe	Represents the system's pipeline system	• Pipe size • Valve size
Water node	Represents the system's pipeline system	• Elevation (coordinate)
Water dam	Represents the system's water storage capacities	• Elevation (coordinate) • Top elevation (ΔZ) • Volume
Water pressure boundary	Represents the system's defined boundaries	• Temperature • Pressure

Water pump configuration and calibration

The pump specification sheet that includes the pump's curve is used to calibrate the water pump. If this is information is unavailable, SCADA data, manual measurements – taken from ultrasonic flow meter readings – and pump performance plates are used. A mine's pump chamber usually consists of multiple pumps, each with multiple stages, configured in series or parallel. The objective is to model the entire pump system while systematically increasing complexity and maintaining the boundary conditions.

Figure 17 illustrates a parallel pump configuration in PTB commonly found in a mining pump chamber. The water nodes and water pipes are used to connect the pumps to one another, to the dam(s) (which in this case is the inlet boundary), and to the outlet boundary.

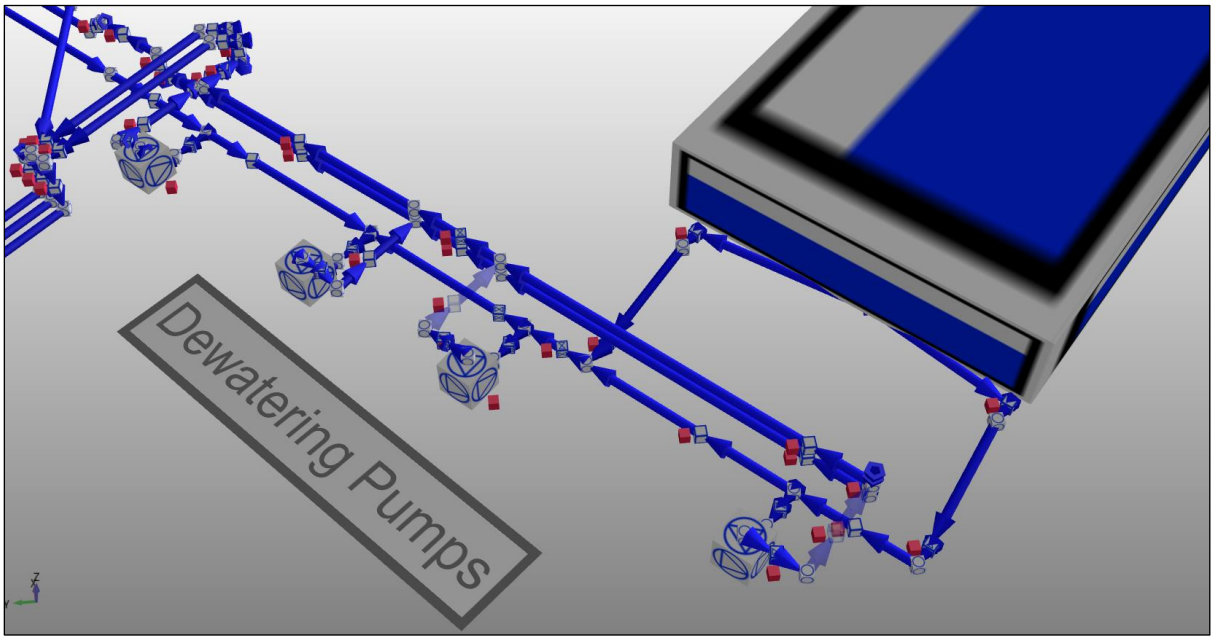

Figure 17: Parallel pump configuration

The calibration process of a water pump can be time-consuming when ensuring that a verified simulation is developed. Table 5 summarises the calibration process.

Table 5: Water pump calibration approach

Step	Description	Comments
1	Separate each water pump into isolated systems.	
2	Use water pressure boundaries for the inlet and outlet conditions of each system.	Obtain from SCADA or measured data.
3	Calibrate each pump individually.	Focus on water flow, pressures, and power.
4	Add pumps sequentially to an isolated system.	Pump performance is affected by series/parallel configurations. This needs to be addressed sequentially in an isolated system.
5	Ensure the end product system is calibrated.	Include the pump scheduling (on/off) for the dewatering system and ensure everything works accordingly.

Controller calibration

PI controllers and step controllers are used to calibrate the remaining functions of the system, such as pressures, flow rates, schedules, and dam levels. The input values for these controllers are initially estimated and then adjusted through iteration. Typical issues that arise with calibrating controllers are their output responses. Figure 18 depicts a sluggish reaction to the system inputs. This can be caused by a PI controller's integral gain being too low or a step controller's boundary conditions being too far apart. Figure 19 depicts an output with too many oscillations and that never reaches a steady state. This can be caused by a PI controller's integral gain being too high or a step controller's boundary conditions being unobtainable for the defined inputs.

Adjustments are made based on the calculated outputs and the respective errors calculated in the verification process. For example, a PI controller's integral gain or a step controller's boundary conditions are adjusted in varying intervals until the desired output is achieved. The iterative cycle is carried out until the desired simulation error boundary is met.

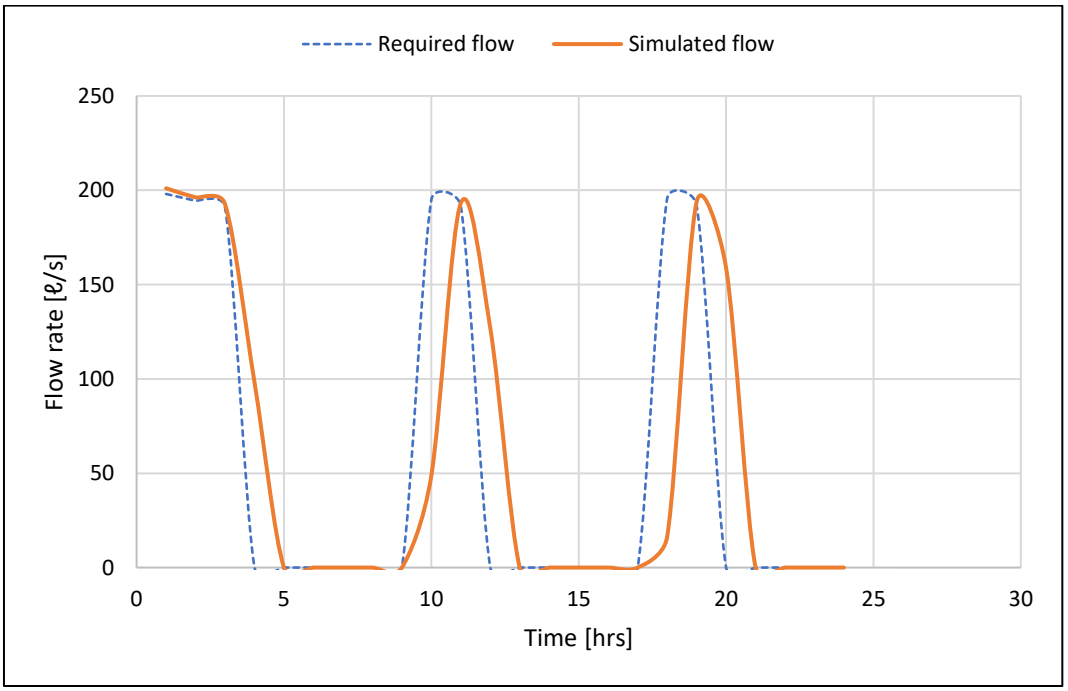

Figure 18: Step controller's water flow rate output with a sluggish reaction

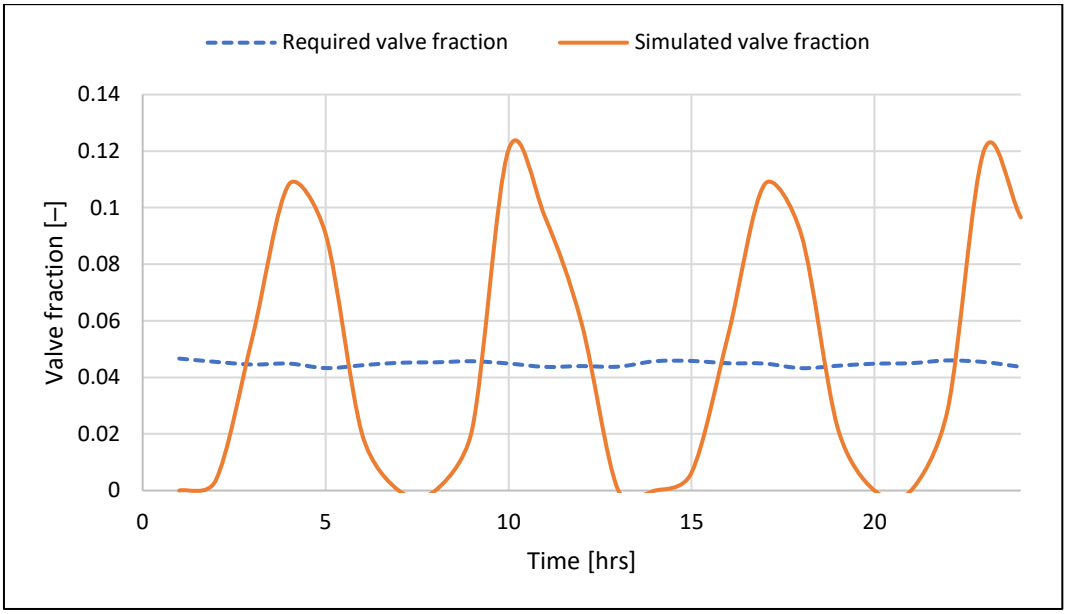

Figure 19: PI controller's valve fraction output with too many oscillations

Full cycle configuration and calibration

Calibrating a full system can become extremely time-consuming as changes made on one component can affect the entire system. Therefore, isolating and calibrating components allow for issues to be identified and rectified in smaller systems, which ease the simulation process. Once the major individual components have been calibrated, they are incorporated into the full cycle configuration as depicted in Figure 20.

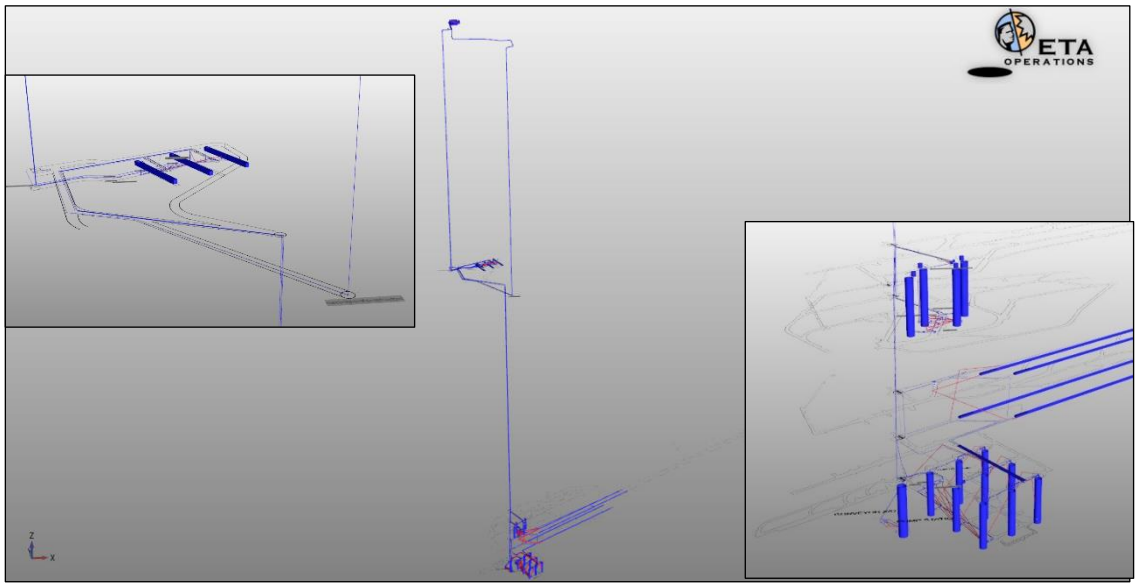

Figure 20: Fully integrated dewatering simulation model in PTB

It is important to note that this does not ensure the full cycle is entirely calibrated. Table 6 summarises the proposed strategy for achieving a fully integrated and calibrated simulation.

Table 6: Full cycle calibration approach

Step	Description	Comments
1	Systematically add complexity to the basic cycle.	
2	Start with the water pressure boundaries.	Ensure that the boundary conditions are defined accurately.
3	Add the pipe layout.	Ensure that this accurately represents the real-life pipe system.
4	Add all the water storage capacities.	Ensure that this accurately represents the real-life water storage capacities.
5	Add the water pumps.	Ensure that all the outputs remain similar to the isolated system. If not, do a thorough investigation of the component's calibration.
6	Add the controllers.	Ensure that all the outputs remain similar to the isolated system. If not, do a thorough investigation of the component's calibration.

For additional information on the individual components, refer to Appendix D: Detailed PTB Water Component Inputs and Outputs. This section defines the important input parameters for the components as obtained during the system investigation.

2.3.3. Simulation verification

The objective of the verification step is to confirm whether the outputs of the simulation match that of the actual data [9], [10], [22], [55]. Three verification methods were identified in literature, namely: mean absolute error (MAE), the mean square error (MSE), and the coefficient of determination. The error limits applicable to each method are highlighted in Table 7.

Table 7: Verification methods' error limits defined by Visagie [22]

Verification method	Error limit
MAE	$Error_{\%} < 5$
MSE	$MSE < 1.7e^{-3}$
Coefficient of determination	$r^2 < 0.95$

In keeping with the calibration limit identified by Mathews [55] in Section 2.3.2 above, the MAE method will be used in this study with the formula defined as follows [22], [55]:

Equation 1

$$Error_{\%} = \frac{1}{N}\sum_{n}^{N} |A_n - S_n|$$

Where:

- $Error_{\%} =$ Mean absolute error [%]
- $N =$ Total number of timestamps in the simulated period
- $A =$ Actual value at timestamp
- $n =$ Timestamp
- $S =$ Simulated value at timestamp

A verified simulation provides assurance that the components were calibrated correctly and that the simulation is representative of the real-life system. In this case, the simulation model will be at least 95% accurate.

The PTB platform is designed to begin at initial (non-operational) conditions that, based on the calibration characteristics, reach steady-state (operational) conditions [55]. It is imperative that the simulation reaches steady state within the defined time [55]. The final steady-state outputs of the simulation are verified in tabular format to compare the simulated and actual results [55]. Verifying these results ensures that the system is operating correctly as a whole [55].

The performance results and dynamic conditions are, on the other hand, compared by plotting the simulated results and the actual results on the same axis. This allows for dynamic verification to be conducted, which ensures that individual components are operating correctly and the model is accurately simulating a dynamic environment [55].

The MAE method, therefore, is applied to the outputs of different components to indicate the accuracy of the model. The simulation error is calculated for each major component in their isolated systems and in the full cycle configuration. The key parameters that require verification are listed in Table 8.

Table 8: Suggested key parameters to verify

Component	Parameter	Unit
Water pump	Discharge flow rate	[ℓ/s]
Water pipe	Flow rate	[ℓ/s]
Water dam	Level	[%]

A verified simulation is valuable for various operational studies. For the research purpose, however, the verified simulation is used to predict a dewatering system's response to a total power failure.

2.4. Total power failure simulation

Once the model accurately simulates the actual dewatering system, a total power failure needs to be simulated. This is achieved by switching the pumps in the system off and diverting water as accurately as possible. There are emergency procedures that must be followed during a power failure [20] such as making changes to the dewatering system to divert water to and from areas to ensure the safety of mining personnel. These changes include amongst others:

- Manually opening/closing valves.
- Blocking annex holes.
- Closing water doors.

- Removing or adding restrictions to water drains.

An example of a total power failure's effect on a dewatering system is illustrated in Figure 21 and Figure 22. Figure 21 illustrates a simplified dewatering system during normal operating conditions:

- One fissure water and one service water source.
- One dewatering level with four dewatering pumps and three dams.
- Water flow to shaft bottom is prevented by a valve.
- The surface dam is the outlet boundary.

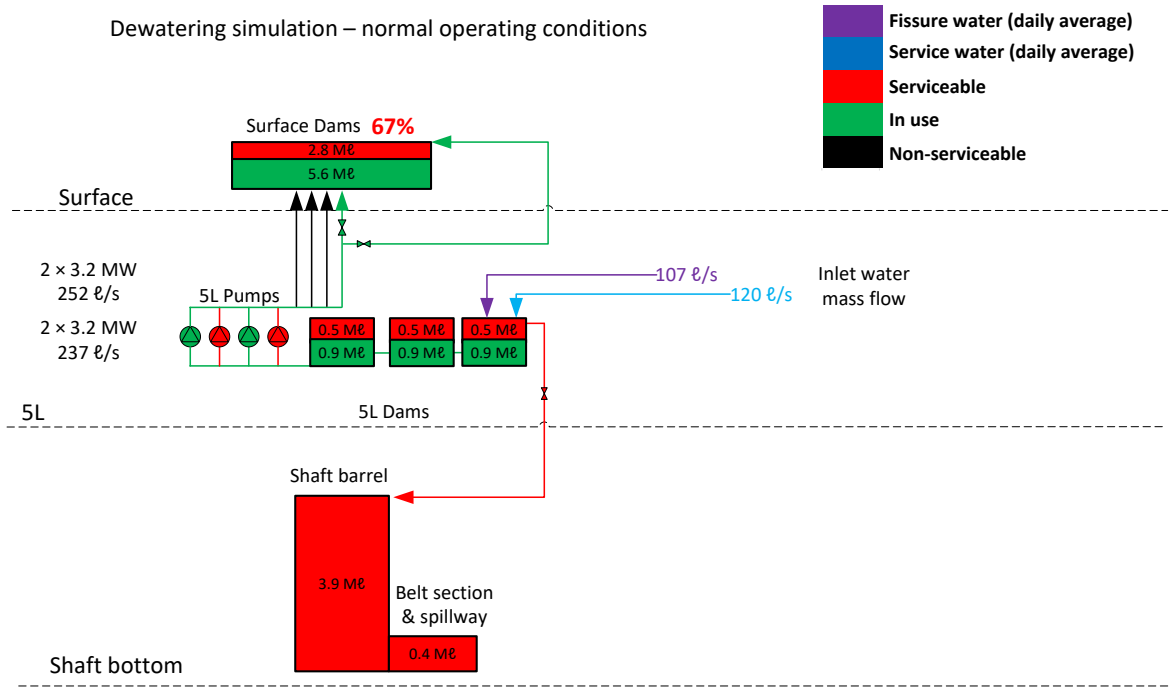

Figure 21: Dewatering system under normal operating conditions

Figure 22 illustrates the same dewatering system as Figure 21 but during a power failure:

- Dewatering pumps are non-operational.
- The valve that allows flow to shaft bottom is opened to prevent 5L's dams flooding.

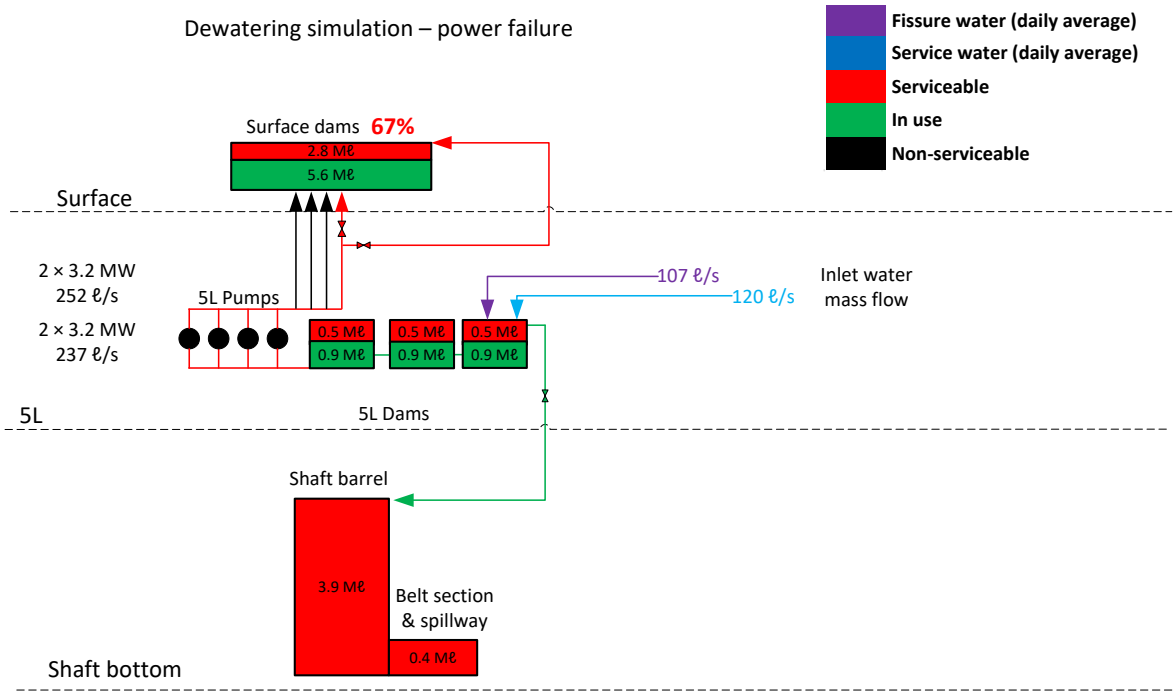

Figure 22: Dewatering system during a power failure

The information required for this process must be kept in mind when conducting the system investigation. It may require a series of simulation verification steps to ensure the model's control components are responding correctly to new criteria based on the mine's emergency procedures.

2.4.1. Validation of results

After the power failure scenario has been simulated and verified, the results must be validated to ascertain whether the system meets the stipulated requirements. Romero et al. [8] suggested that the general guideline for designing underground dewatering dam capacity is that the system should be able to store between 8 and 24 hours of influx without pumping. However, each mine has its own requirements that need to be adhered to, to ensure safety of its personnel.

Once the calibration and verification phases have been completed, the simulation will be at least 95% accurate in imitating the real-world system. Given that, any proposed changes can

be tested in the simulation environment with the premise being that the system's response in the simulation will be within 5% of how the real-world system will respond.

A real-life test is not possible due to the risk it poses to personnel and equipment. The validation of the method is deemed successful if the defined requirement, namely the number of hours before flooding, is met.

2.4.2. Scenario simulations

If the defined requirement is not met, the model can run contingencies. Simulating scenarios is extremely advantageous, as identified in Section 1.4. It is, therefore, a vital aspect of the proposed method. Scenario simulations were heavily supported by [31], [34], [37]–[41], [43]–[46], [48], [50] in that several scenarios can be tried and tested by the model without expenditure and strain on the actual system. Every suggested change to the system is made in the simulation environment and tested to determine its efficacy in meeting the requirement(s). This creates an iterative cycle in the method so the requirement(s) can be met.

A thorough understanding of the system is vital in contingency planning. The proposed changes need to be feasible for the system under investigation otherwise the scenarios will become redundant. Possible changes usually implemented are:

- Opening/closing valves according to new schedules.
- Constructing new pipelines to move water to other areas.
- Closing unused areas to be used for additional water storage.
- Constructing new water storage areas.

2.5. Implementation of changes

Once the proposed change(s) to the system have been proven to meet all the defined requirements, the changes are made to the real-life system. This inevitably changes the baseline system, which needs to be addressed and updated in the simulation model.

This step in the process also accounts for any changes that may have been made to the system while the calibration verification steps were being carried out. The simulation should always reflect the most recent version of the real-life system.

2.6. Conclusion

This chapter presented the steps for developing a dynamic and integrated simulation model of a mine dewatering system. The model can simulate a total power failure and assess the systems response thereto. The platform further provides the opportunity to run contingency planning scenarios (if required) so that the defined requirements can be met.

The key points required to create the simulation model include:

- System investigation: A thorough understanding of the dewatering system needs to be established before that system can be simulated.
- Baseline simulation calibration: A basic simulation model is created to depict the mine dewatering system layout.
- Total power failure simulation: The verified simulation model is used to determine the dewatering system's response to a total power failure.
- Implementation: Any proposed changes identified through the simulation investigations need to be implemented in the real-life system.

The next chapter applies the method to an existing dewatering system to assess its response to a total power failure and discusses the results obtained.

3. RESULTS AND DISCUSSION

3.1. Preamble

This chapter applies the proposed method to a real-world case study. The aim is to test whether the developed simulation-based method can be used in practice and to compare it with the mining industry's existing method. The mine in question is referred to as Mine A. It is situated in South Africa, and is a multishaft medium- to deep-level mining complex. The operation's managing structure has a 48-hour total power failure emergency requirement, which entails that no significant harm should come to personnel or equipment within that period. To address the purpose of the study, this means that no active levels or areas should be filled with water during the 48-hour period.

3.2. Industry method

Mine A conducted a theoretical calculation of their available emergency capacities based on design specifications. Figure 23 illustrates the capacities deemed available during an emergency and the time taken for each capacity to be filled according to a defined flow rate.

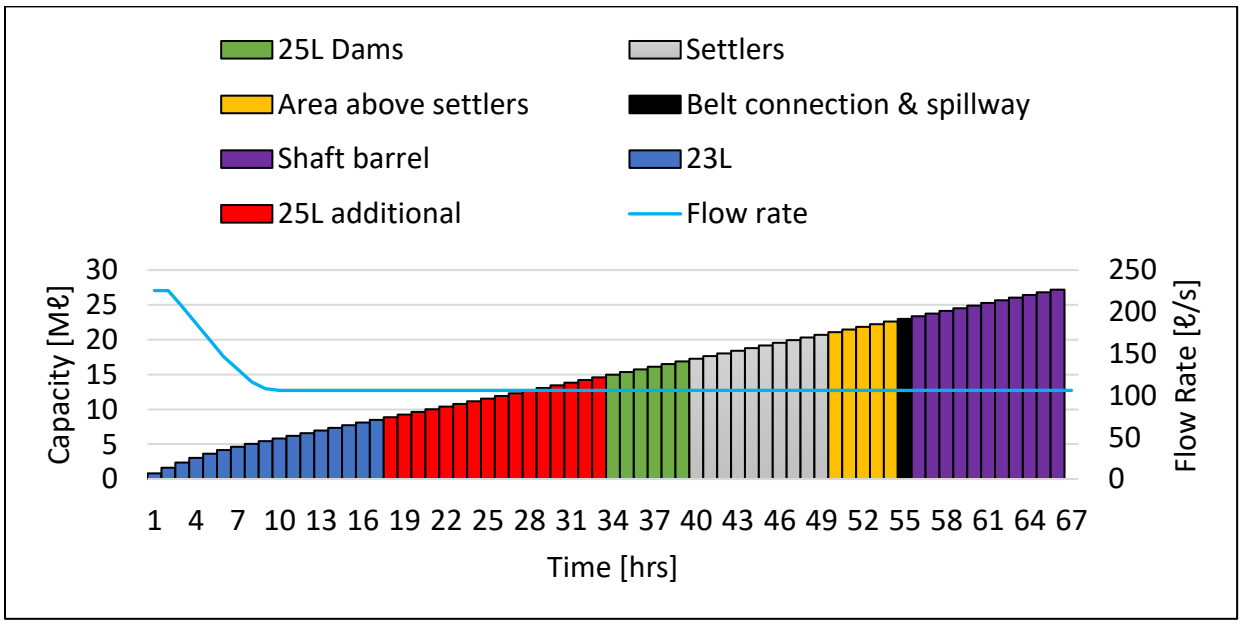

Figure 23: Mine A's theoretical emergency capacity

Table 9 provides more detail regarding the capacities considered during the theoretical calculation carried out by Mine A.

Table 9: Theoretical calculations done by Mine A

Legend on Figure 23	Description	Theoretical capacity [Mℓ]
25L dams	The available capacity of the clear water dams on the lowest level of the mine (excluding shaft bottom).	2.40
Settlers	The six settlers preceding the clear water dams.	3.58
Area above settlers	The area above the settlers that is available to use.	1.98
Belt connection and spillway	The belt connection and spillway are located below 25L and calculated separately to shaft bottom's capacity.	0.47
Shaft barrel	The shaft barrel includes the volume from the footwall of 25L to shaft bottom.	4.35
23L	A void on 23L is available. A wall was built on 23L to close off a haulage that can be used as capacity.	8.75
25L additional	This is the additional volume available on 25L before the pump area is deemed flooded.	6.00
	Total available capacity:	**27.53**

From the results illustrated in Figure 23, the defined requirement of 48 hours is achievable with the final available capacity filling after 67 hours. From the graphical results it is evident that the calculation is a theoretical approximation of the design specifications. However, in reality, the values could differ. The approximation further does not adopt an integrated approach by assuming that the capacities will systematically fill up and the total flow rate will affect each capacity in the same way.

3.3. Proposed method application

3.3.1. System investigation

Mine A's cross-sectional shaft layout is illustrated in Figure 24, which shows that Mine A has two shaft sections, namely a main shaft and a sub-shaft.

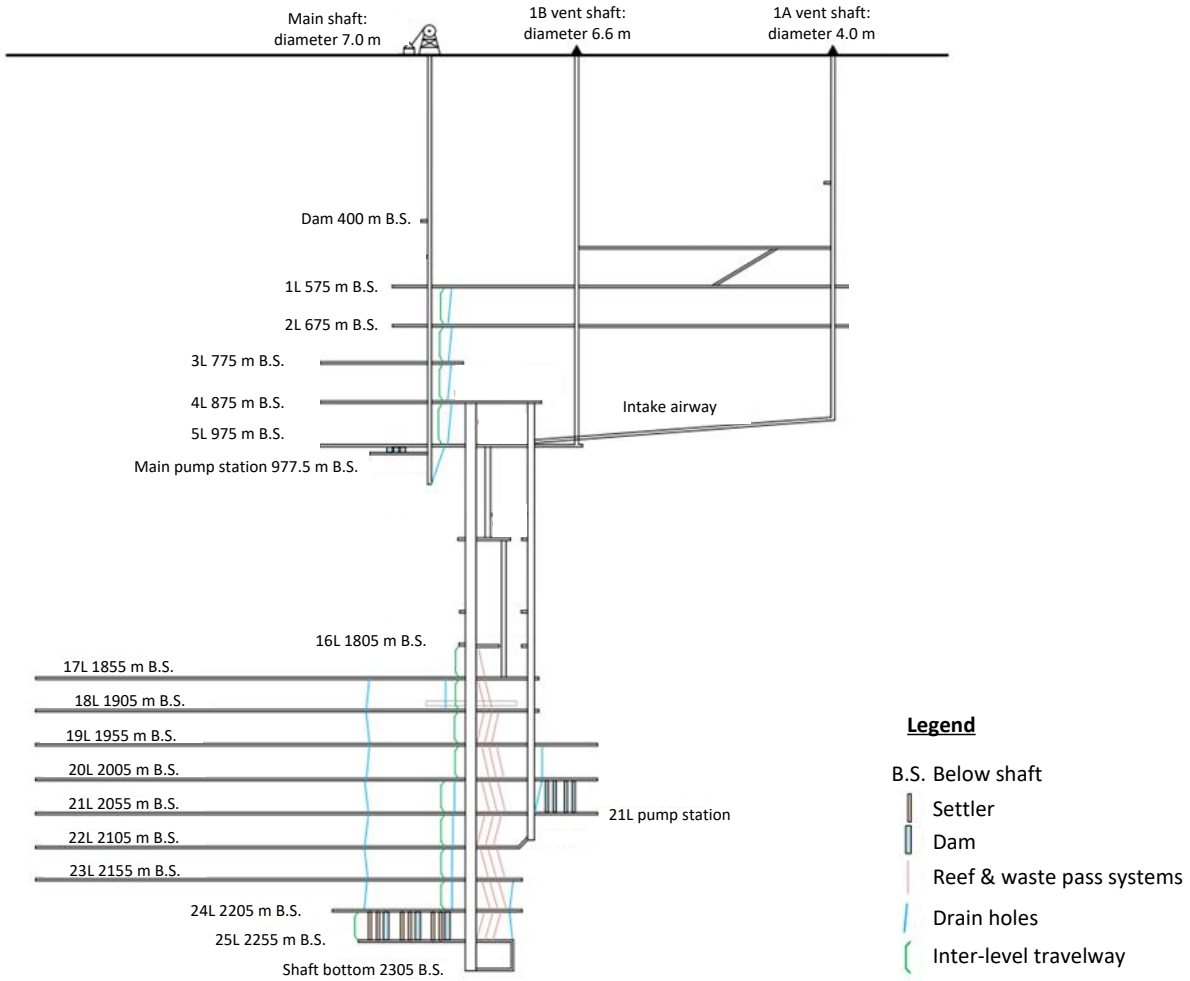

Figure 24: Mine A's shaft cross-section layout

Mine A has potable water that is supplied by the local municipality, service water that is supplied by a surface refrigeration system, and fissure water that is located at different points in the shaft. Water is supplied to three active mining levels (19L, 20L, and 21L) and three auxiliary levels (5L, 24L, and 25L) for the following purposes:

- All levels – drinking (potable water).
- 20L – air cooling units.
- 20L – bulk air coolers.
- Mining levels – mining activities (such as drilling and watering down).

The potable water and service water are supplied from surface via a network of piping and controlled by valves at different points in the respective networks. Once used, the water is

gravity-fed along the haulage and/or pumped by spindle pumps to drain holes so that it can flow down to the settlers.

The depth of the entire shaft section requires three lift stages for dewatering – 25L, 21L, and 5L – where only 24L has settlers. All the water is, therefore, directed to the 24L settlers. Thereafter, the water flows to the 25L dams from where it is pumped first to 21L, then 5L, and finally to surface. Once the water reaches the surface dam, it is processed through the surface fridge plant system, cooled, and then sent underground again. Any excess water on surface is pumped to evaporator dams where it is stored until evaporation occurs.

System parameter specification

Shaft bottom is the lowest point in the shaft. It was used as the first boundary condition moving from bottom to top in the system. Shaft bottom covers the void in the shaft from the footwall of the last pump station until absolute bottom. Three spindle pumps are located at shaft bottom to keep the water level as low as possible. However, one pump was out of order during the investigation.

Shaft bottom has three pumps that pump the water up to a holding dam on 25L before being pumped up to the settler area on 24L. Two spindle pumps are available on 25L for this purpose. The first dewatering lift stage in the shaft is 25L. Three dams and four dewatering pumps manage the water demands. The second lift stage is 21L with four dams and four pumps, and the third stage is 5L with three dams and four pumps. From 5L, the water is pumped to surface where the surface dam is the outlet boundary of the system. As mentioned, the water is either pumped to the evaporator dams or processed through the fridge plant from this point. Since these processes only made the simulation time longer, they were excluded.

The service water is supplied from surface and is a key inlet boundary along with the fissure water. The fissure water sources, along with the component specifications and boundary conditions, were investigated during the physical and digital investigations. The potable water for Mine A was redundant as potable water is consumed underground and does not have a major impact on the dewatering system.

Figure 25 depicts the defined system parameters for Mine A. As previously mentioned, the system parameters were specified concurrently with the physical and digital investigations. The information in Figure 25 is the culmination of a complete, iterated system investigation.

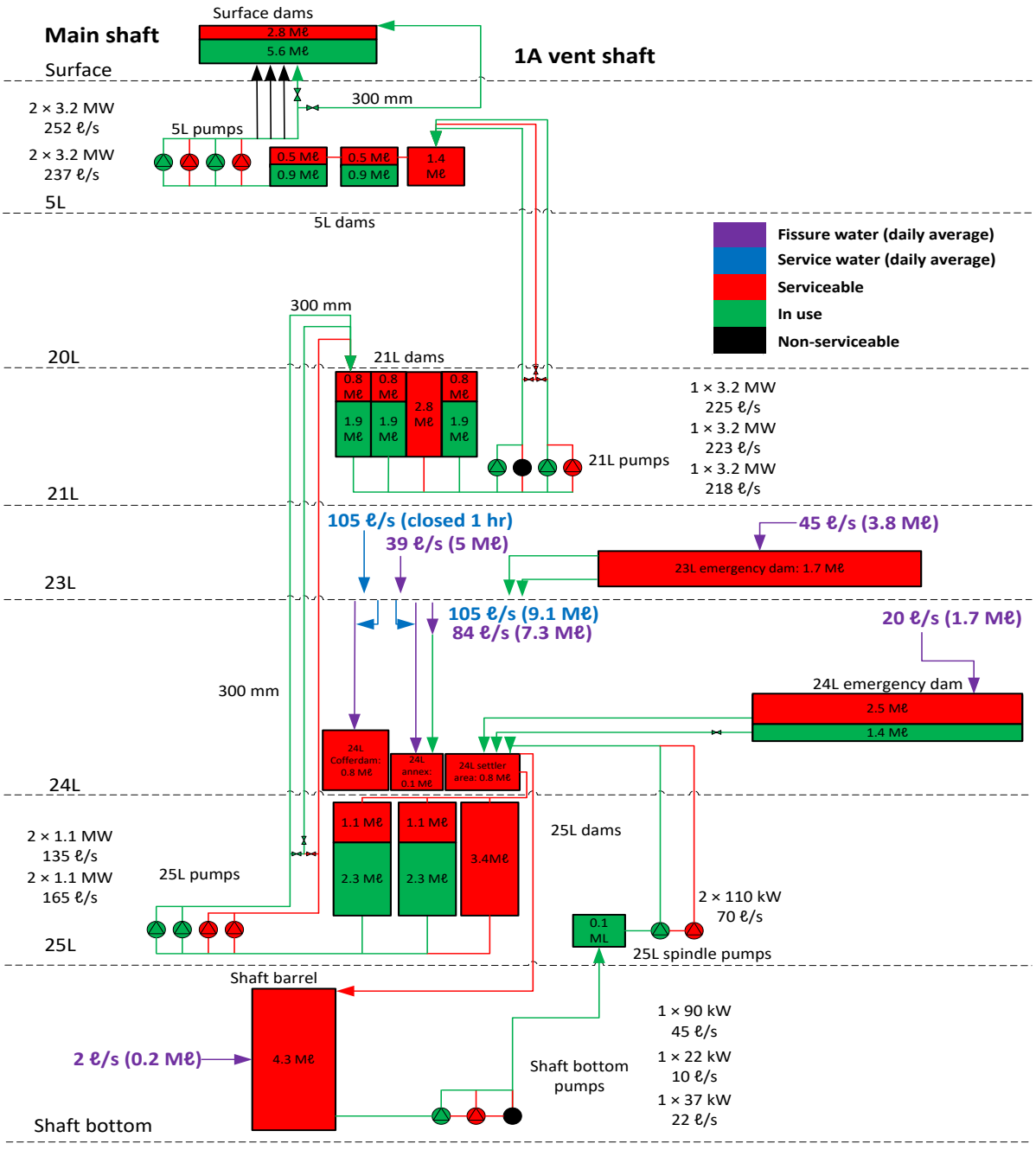

Figure 25: Mine A's defined system parameters

Physical investigation

A detailed underground audit, similar to Appendix B: Detailed Underground Audit, was conducted for the physical investigation. The information gathered was used to update the capacities, pump specifications, and fissure water flow rates in Figure 25 and provided the foundation for the simulation's skeleton. The pipe layouts and distances were noted on the DXF layouts; the column sizes and elevations were measured with a tape measure and laser distance meter; and the valve sizes and positions were observed.

Pump specifications were obtained from the plates on the pumps and tests were conducted to measure each pump's flow rate. An ultrasonic water flow meter was connected to the outlet pipe of a pump at least 2 m from any bends or deviations. The flow meter was configured to store data for one hour while the pump ran to ensure steady state was reached and enough data was obtained. Each pump in the system was tested in this manner and the results were used for calibration.

During the physical investigation, one dam on each dewatering lift stage level was empty and could be measured with a laser distance meter. It was assumed that the remaining dams were similar. A similar approach was taken for the settlers – two settlers were empty. The surface dam, settler area (area above the settlers), 24L cofferdam, 24L annex, and shaft bottom were also measured with a laser distance meter and the capacities were subsequently calculated.

The 23L and 24L emergency dam walls were measured with a laser distance meter, but no entry was permitted behind the wall to measure the available area. Thus, DXF documents were used to determine the dip angle and relative capacity. Due to the dip angle, the haulage capacity could not be calculated as a rectangle but was rather calculated as a triangle. This is illustrated in Figure 26.

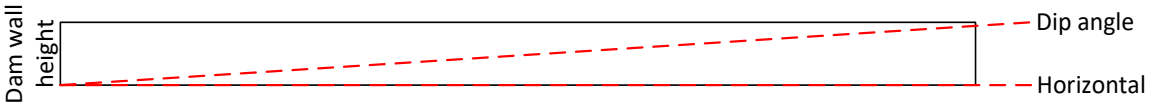

Figure 26: Dip angle effect on haulage capacity calculation

The settler area was also split into three sections due to findings during the physical investigation for the cofferdam, annex, and settlers. This made describing water outlet points and area identification easier on 24L.

Table 10 compares the design dewatering capacities and physically investigated capacities. From this comparison it is evident that physical investigation is a valuable tool for ensuring that the real-life system is replicated accurately.

Table 10: Dewatering capacity comparison

Capacity	Design specification [Mℓ]	Verified capacity [Mℓ]	Difference [ΔMℓ]
5L dams	4.20	4.20	0.00
21L dams	12.80	11.20	−1.60
25L dams	6.00	10.20	4.20
Settlers	3.58	5.10	1.52
Area above settlers	1.98	1.80	−0.18
Shaft bottom	4.82	4.30	−0.28
23L emergency dam	8.75	1.71	7.04
25L additional	6.00	0.00	−6.00
24L emergency dam	0.00	3.90	3.90
24L cofferdam	0.00	0.80	0.80
24L annex	0.00	0.10	0.10

The physical investigation confirmed that all the water is diverted to the 24L settlers before being dewatered through the three lift stages. Therefore, the shaft's total water flow should all be accounted for on 24L. The areas to which the water is diverted on 24L do, however, differ, so a decision was taken to account for the water on 23L first. Although the service water is supplied from surface and used on 19L, 20L and 21L, it gets diverted through a network of drain holes that are linked to 23L. Thus, 23L is the first level where all the service water can be accounted for above 24L.

The fissure water sources are accounted for individually on 23L, 24L and shaft bottom. The fissure water flows into drains from the respective sources where measurements were taken.

A flotation device was placed in the drain and allowed to flow a predefined distance. The time taken for the device to flow along with the area of the drain and the distance travelled were used to calculate the flow rate using Equation 2:

Equation 2

$$Q = \frac{A \times d}{t}$$

Where:

- Q = Volumetric flow rate [m^3/s]
- A = Flow area [m^2]
- d = Distance [m]
- t = time [s]

The physical investigation identified that three dewatering columns on 5L, one pump on 21L, and one pump at shaft bottom were broken and not serviceable. This affected the shaft's redundancy and increased the likelihood of downtime due to equipment breakdowns.

Digital investigation

The following information was available on the SCADA for Mine A's dewatering system:

- Dam levels, per dam, for each lift stage.
- Dewatering flow rate per column on each lift stage.
- Service water flow rate (from surface to underground).

All the relating historical and current data were acquired from the mine's SCADA system through which a few trends were identified:

- The flow and level meters regularly break down.
- Instrumentation is not fixed in a timely manner.
- Data loss is inevitable at some stage.

Mining personnel confirmed that readings may be unreliable due to inadequate maintenance and sensors being tampered with. Figure 27 shows an example of unreliable data as the water flow rate through a dewatering column cannot be negative. Figure 28 shows an example of data loss. In the case of data loss, the respective data points are exported as 'NaN'.

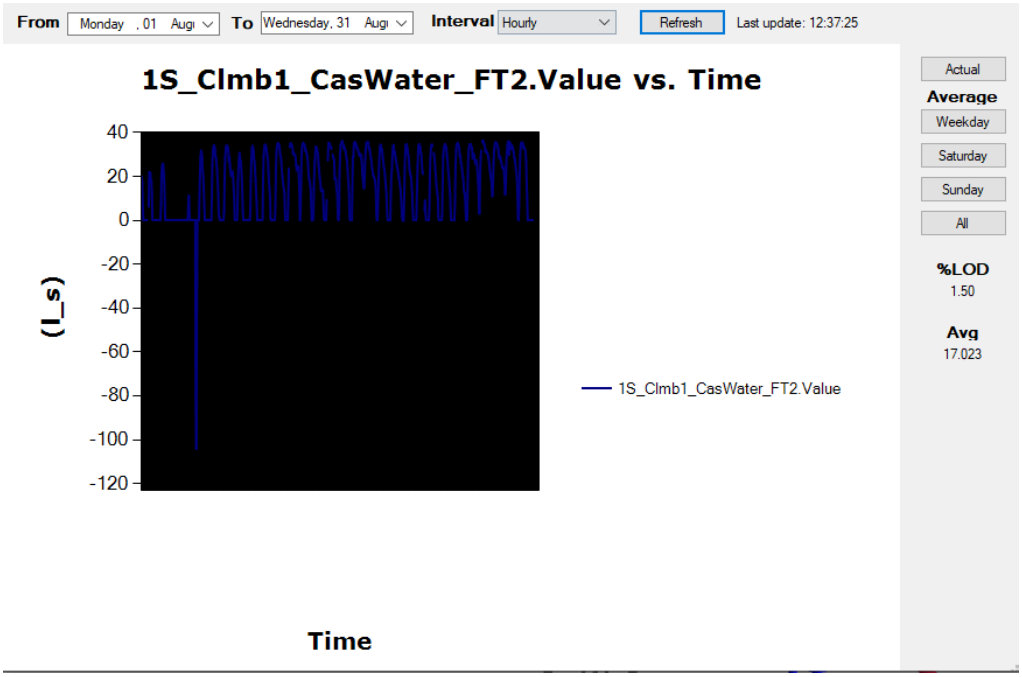

Figure 27: SCADA data extracting with unreliable readings

	A	B	C
1		1S_Clmb1_CasWater_FT2.Value	
2	2022/08/01 00:00	20.08661748	
3	2022/08/01 01:00	16.93068141	
4	2022/08/01 02:00	5.850726153	
5	2022/08/01 03:00	0.095467934	
6	2022/08/01 04:00	0.107461906	
7	2022/08/01 05:00	0.103429052	
8	2022/08/01 06:00	0.087831957	
9	2022/08/01 07:00	0.086108026	
10	2022/08/01 08:00	0.092310017	
11	2022/08/01 09:00	0.123345397	
12	2022/08/01 10:00	0.126521234	
13	2022/08/01 11:00	NaN	
14	2022/08/01 12:00	NaN	
15	2022/08/01 13:00	6.237139449	
16	2022/08/01 14:00	21.99143571	
17	2022/08/01 15:00	21.79748562	
18	2022/08/01 16:00	21.61515939	
19	2022/08/01 17:00	18.24008195	
20	2022/08/01 18:00	17.72682522	
21	2022/08/01 19:00	12.43265652	
22	2022/08/01 20:00	0.533343549	
23	2022/08/01 21:00	0.133807076	
24	2022/08/01 22:00	0.139956221	

Figure 28: Excel export of SCADA data from PTB

This data could not be used to calibrate the simulation as it would affect the accuracy and validity negatively. Therefore, data was extracted from a period that did not present any anomalies. The data from February 2022 was used because it provided a month's worth of data without any anomalies. Furthermore, the daily profiles (of weekdays) were similar, hence a 24-hour averaged profile could be constructed. Figure 29 to Figure 34 graphically illustrate the dam levels and column flow rates for February 2022 on the three lift stage levels over a 24-hour averaged period.

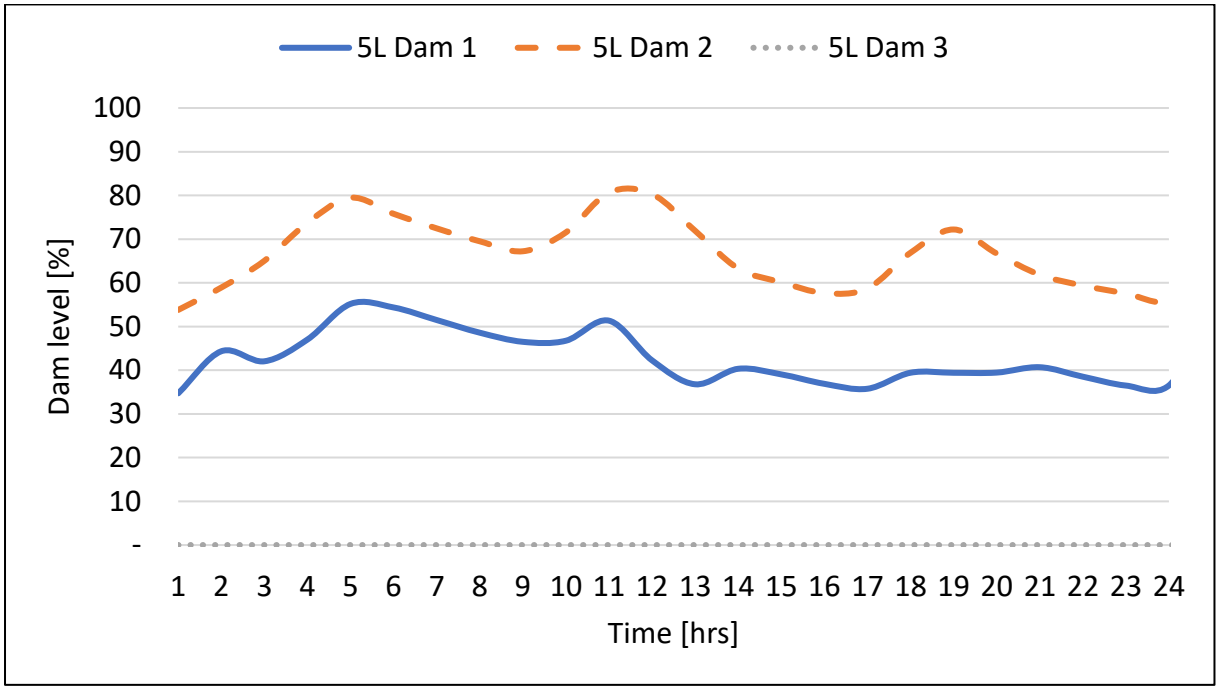

Figure 29: SCADA data for dam levels on 5L

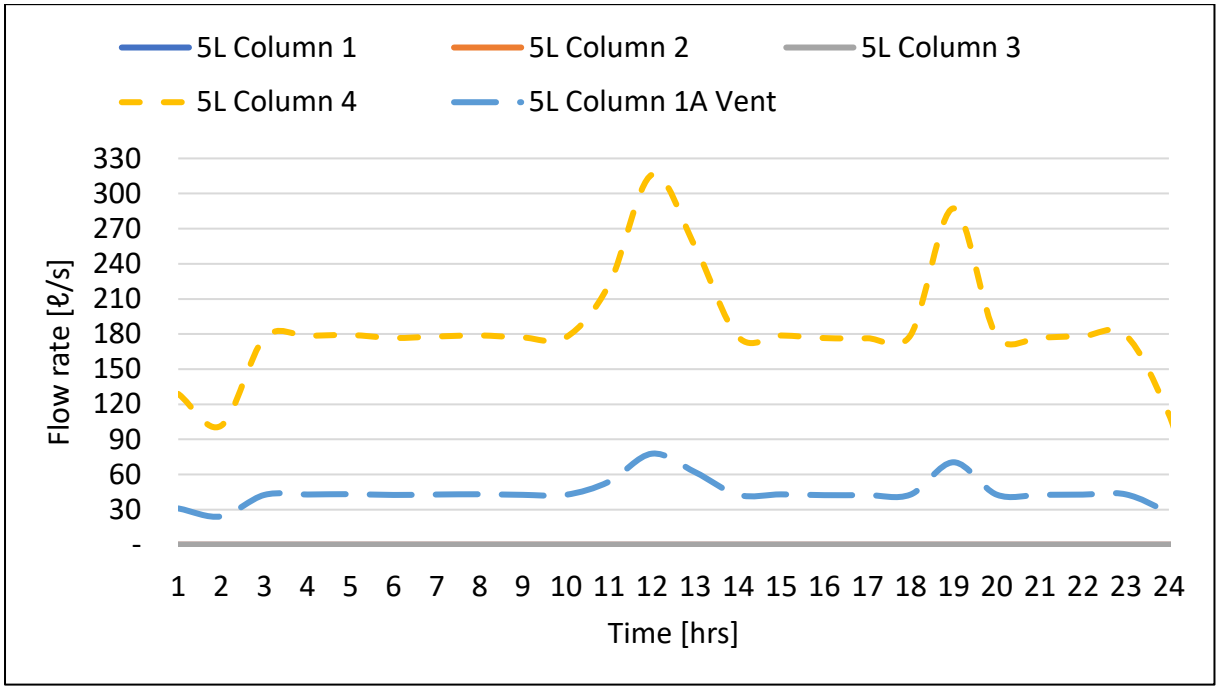

Figure 30: SCADA data for column flow rates on 5L

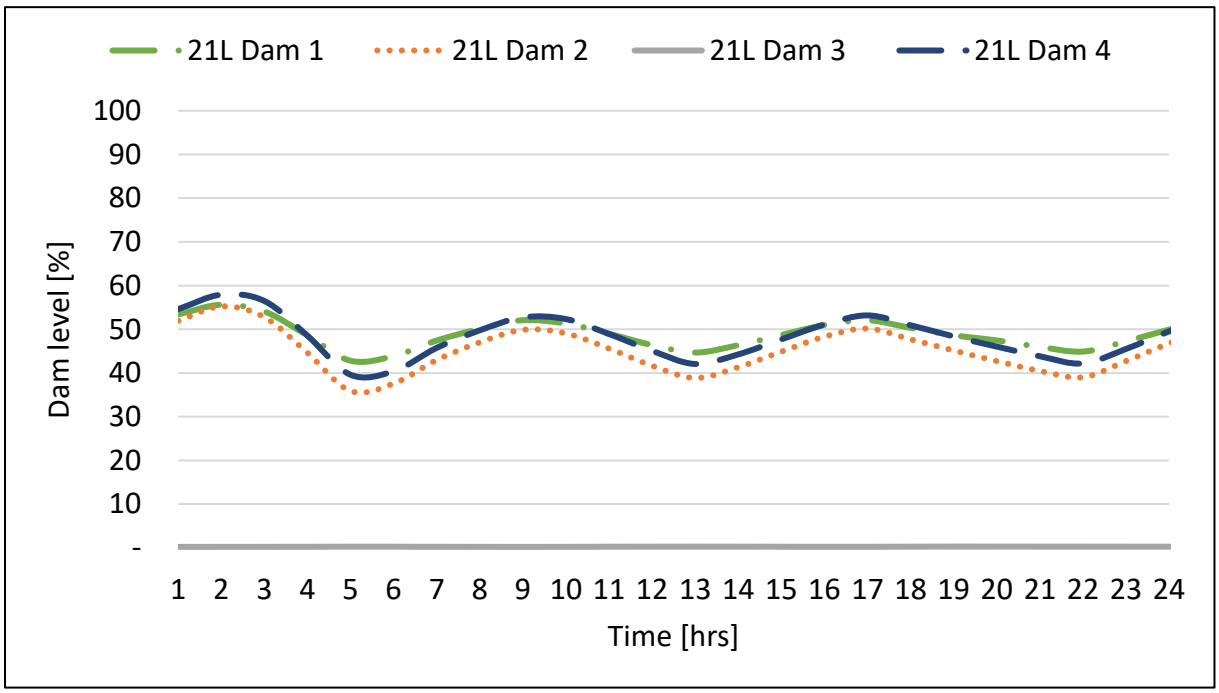

Figure 31: SCADA data for dam levels on 21L

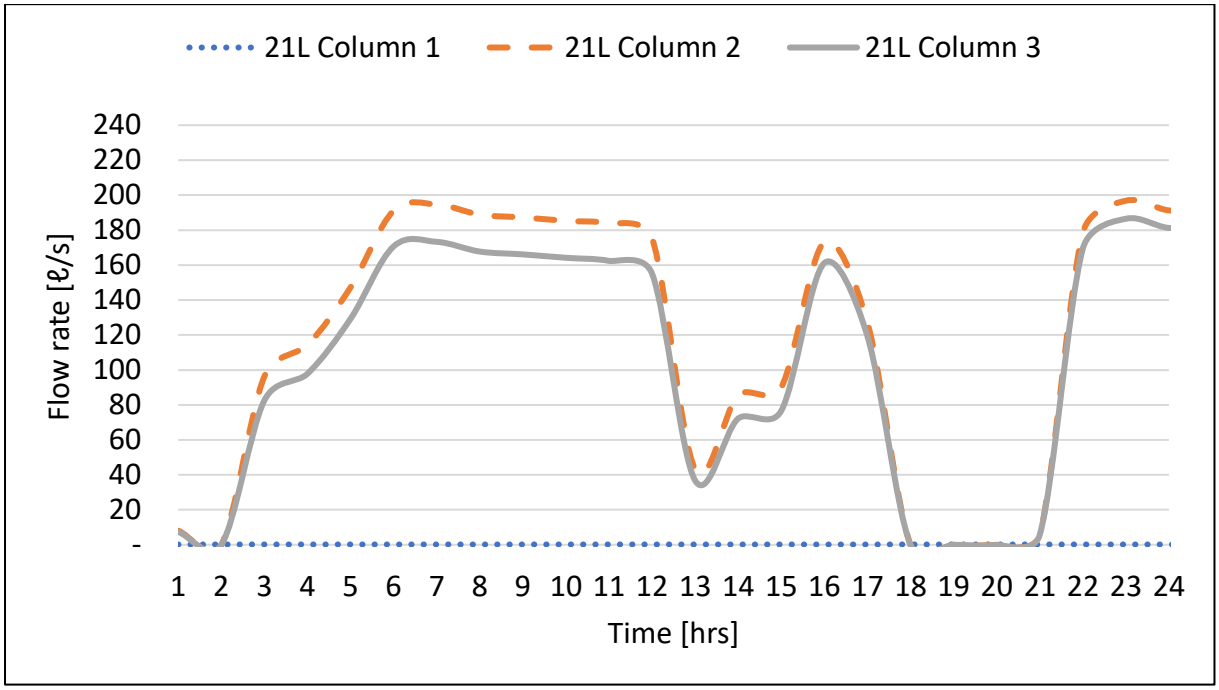

Figure 32: SCADA data for column flow rates on 21L

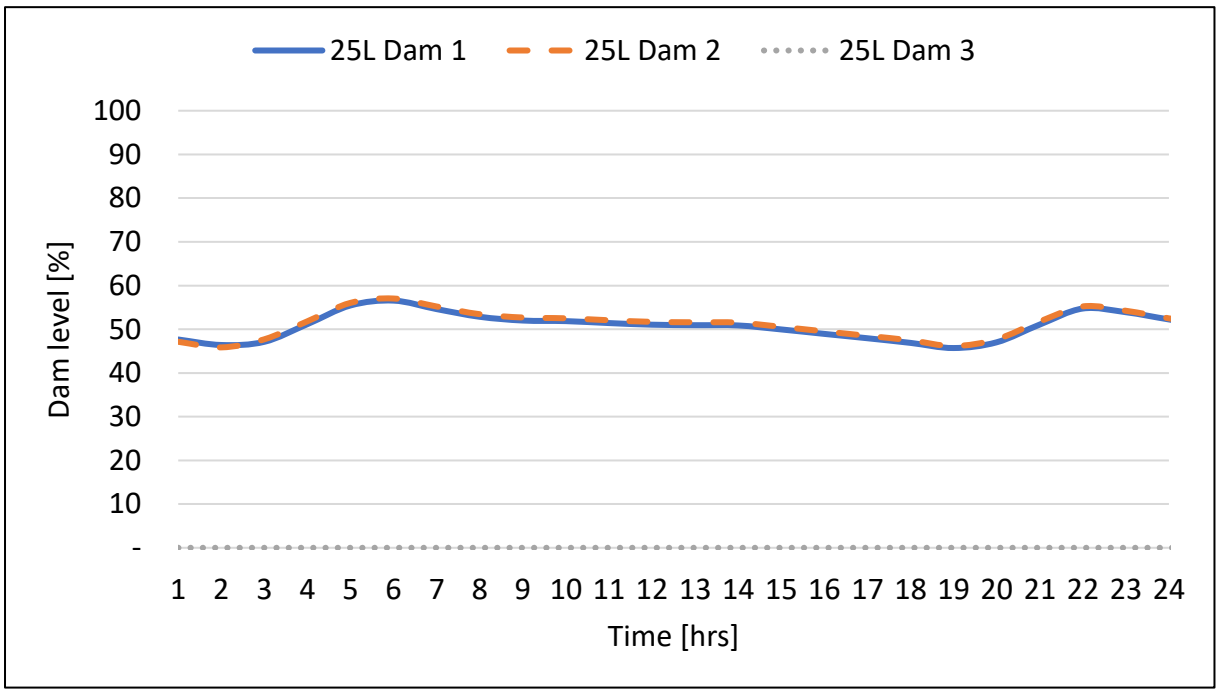

Figure 33: SCADA data for dam levels on 25L

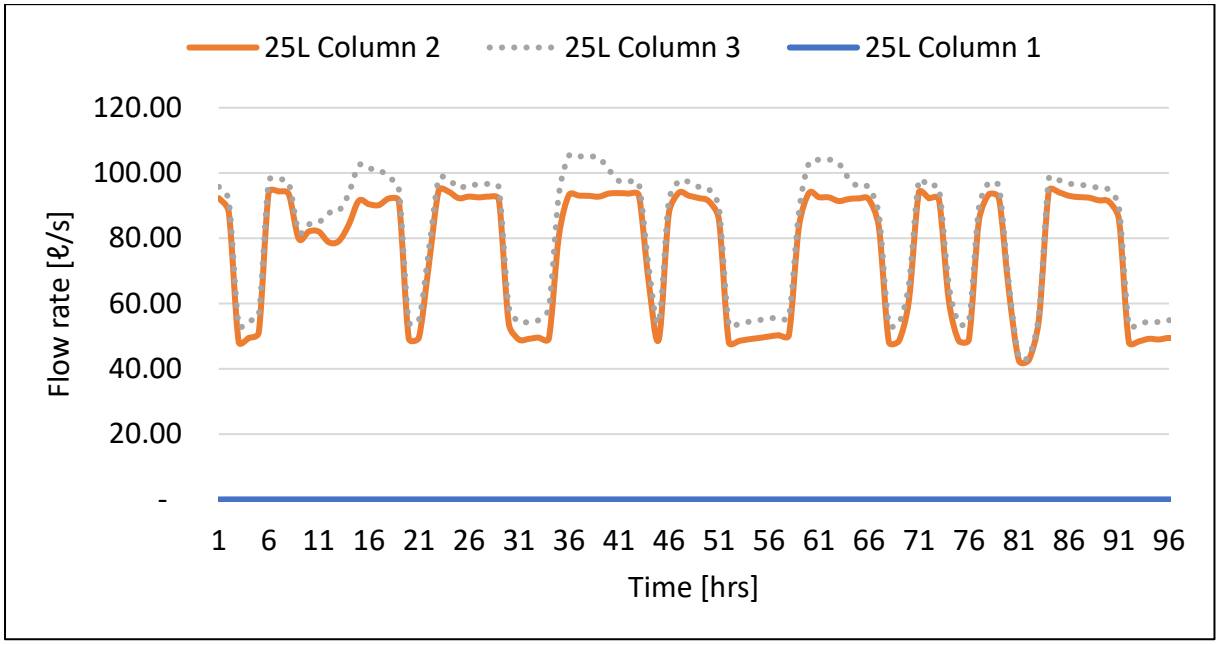

Figure 34: SCADA data for column flow rates on 25L

The SCADA data for the dam levels indicate that only two dams are used per level, leaving the remainder of the dams as extra capacity for emergencies. The data also shows that only two columns are used for dewatering for each level. The physical investigation verified these operating conditions with the findings illustrated in Figure 25.

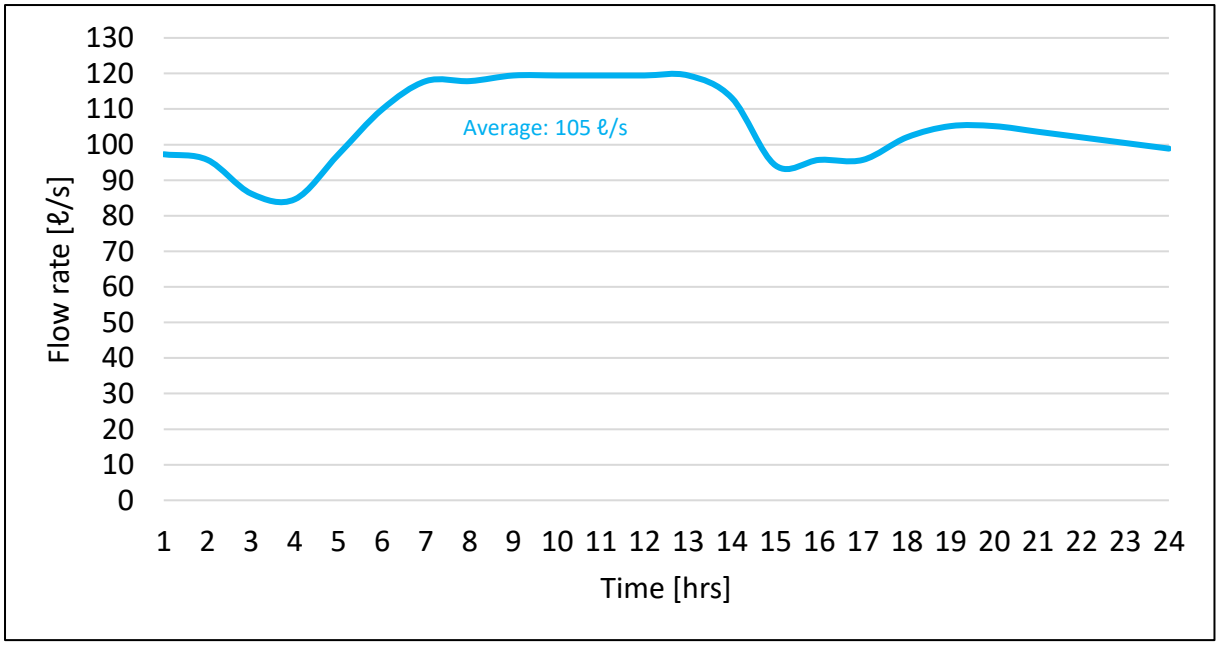

Figure 35: SCADA data for service water flow rate

Figure 35 depicts Mine A's service water flow rate as supplied from surface. The flow meter is positioned on the supply column just before the shaft. The cumulative dewatering flow rate on 25L (Figure 34) was used along with the service water flow rate (Figure 35) to ensure that all the water was accounted for using a mass balance.

Fissure water sources were identified and measured on 23L, 24L and shaft bottom, but the mass balance indicated that an additional 39 ℓ/s needed to be accounted for. This was attributed to the levels above 23L as a singular flow rate as depicted in Figure 11. The fissure water sources were assumed to be linear. Fissure water is dynamic, according to Martínez and Ugorets [46], but their study was conducted over several years and the profile changed according to season. Therefore, the fissure water could be altered according to season in the simulation to reduce the simulation time.

This accounted for all the service water supplied to the shaft. In the next section, the February 2022 SCADA data will be used to calibrate the baseline simulation, which will assist in fulfilling Study Objective B, namely calibrating the simulation using empirical data from the case mine, and the dynamic data will aid in calibrating a dynamic simulation.

3.3.2. Baseline simulation calibration

The basic cycle

The information gathered in Section 3.3.1 was used to build and calibrate the baseline simulation model in PTB, as depicted in Figure 36. The simulation was developed to depict the real-world environment and accurately simulate everyday operations. The components were all represented on a 1:1 scale as identified during the physical investigation. Controllers were used to ensure the simulation was representative of daily operating procedures (such as flow rates, and schedules).

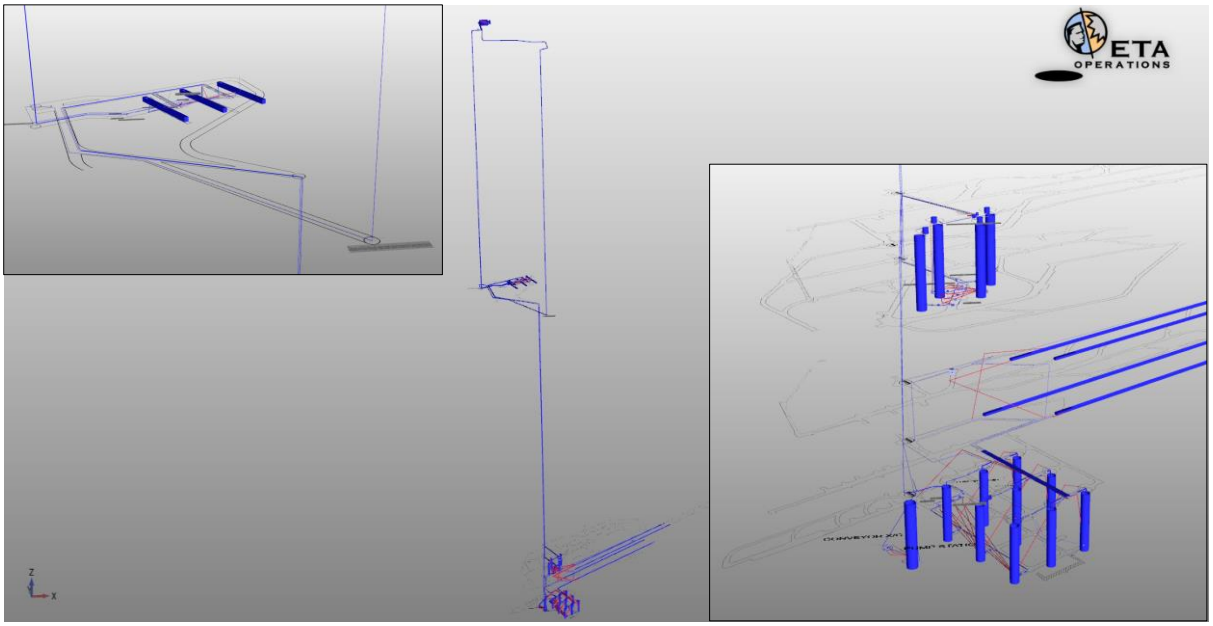

Figure 36: Baseline PTB simulation model of Mine A' dewatering system

Due to there being three lift stages, basic cycle development had to be divided into three stages too. Each stage was calibrated and verified before complexity was added to the individual system until each individual system represented the real-life environment accurately.

With all the water being diverted to the 24L settlers, the first step was to ensure that each pump station was operating correctly, namely that the pumps and dam levels were responding similarly to the SCADA data for the predefined incoming flow rates. The next step was to integrate the 25L and 21L pump stations (illustrated in Figure 37 and Figure 38, respectively) in one model and again to ensure the components were responding accordingly.

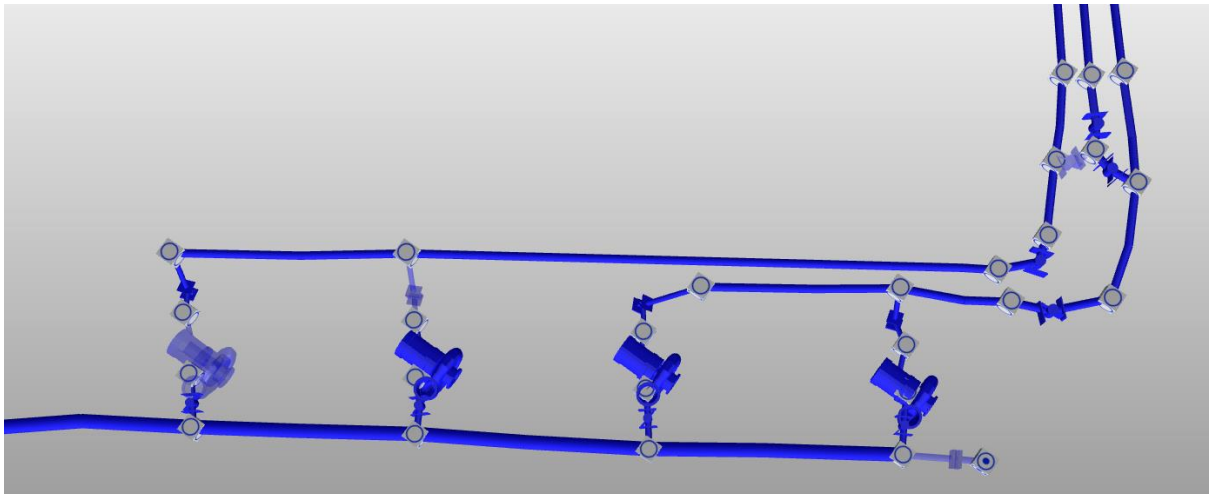

Figure 37: PTB representation of 25L pump station

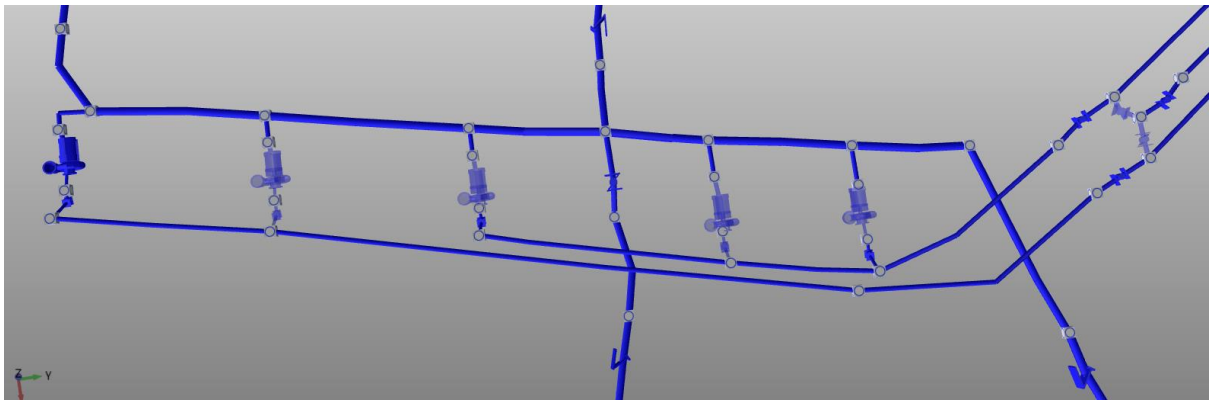

Figure 38: PTB representation of 21L pump station

Finally, the 5L pump station (illustrated in Figure 39) was added to the system. Again, the components were analysed to ensure they were responding correctly.

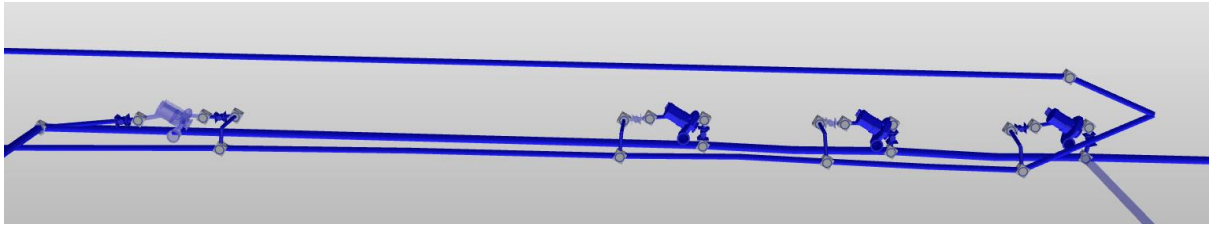

Figure 39: PTB representation of 5L pump station

Simulation calibration and verification

As mentioned in the Chapter 2: Development of Solution, the calibration and verification of the simulation occur concurrently while adding complexity to the basic cycle. This is a highly iterative cycle that becomes increasingly more difficult as complexity is added.

Figure 40 illustrates the water flow rates for Mine A that the dewatering system needs to remove. As mentioned previously, the fissure water sources were accounted for at their respective points. The service water was presumed to accumulate at 23L where it was accounted for as a singular flow rate.

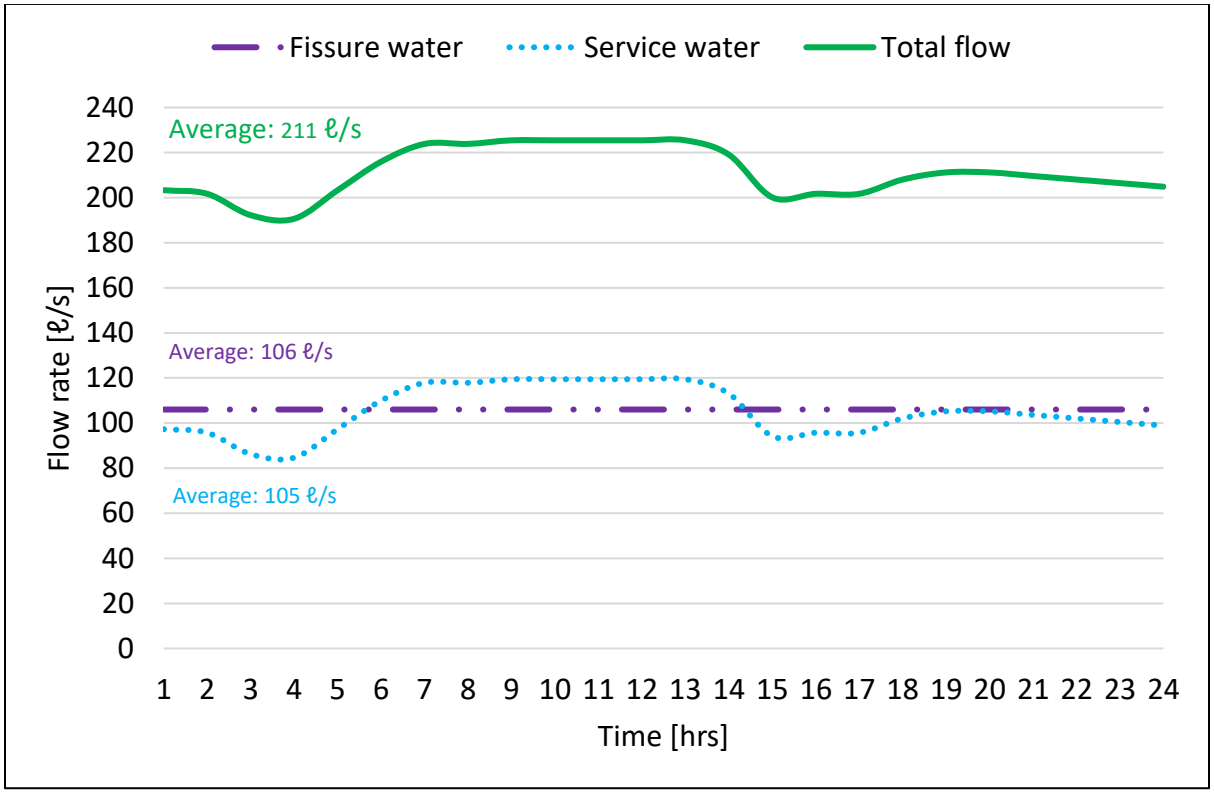

Figure 40: Water flow rates for Mine A

The model was simulated over a 96-hour period to ensure that the components reached steady state. PI controllers were used to control the flow rates of the different water sources. Due to the fissure water input profiles being linear, calibration was easier while the service water was slightly more difficult. However, the flow rates were input values and were calibrated to match the data precisely. The verification is summarised in Table 11.

Table 11: Fissure water flow rate verification

Water source	Flow rate [ℓ/s]	Simulated flow rate [ℓ/s]	Error [%]
Fissure water above 23L	39	39	0.00
Fissure water on 23L	45	45	0.00
Fissure water on 24L	20	20	0.00
Fissure water at shaft bottom	2	2	0.00
Service water	105	105	0.00

Table 11 provides an indication of the average flow rate for the service water due to its dynamic profile. Figure 41 does provide clarification as to how closely the simulated values matched the actual data.

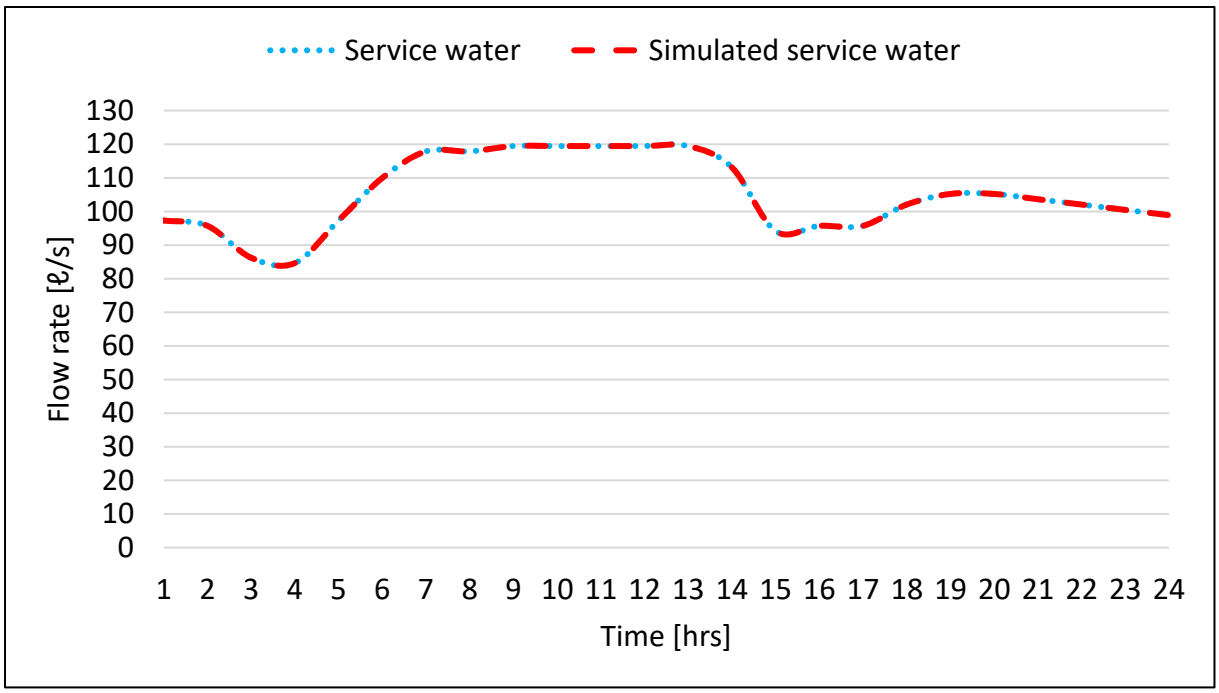

Figure 41: Actual vs simulated service water flow rate

The dynamicity of the 25L dewatering was also closely matched by the simulation results and was within the 5% calibration requirement. Figure 42 compares the 25L results graphically. The 21L and 5L total dewatering comparisons further fulfilled the 5% calibration requirement with the profiles closely correlating to the actual data depicted in Figure 30 and Figure 32, respectively.

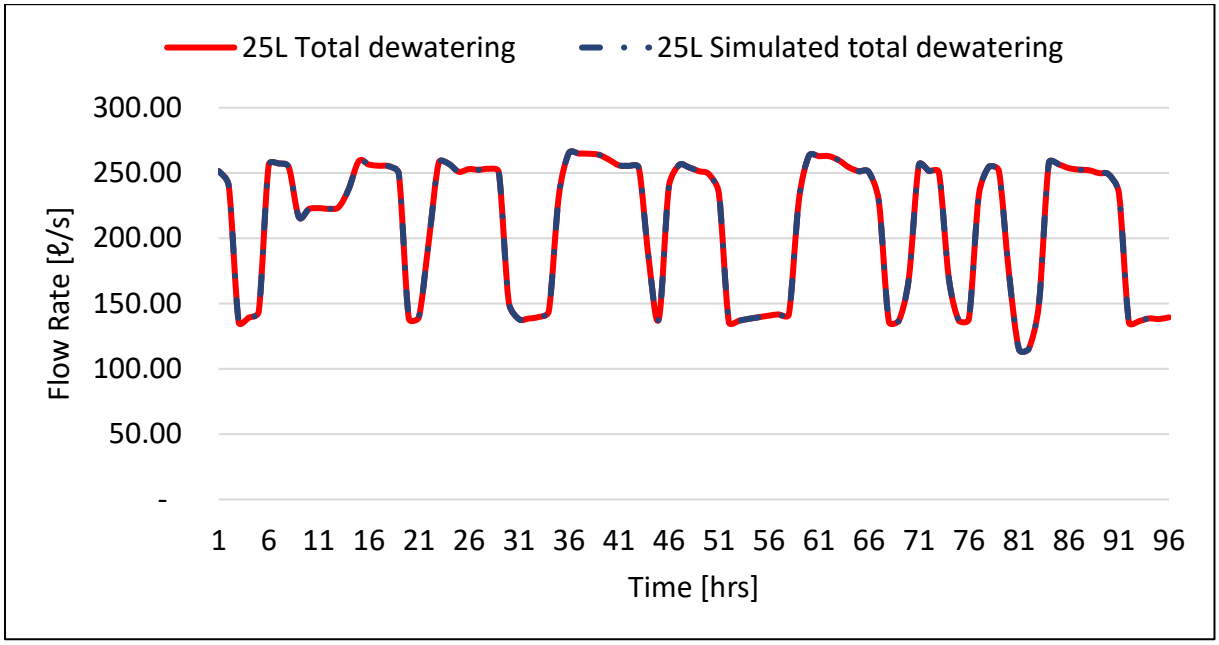

Figure 42: Actual vs simulated 25L total dewatering flow rate

The closely matched flow rate profiles indicated that the pumps on each level were calibrated correctly and the scheduling thereof matched real-life operating conditions. The significance thereof lay in the corresponding dam levels. This indicated whether the input parameters and capacities were calculated correctly.

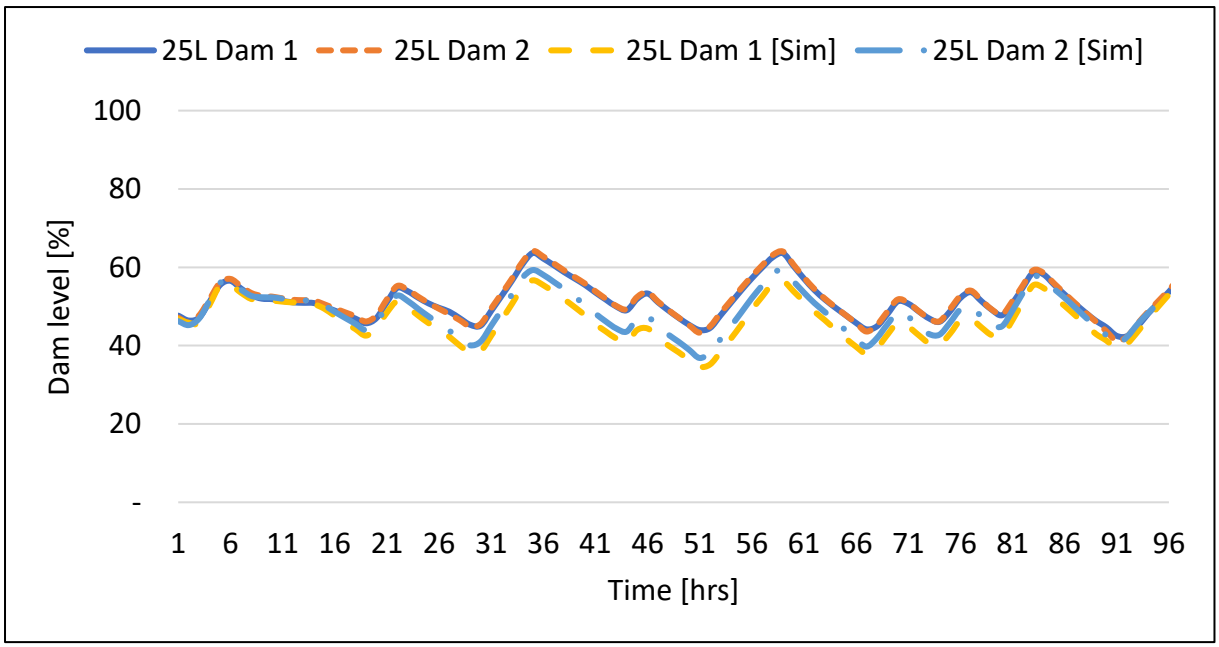

Figure 43: Actual vs simulated 25L dam levels

As shown in Figure 43, the corresponding dam levels on 25L were also closely matched. The same trends were apparent on 21L and 5L. Table 12 summarises the MAE for the dynamic profiles in the simulation.

Table 12: Summary of the accuracy of the baseline simulation components

Dynamic calibration	Dam level	Simulated dam level	Error [%]
25L Dam 1 level [%]	51.27	46.41	4.86
25L Dam 2 level [%]	51.56	48.40	3.16
25L total dewatering flow rate [ℓ/s]	211.00	209.44	0.31
21L Dam 1 level [%]	48.14	46.14	4.15
21L Dam 2 level [%]	44.10	44.39	0.66
21L Dam 4 level [%]	47.17	45.11	4.36
21L Total dewatering flow rate [ℓ/s]	231.41	223.73	3.12
5L Dam 1 level [%]	44.71	44.72	0.02
5L Dam 2 level [%]	66.61	63.57	4.57
5L total dewatering flow rate [ℓ/s]	222.30	228.88	2.96

Overall, the simulation model's calibration was successful as none of the components fell short of the 5% calibration requirement. The model could, therefore, reproduce the dewatering operating conditions of Mine A accurately.

3.3.3. Simulating a total power failure

The physical investigation also brought the following information to light:

- A network of drain holes on the levels above 23L ensure that water is gravity-fed to 24L and miss any capacities above 23L as a result. The capacities available for a total power failure can, therefore, only be considered from 23L downward.
- The two empty settlers are not serviceable and cannot be used in an emergency.
- The 24L emergency dam as well as the 24L cofferdam and 24L annex area do not have valves on their outlets and cannot store water currently, rendering their capacities redundant.

- A drain hole was found behind the 23L emergency dam which renders the dam's capacity redundant.
- If upgrades are made to the 24L emergency dam outlets, such as installing valves and usable columns, they can only store the fissure water currently flowing through them. This is due to the series of annex holes that divert the rest of the water directly to the settler area.
- The 24L emergency dam does not have overflow pipes to divert water to the settler area if the capacity fills. The water flows over the walls towards the shaft and then to shaft bottom.

These factors significantly decrease the available capacity during an emergency. Table 13 compares the available emergency capacities during a total power failure.

Table 13: Available emergency capacity comparison

Capacity	Design specification [Mℓ]	Verified capacity [Mℓ]	Difference [ΔMℓ]
Spare capacity of 25L dams	2.40	5.60	3.20
Settlers	3.58	0.00	−3.58
Area above settlers	1.98	0.80	−0.18
Shaft bottom	4.82	4.30	−0.52
23L emergency dam	8.75	0.00	−8.75
25L additional	6.00	0.00	−6.00
24L emergency dam	0.00	0.00	0.00
24L cofferdam	0.00	0.00	0.00
24L annex	0.00	0.00	0.00
Total	**27.53**	**10.70**	**−16.83**

Mine A's 48-hour requirement was tested in the simulation environment according to the updated capacities as found through the investigation. The shaft was deemed to have reached its maximum flood capacity once shaft bottom has flooded. This reference was chosen because once shaft bottom has flooded, the pump chamber would fill with water, posing a risk to the equipment and personnel therein.

A total power failure was set to occur at the 34-hour mark during the 96-hour simulation period. This point was chosen due to the high service water demand in the shaft to ensure a worst-case scenario was simulated. It was assumed that all tasks relating to Mine A's emergency procedure would be carried out after an hour. These tasks included but were not limited to closing the service water valve on surface and opening the drains on 24L to the 25L spare dams.

Using Equation 1, the service water was calculated to drain through the system to the 24L settlers over a seven-hour period. Thereafter, only fissure water would affect the system. Figure 44 shows the water flow rates during a total power failure.

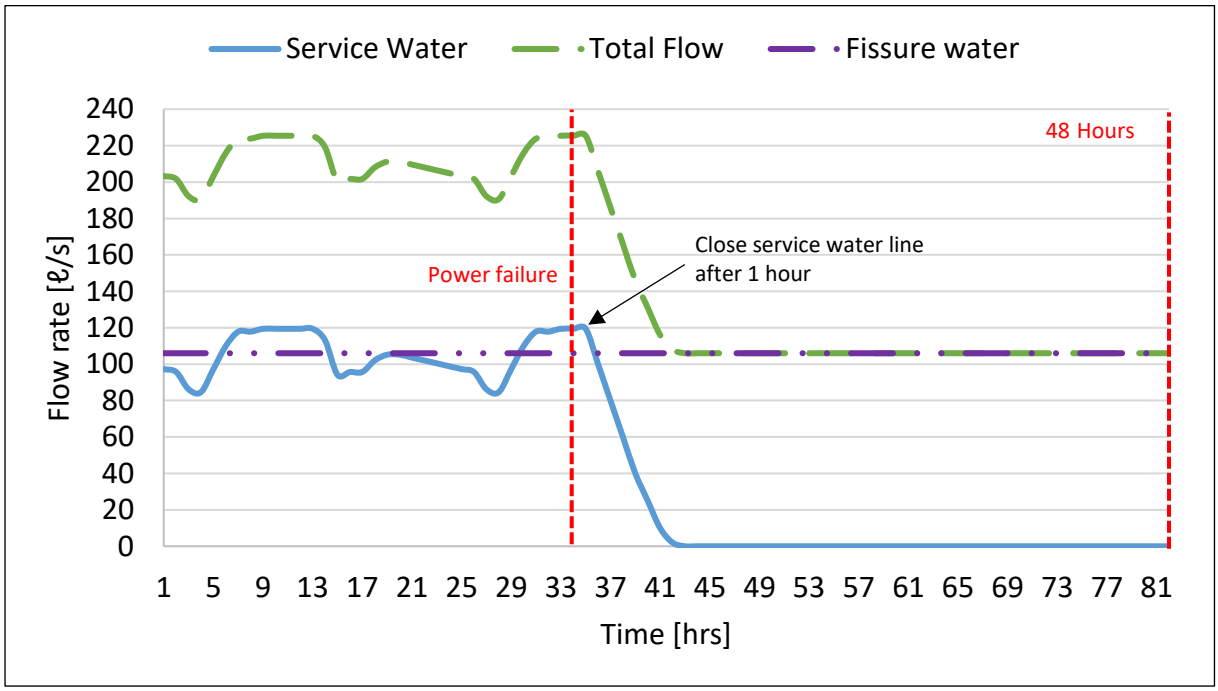

Figure 44: Mine A total power failure flow rates

The process of opening and closing valves along with the new service water flow rate and pump schedules had to be implemented in the baseline scenario simulation. Thereafter, a series of validation steps were carried out to ensure the system was responding correctly to the changes.

Figure 45 illustrates the dam level profiles during a total power failure for the available emergency capacities. Evidently, from the figure, shaft bottom flooded after 22 hours, which was 26 hours short of the defined requirement.

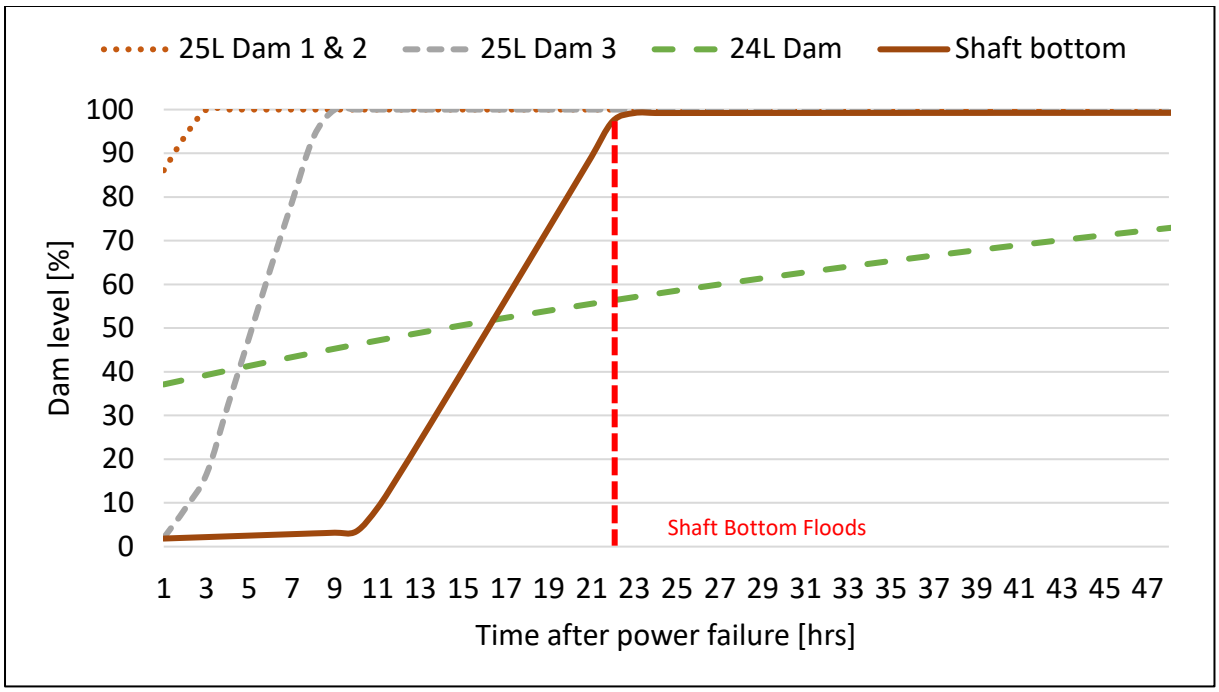

Figure 45: Mine A's total power failure capacity results

3.3.4. Scenario simulations

Mine A's emergency capacities did not fulfil the requirement and shaft bottom flooded after just 22 hours. This prompted a series of scenario simulations in order for the requirement to be satisfied. The scenario simulations were conducted in collaboration with Mine A's engineering team, who assisted in finding solutions to the various problems found during the investigations.

Scenario 1: improve the 24L emergency dam capacity usage

The first problem to be addressed was the use of the 24L emergency dam. The following upgrades/improvements were suggested:

- Increase the two existing 100 mm outlet pipes to 250 mm pipes with valves. This would ensure that enough water could drain during normal operation, keeping the dam level as low as possible.
- Install two 300 mm overflow columns on the emergency dam to the settler area. This would divert water before the dam wall overflowed, preventing water from travelling directly to the shaft.
- Move annex hole 24.1's outlet pipe to behind the 24L emergency dam wall. This would allow additional water to be stored behind the 24L capacity before flowing to the settler area and dams.

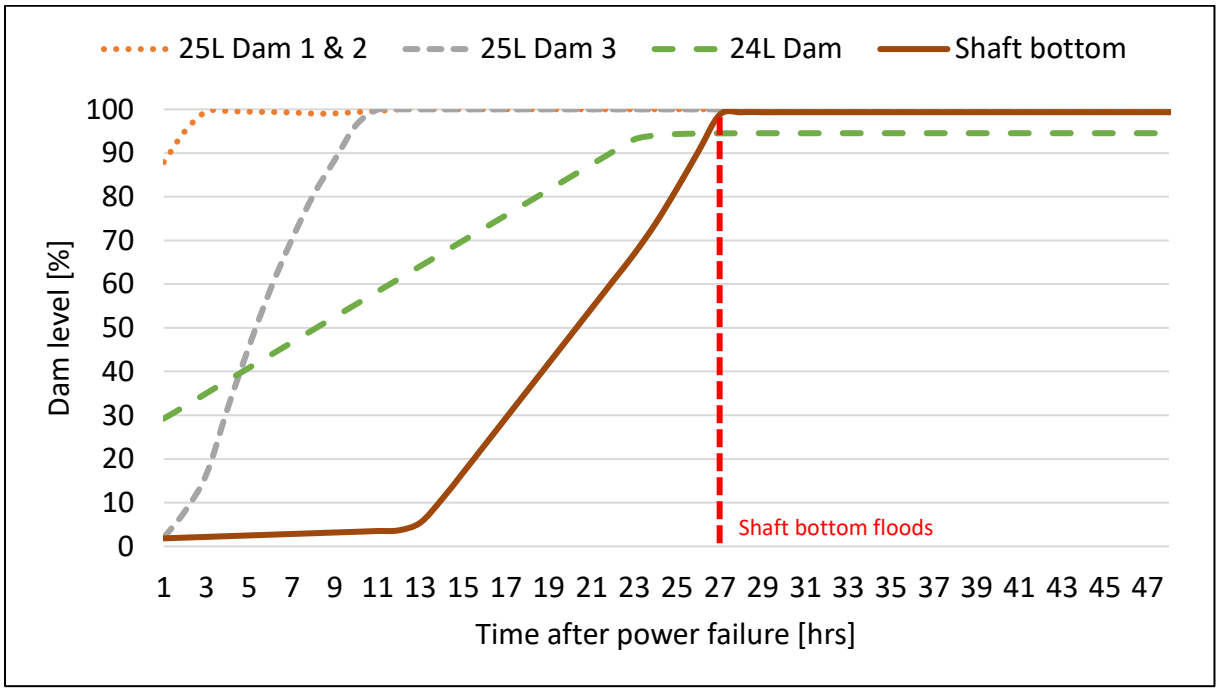

Figure 46: Mine A's emergency capacity results from Scenario 1

From Figure 46, it is clear that the suggested changes provided an additional five hours to the flood time. This was attributed to using the 24L emergency dam fully and diverting an annex hole's flow to the emergency dam first. However, the requirement was still not met, which prompted further investigation. The second scenario was closely related to the first; therefore, the changes made in Scenario 1 were kept and the suggestion made in Scenario 2 was added.

Scenario 2: increase the 24L emergency dam walls

The second scenario aimed to determine the effect of increasing the 24L emergency dam walls to increase the available capacity. Currently, the dam walls are 2.1 m, which relates to a 3.9 Mℓ storage capacity, as a result of the dip angle and haulage size measured on the DXF.

The proposal was to increase the dam wall height to 3.5 m, which would increase the capacity to 8.3 Mℓ. A height of 3.5 m was chosen as the vent department required at least a 0.5 m gap between the wall and the hang wall. This ensured that enough ventilation air flowed through the area to avoid methane buildup. The results are illustrated in Figure 47.

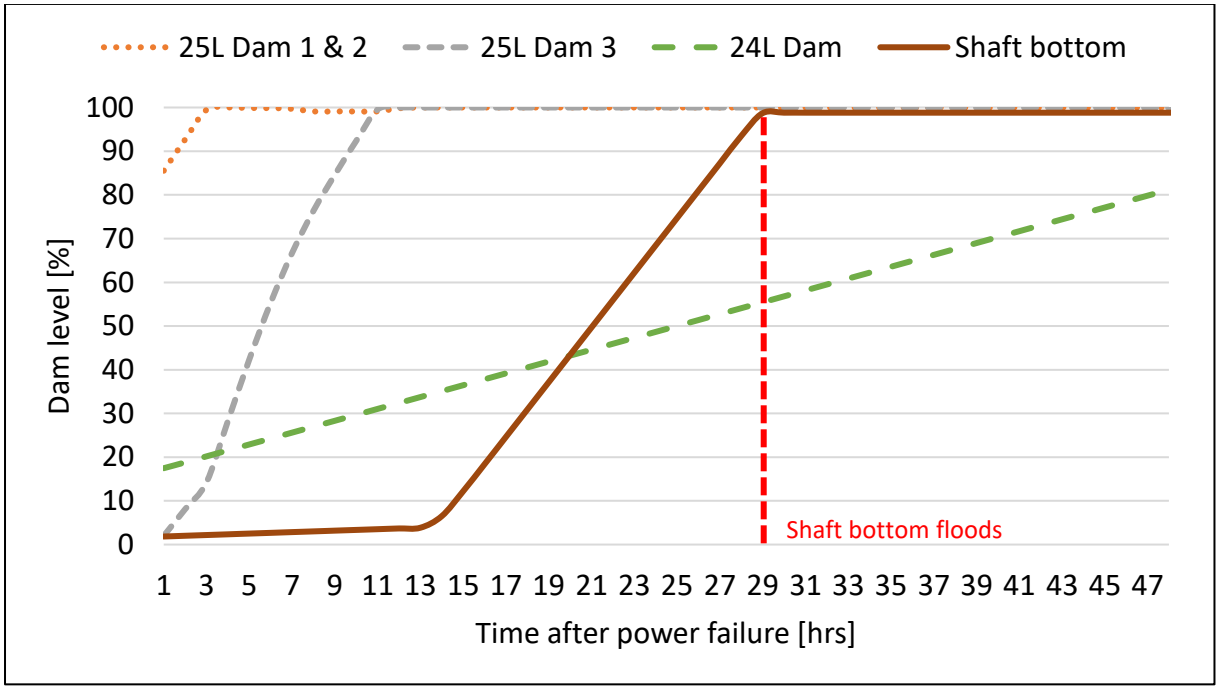

Figure 47: Mine A's emergency capacity results from Scenario 2

Although only two hours were gained from the proposed changes, the 24L emergency dam capacity increased significantly, which incited the changes proposed in Scenario 3.

Scenario 3: seal off the annex and cofferdam areas

Scenario 3's proposed changes were based on using the increased 24L emergency dam capacity effectively. Figure 48 and Figure 49 depict the 24L cofferdam area and 24L annex area, respectively. These are the two outlet areas for all of the annex holes on 24L. The only

exclusion was annex 24.1, which had to be diverted to behind the 24L emergency dam already according to Scenario 1.

Figure 48: 24L cofferdam area

Figure 49: 24L annex area

The proposed change for Scenario 3 was to seal off the two areas completely. The following upgrades had to be made:

- The 24L cofferdam area already had outlet pipes, but all required valves to ensure water could be stored in the capacity during an emergency.
- The 24L annex area required two 200 mm outlet pipes for normal operation.
- Both areas required two 300 mm overflow pipes (had to be elevated higher than the outlet pipes) to divert water to behind the 24L emergency dam.

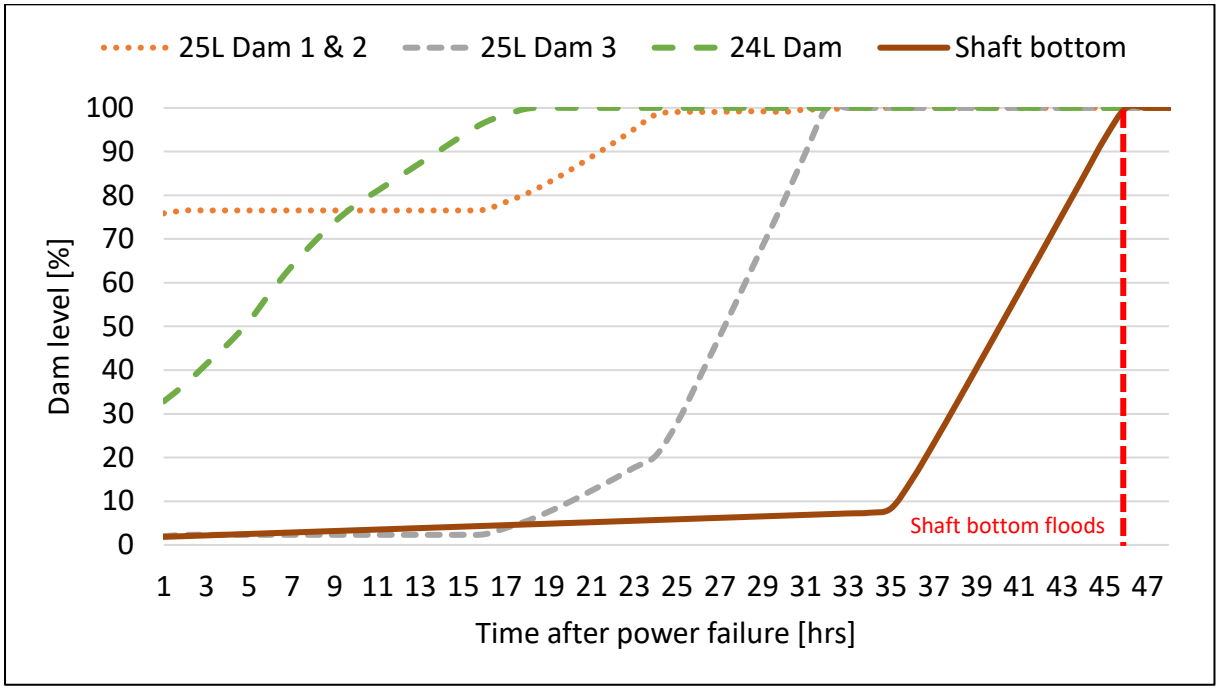

Figure 50: Mine A's emergency capacity results from Scenario 3

Figure 50 illustrates the results following the proposed changes for Scenario 1, 2, and 3 combined. While the flood time had increased by 24 hours, the requirement had still not been met.

Scenario 4: install a water door

The fourth scenario proposition was to build water doors on 24L in front of the two existing 24L emergency dam walls on either side of the haulage. A water door allows for normal operating conditions to continue. Ventilation flow remains the same and people can move freely in and out of the area. During an emergency, the doors are closed, allowing all water to be stored behind it.

A water door completely seals the area; therefore, dip angles do not affect the capacity. The entirety of 24L behind the water can thus be used, which increases the 24L emergency dam capacity to 35 Mℓ. Figure 51 illustrates the location of key points on 24L and Table 14 provides the legend applicable to Figure 51.

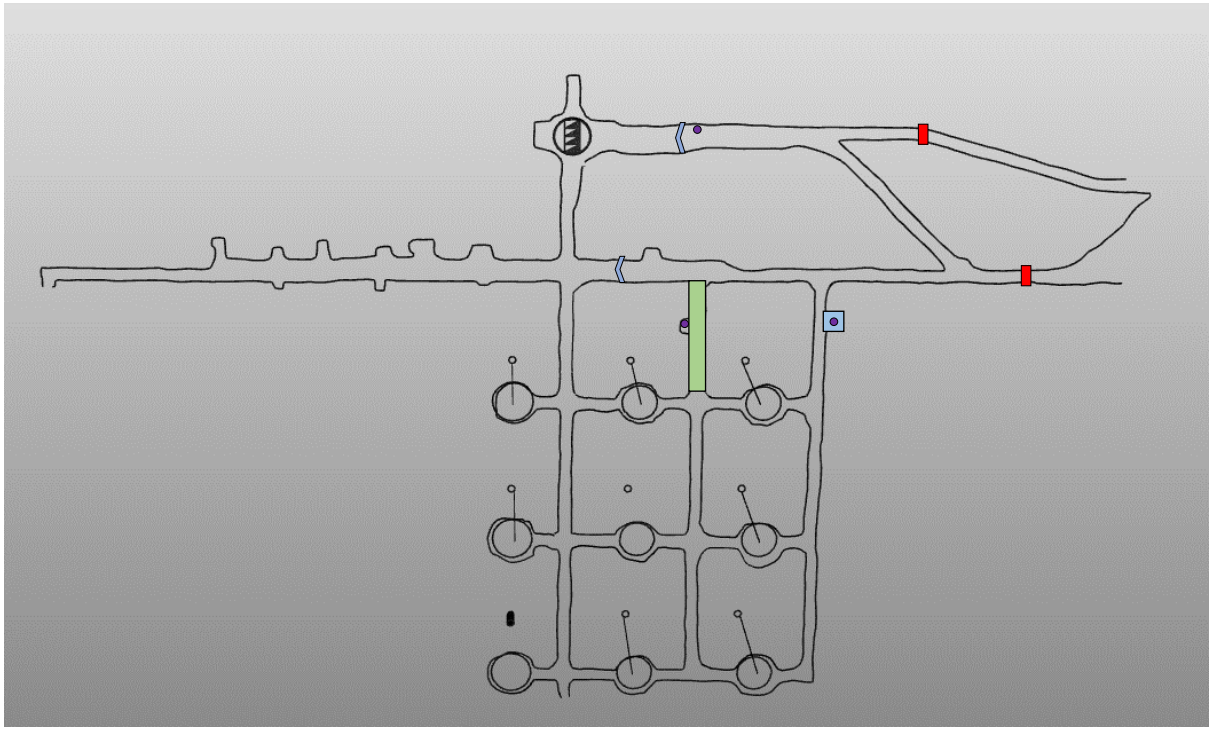

Figure 51: 24L key areas on DXF

Table 14: Legend for Figure 51

Component	Description
	24L cofferdam area
	24L annex area
	Annex hole outlets on 24L
	24L emergency dam walls
	Proposed water door placements

Figure 52 illustrates the results following the proposed changes. The results indicate that a collective implementation of all the proposed changes would allow the 48-hour requirement to be met.

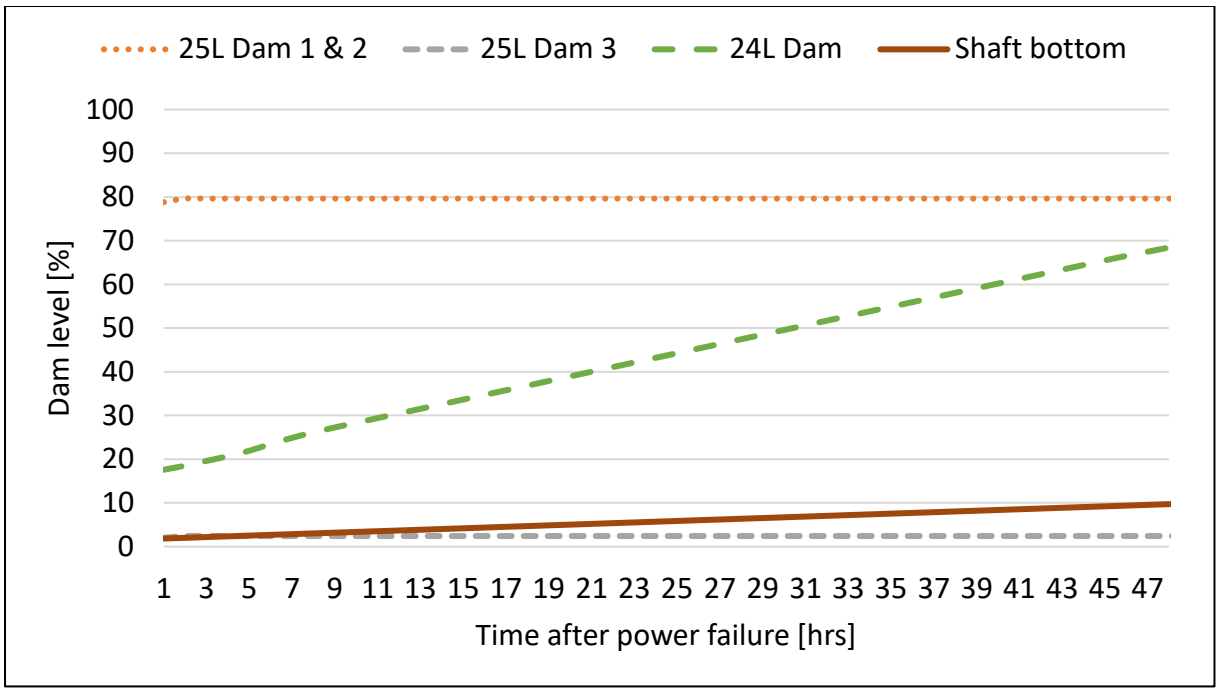

Figure 52: Mine A's emergency capacity results from scenario 4

3.3.5. Validation of results

Section 3.3.2 demonstrated that the simulation met the calibration requirement, indicating the simulation was at least 95% accurate in replicating the real-world system. Based on that, any changes made to the simulation during the scenario process ensured that the simulation environment would respond to within 5% of what is expected in reality. Therefore, the validation was successful given that a collective implementation of all four scenarios met the 48-hour requirement in the simulated environment.

3.3.6. Implementation of changes

All four scenarios will need to be combined and implemented at Mine A to ensure the shaft conforms to the 48-hour requirement. This will inevitably change the baseline simulation, which needs to be addressed. The same process can be followed as described in the proposed

method to ensure all the facets are covered. The process will, however, be shorter due to the majority of the information already being gathered.

3.4. Conclusion

This chapter applied a generic method to develop, calibrate, and verify a simulation model on a case mine dewatering system. The aim of the simulation model was to determine how the shaft would respond to a total power failure and compare it with the exiting method in industry. Table 15 summarises the industry method and simulated results.

Table 15: Summary of results for Mine A's flood time

No.	Description	Total hours
0	Industry method	67
1	Simulated existing configuration	22
2	Simulated Scenario 1	27
3	Simulated Scenario 2	29
4	Simulated Scenario 3	46
5	Simulated Scenario 4	> 48

The industry method followed a static simulation based on design specifications that were found to be inaccurate during the investigation phase of implementing the proposed method. Another factor that contradicted the industry method in the proposed method was the integrated approach. The simulation model showed that capacities would fill up simultaneously at stages whereas the industry method assumed capacities would fill systematically.

The proposed method ensured that a verified simulation was developed, which was crucial as it eliminated errors from the start, ensuring the model could replicate real-world operating conditions accurately. Finally, the simulation model was developed using dynamic data that accounted for peak flow rates.

The deviations from the industry method highlighted key factors to developing an accurate simulation model, namely that verification, integration, and dynamicity can greatly affect the

results and subsequent safety risks. It further indicated the importance of simulating highly hazardous events because if the mine had made provisions based on the 67-hour calculation time, many people and very expensive equipment would have been at risk.

It was demonstrated that this method could be used to simulate a mine dewatering system's response to a total power failure. The simulation platform allowed for hypotheses to be tested through scenario simulations, which ensured that predefined requirements could be met. The method's generic approach further allowed for it to be implemented on other mineshafts. The results of two other shafts are provided in Appendix E: Simulation Results of Mine B and Mine C.

4. CONCLUSION

4.1. Study overview

Mines emphasise health and safety, which prompted research into ensuring that adequate safety measures are in place. One safety measure under investigation is the removal of water to improve the working conditions and integrity of the shaft. Studies were conducted on dewatering system design, water infiltration, and groundwater flow while simulation-based methodologies were identified as a successful approach in addressing problems related thereto. Little research was, however, conducted on the shaft's capability to store water during a total power failure – an increasingly guaranteed event. This prompted the research aim and objectives.

This study focused on applying a newly developed simulation-based methodology to a case mine to predict the flood times during a total power failure. The simulation model further provided a platform for testing contingency planning hypotheses through scenario simulations.

A verified, integrated, and dynamic dewatering system was developed in PTB to replicate Mine A's operating conditions. The dewatering simulation model was built and calibrated using data obtained during physical investigations (pump tests and ultrasonic flow meter readings) and digital investigations (SCADA data) to ensure the simulation components could replicate the real-world operating conditions to within an MAE of 5%.

A total power failure was run in the simulation environment assuming that the model's response would be within 5% of the real-world environment due to the calibration process. Mine A did not meet the mine's flooding requirement of 48 hours and flooding took place after just 22 hours. This along with the industry method's error of 67% when compared with the simulation method incited a series of scenario simulations.

Four scenarios were run with each scenario building on the previous until the 48-hour requirement was met. The simulation was, therefore, validated in that it conformed to the

need of aiding emergency planning by identifying what is required for the shaft to meet the requirement.

The validation and outcomes of the simulation highlight the importance of using simulation-based methodologies to aid decision-making and emergency planning on a mine. The platform allows for planning to be done without installing expensive infrastructure and performing expensive tests without any certainty of success.

4.2. Shortcomings

Some challenges that were faced during this study include:

- The mine did not have a set pumping schedule, which made pump calibration and control problematic.
- Some areas in the mine were not accessible, which increased the need for assumptions to be made regarding component sizes, locations, and water flow rates.
- There was a lack of measuring instrumentation (such as pump power or running amps and water usage at working areas), which created difficulty in calibrating the model.
- A total power failure could not be tested in reality due to the safety risks involved.

These challenges do affect the accuracy of the simulation as assumptions had to be made during the calibration process. As a result, the shortcomings of the study are:

- The study could not test the validity of the simulated results once changes were made.
- The study did not distribute water flow rates to sections above 23L, which could affect the flood time.
- The study used digital data as input values which, depending on the accuracy of the data, could affect the accuracy of the results, particularly after changes are made.
- The study did not account for human error during the emergency such as failing to open/close valves where necessary or diverting water incorrectly.
- The study did not account for any infrastructure failure, installation errors, or calculation errors, assuming the proposed changes would work as intended.

4.3. Recommendations for future work

The recommendations for future work include:

- Expanding the scope of the simulation model to include the water supply from the origin. This will require extensive and detailed audits throughout the mine to ensure water is accounted for at the correct locations in the mine. This may improve simulation accuracy.
- Applying the method in localised sections of the mine. Especially for sections that are prone to flooding, the scope can be reduced and simulation used to determine causal factors that will aid with developing improved dewatering schemes.
- Applying the method to other industries where water inundations are common or dewatering systems are required; for example, construction and tunnelling sites.
- Conveying the thorough understanding of the system obtained through the process to employees and using it for training and planning purposes. Therefore, research can be conducted on implementing the method's results for training and emergency planning.
- Validating the method. The simulation results and decisions made based on these results need to be tested using real-life data.

REFERENCE LIST

[1] T. L. Dickinson, T. G. Thorowgood, and J. L. Estep, *Evolutionary and Revolutionary Technologies for Mining*. National Academies Press, Washington, DC, 2002. doi: 10.17226/10318.

[2] M. B. Revuelta, "Mineral resource extraction," in *Springer Textbooks in Earth Sciences, Geography and Environment*, Springer, Cham, 2018, pp. 311–421. doi: 10.1007/978-3-319-58760-8_5.

[3] B. Friedenstein, C. Cilliers, and J. van Rensburg, "Simulating operational improvements on mine compressed air systems," *S. Afr. J. Ind. Eng.*, vol. 29, no. 3, pp. 69–81, Nov. 2018, doi: 10.7166/29-3-2049.

[4] J. Vosloo, L. Liebenberg, and D. Velleman, "Case study: Energy savings for a deep-mine water reticulation system," *Appl. Energy*, vol. 92, pp. 328–335, Apr. 2012, doi: 10.1016/J.APENERGY.2011.10.024.

[5] L. G. Venburg, "Dewatering of mines: A practical analysis," in *International Mine Water Association*, San Francisco, CA, 2017, pp. 219–232.

[6] D. Stephenson, "Distribution of water in deep gold mines in South Africa," *Int. J. Mine Water*, vol. 2, no. 2, pp. 1–30, 2006.

[7] I. Prosser, L. Wolf, and A. Littleboy, "Water in mining and industry," in *Water*, CSIRO Publishing, Canberra, 2011, pp. 135–146.

[8] A. Romero, D. Millar, M. Carvalho, J. M. Maestre, and E. F. Camacho, "A comparison of the economic benefits of centralized and distributed model predictive control strategies for optimal and sub-optimal mine dewatering system designs," *Appl. Therm. Eng.*, vol. 90, pp. 1172–1183, Nov. 2015, doi: 10.1016/j.applthermaleng.2015.01.031.

[9] A. Nell, “Development of a dewatering control strategy to prevent flooding within deep-level mines,” M. Eng. dissertation, North-West University, Potchefstroom, 2022.

[10] A. Wagner, “An integrated simulation-based method for deep-level mine dewatering planning,” M. Eng. dissertation, North-West University, Potchefstroom, 2022.

[11] R. Venter, “Reconfiguring deep-level mine dewatering systems for increased water volumes,” M. Eng. dissertation, North-West University, Potchefstroom, 2020.

[12] A. J. Gunson, “Quantifying, reducing and improving mine water use,” PhD thesis, University of British Columbia, Vancouver, 2013. doi: 10.14288/1.0071942.

[13] A. Botha, “Optimising the demand of a mine water reticulation system to reduce electricity consumption,” M. Eng. dissertation, North-West University, Potchefstroom, 2010.

[14] G. M. Mudd, “Mining and water resources,” *Encyclopedia of the World’s Biomes*, pp. 45–54, Jan. 2020, doi: 10.1016/B978-0-12-409548-9.12131-1.

[15] D. H. Velleman, J. Venter, and R. Pelzer, “Automated demand side management of clear water pumping and storage for shifting load out of Eskom’s domestic peak in the mining industry,” in *9th Industrial and Commercial Use of Energy Conference*, 2012, pp. 1–4.

[16] E. Mavhura, “A systems approach for assessing emergency preparedness in underground mines of Zimbabwe,” *Resour. Policy*, vol. 62(C), pp. 1–8, 2019, doi: 10.1016/j.resourpol. 2019.03.005.

[17] W. Yang, X. Xia, G. Zhao, Y. Ji, and D. Shen, “Overburden failure and the prevention of water and sand inrush during coal mining under thin bedrock,” *Min. Sci. Technol.*, vol. 21, no. 5, pp. 733–736, Sep. 2011, doi: 10.1016/J.MSTC.2011.04.002.

[18] A. Lane, J. Guzek, and W. van Antwerpen, “Tough choices facing the South African mining industry,” *J. S. Afr. Inst. Min. Metall*., vol. 115, no. 6, 2015.

[19] J. A. Jacobs, M. J. Mathews, and M. Kleingeld, “Failure prediction of mine de-watering pumps,” *J. Failure Anal. Prev.*, vol. 18, no. 4, pp. 927–938, Aug. 2018, doi: 10.1007/s11668-018-0488-3.

[20] *Mine Health and Safety Act No. 29 of 1996 and Regulations*.

[21] Sibanye Stillwater, *Beatrix: Power Failure in February 2018*, Welkom, 2018.

[22] A. J. A. Visagie, “Modelling the effect of changes in mining compressed air networks on refuge chambers,” M. Eng. dissertation, North-West University, Potchefstroom, 2020.

[23] J. Szczepiński, “The significance of groundwater flow modeling study for simulation of opencast mine dewatering, flooding, and the environmental impact,” *Water (Basel.)*, vol. 11, no. 4, p. 848, Apr. 2019, doi: 10.3390/w11040848.

[24] K. T. Witthuser, M. Holland, T. Seidel, and C. M. Konig, “Numerical modelling of mine dewatering and flooding in the Evander gold basin, South Africa,” *S. Afr. J. Geol.*, vol. 118, no. 1, pp. 71–82, Mar. 2015, doi: 10.2113/gssajg.118.1.71.

[25] K. Różkowski, R. Zdechlik, and W. Chudzik, “Open-pit mine dewatering based on water recirculation: Case study with numerical modelling,” *Energies (Basel.)*, vol. 14, no. 15, p. 4576, Jul. 2021, doi: 10.3390/en14154576.

[26] B. Meyer, “The 2008 flooding of Amandelbult Mine, the impact of the flood and the road to recovery,” in *Anglo American Mining Conference*, 2008.

[27] M. Onifade, “Towards an emergency preparedness for self-rescue from underground coal mines,” *Proc. Saf. Env. Prot.*, vol. 149, pp. 946–957, May 2021, doi: 10.1016/J.PSEP.2021.03.049.

[28] S. Foster and G. Tyson, “Mining enterprises and groundwater,” International Association of Hydrogeologists, 2018.

[29] *Occupational Health and Safety Act No. 85 of 1996 and Regulations*.

[30] K. M. Kowalski-Trakofler, C. Vaught, M. J. Brnich Jr., and J. H. Jansky, “A study of first moments in underground mine emergency response,” *J. Homel. Secur. Emerg. Manag.*, vol. 7, no. 1, 2010 doi: 10.2202/1547-7355.1652.

[31] D. Alexander, “Disaster and emergency planning for preparedness, response, and recovery,” in *Oxford Research Encyclopedia of Natural Hazard Science*, Oxford University Press, Oxford, 2015. doi: 10.1093/acrefore/9780199389407.013.12.

[32] S. Singh, E. Shebab, N. Higgins, “Data management for developing digital twin ontology model,” *Proc. Inst. Mech. Eng. B. J. Eng. Manuf.*, vol. 235, no. 14, pp. 2323–2337, Dec. 2021, doi: 10.1177/0954405420978117.

[33] O. Zavila, P. Dobes, J. Dlabka, and J. Bitta, “The analysis of the use of mathematical modeling for emergency planning purposes,” *Sci. Popul. Prot.*, vol. 2., 2015.

[34] A. D’Uffizi, M. Simonetti, G. Stecca, and G. Confessore, “A simulation study of logistics for disaster relief operations,” *Procedia CIRP*, vol. 33, pp. 157–162, 2015, doi: 10.1016/ j.procir.2015.06.029.

[35] N. N. Samany, M. Sheybani, and S. Zlatanova, “Detection of safe areas in flood as emergency evacuation stations using modified particle swarm optimization with local search,” *Appl. Soft. Comput.*, vol. 111, art. 107681, Nov. 2021, doi: 10.1016/J.ASOC.2021.107681.

[36] M. Rahman, N. Chen, M. M. Islam, “Development of flood hazard map and emergency relief operation system using hydrodynamic modeling and machine learning algorithm,” *J. Clean. Prod.*, vol. 311, art. 127594, Aug. 2021, doi: 10.1016/J.JCLEPRO.2021.127594.

[37] H. M. Lyu, S. L. Shen, A. Zhou, and J. Yang, “Perspectives for flood risk assessment and management for mega-city metro system,” *Tunn. Undergr. Space Technol.*, vol. 84, pp. 31–44, Feb. 2019, doi: 10.1016/J.TUST.2018.10.019.

[38] S. Dazzi, R. Vacondio, P. Mignosa, and F. Aureli, “Assessment of pre-simulated scenarios as a non-structural measure for flood management in case of levee-breach inundations,” *Int. J. Disaster Risk Reduct.*, vol. 74, art. 102926, May 2022, doi: 10.1016/j.ijdrr.2022.102926.

[39] E. Brunetti, J. P. Jones, M. Petitta, and D. L. Rudolph, “Assessing the impact of large-scale dewatering on fault-controlled aquifer systems: a case study in the Acque Albule basin (Tivoli, central Italy),” *Hydrogeol. J.*, vol. 21, no. 2, pp. 401–423, Mar. 2013, doi: 10.1007/s10040-012-0918-3.

[40] E. Pujades, E. Vàzquez-Suñé, J. Carrera, and A. Jurado, “Dewatering of a deep excavation undertaken in a layered soil,” *Eng. Geol*,. vol. 178, pp. 15–27, Aug. 2014, doi: 10.1016/ j.enggeo.2014.06.007.

[41] Z. Chen, H. Jintao, H. Zhan, and F. Yesheng, “Optimization schemes for deep foundation pit dewatering under complicated hydrogeological conditions using MODFLOW-USG,” *Eng. Geol*., vol. 303, art. 106653, Jun. 2022, doi: 10.1016/j.enggeo.2022.106653.

[42] S.-L. Shen, H.-M. Lyu, A. Zhou, L.-H. Lu, G. Li, and B.-B. Hu, “Automatic control of groundwater balance to combat dewatering during construction of a metro system,” *Autom. Constr*., vol. 123, art. 103536, Mar. 2021, doi: 10.1016/j.autcon.2020.103536.

[43] C.-F. Zeng, S. Wang, X.-L. Xue, G. Zheng, and G.-X. Mei, “Evolution of deep ground settlement subject to groundwater drawdown during dewatering in a multi-layered aquifer-aquitard system: Insights from numerical modelling,” *J. Hydrol.*, vol. 603, art. 127078, Dec. 2021, doi: 10.1016/j.jhydrol.2021.127078.

[44] E. Pujades, A. Jurado, J. Carrera, E. Vázquez-Suñé, and A. Dassargues, “Hydrogeological assessment of non-linear underground enclosures,” *Eng. Geol*., vol. 207, pp. 91–102, Jun. 2016, doi: 10.1016/j.enggeo.2016.04.012.

[45] L. Zu-jiang, Z. Ying-ying, and W. Yong-xia, “Finite element numerical simulation of three-dimensional seepage control for deep foundation pit dewatering,” *J. Hydrodynam.*, vol. 20, no. 5, pp. 596–602, Mar. 2008.

[46] C. Martínez and V. Ugorets, “Use of numerical groundwater modelling for mine dewatering assessment,” in *2nd International Congress on Water Management in the Mining Industry*, Santiago, Chile, 9–11 June 2010, pp. 317–326.

[47] W. Pulles, “Best practice guideline A6: Water management for underground mines,” Water Affairs and Forestry, Pretoria, 2008.

[48] L. Hu, M. Zhang, Z. Yang, Y. Fan, J. Li, H. Wang, and C. Lubale, “Estimating dewatering in an underground mine by using a 3D finite element model,” *PLoS One*, vol. 15, no. 10, art. e0239682, Oct. 2020, doi: 10.1371/JOURNAL.PONE.0239682.

[49] H. Yuan, Z. Gai-ling, and Y. Guo-yong, “Numerical simulation of dewatering thick unconsolidated aquifers for safety of underground coal mining,” *Min. Sci. Technol.*, vol. 19, no. 3, pp. 312–316, 2009.

[50] H. A. Mengistu, M. B. Demlie, T. A. Abiye, Y. Xu, and T. Kanyerere, “Conceptual hydrogeological and numerical groundwater flow modelling around the Moab Khutsong deep gold mine, South Africa,” *Groundw. Sustain. Dev*., vol. 9, art. 100266, Oct. 2019, doi: 10.1016/j.gsd.2019.100266.

[51] C. Li, J. Li, Z. Li, and D. Hou, “Establishment of spatiotemporal dynamic model for water inrush spreading processes in underground mining operations,” *Saf. Sci*., vol. 55, pp. 45–52, Jun. 2013, doi: 10.1016/j.ssci.2013.01.001.

[52] R. Álvarez, A. Ordóñez, E. de Miguel, and C. Loredo, “Prediction of the flooding of a mining reservoir in NW Spain,” *J. Environ. Manage.*, vol. 184, pp. 219–228, Dec. 2016, doi: 10.1016/J.JENVMAN.2016.09.072.

[53] R. L. Burritt and K. L. Christ, “Water risk in mining: Analysis of the Samarco dam failure,” *J. Clean. Prod.*, vol. 178, pp. 196–205, Mar. 2018, doi: 10.1016/J.JCLEPRO.2018.01.042.

[54] G. Seetal, “Evaluating water supply control at a centralised hydro-powered mine,” M. Eng. dissertation, North-West University, Potchefstroom, 2021.

[55] I. Mathews, “A simulation-based prediction model for coal fired power station condenser maintenance,” M. Eng. dissertation, North-West University, Potchefstroom, 2020.

[56] E. C. Hunter and G. T. C. Emere, “The use of cylindro-conical settlers for the clarification of underground water,” *J. S. Afr. Inst. Min. Metall.*, pp. 201–206, May 1977.

APPENDICES

Appendix A: Dewatering System Components Breakdown

A.1. Spindle pumps

Spindle pumps typically assist the dewatering system. Some functionalities include:

- Pumping water to a dam or drain holes to avoid sections filling with water.
- Pumping water to other spindle pump areas to assist dewatering a level.

A small cubby is usually built for the spindle pump so that the impeller is always submerged since the pump trips once the water drops below a certain level. Figure 53 depicts a spindle pump in a cubby on a mining level as well as a spindle pump as illustrated by a supplier.

Figure 53: Mining spindle pump[13]

[13] Balz Pumps, "VS 100 M-Type." https://www.balzpumps.co.za/?page_id=10196 (accessed Aug. 16, 2022).

Table 16 indicates the specifications of available spindle pumps as provided by a supplier.

Table 16: Spindle pump specifications[13]

Model/power	Maximum head [m]	Maximum flow [ℓ/s]	Impeller diameter [mm]
VS100 – 7.5 kW – 4P	22	30	250
VS100 – 15 kW– 4P	27	70	270
VS100 – 22 kW– 2P	62	34	220
VS100 – 37 kW – 2P	80	38	250
VS100 – 45 kW– 2P	102	33	270

A.2. Pipes and valves

Pipes of varying materials and accompanying valves are used in underground mining to move water to and from different sections. The pipe and valve specifications (such as thickness, material, and cladding) are chosen according to defined design parameters. Automatic valves and/or manual valves divert the water accordingly and are available in various configurations, such as globe valves, ball valves, and butterfly valves. Figure 54 illustrates three underground dewatering pipes with varying degrees of insulation with the top pipe having a ball valve.

Figure 54: Three underground dewatering pipes

A.3. Drains

Figure 55 illustrates a drain in a mine haulage. Haulages and travelways are inclined so that water flows towards the shaft. The drains are subsequently built to keep the travelways dry but still allow water to flow towards a drain hole, spindle pump cubby, or the shaft.

Figure 55: Mine drain

A.4. Annex and drain holes

Figure 56 and Figure 57 illustrate a mine drain hole and a mine annex hole, respectively. Pipes and/or drains transport water to drain holes, which are holes from an upper level to a lower level. The annex hole is the outlet of the drain hole on the lower level, which is usually accompanied by piping to move the water to another drain hole, a spindle pump, or a dam.

Figure 56: Mine drain hole

Figure 57: Mine annex hole

A.5. Settlers

Settlers are essentially purification dams. Lime and other additives are added to water so that the heavier contaminating particles (suspended solids) can settle to the bottom and the cleaned water can flow into clear water dams before being pumped out [56]. Figure 58 depicts a top view of a settler underground while Figure 59 provides a diagrammatic representation of the water purification process underground.

Figure 58: Top view of a mine settler

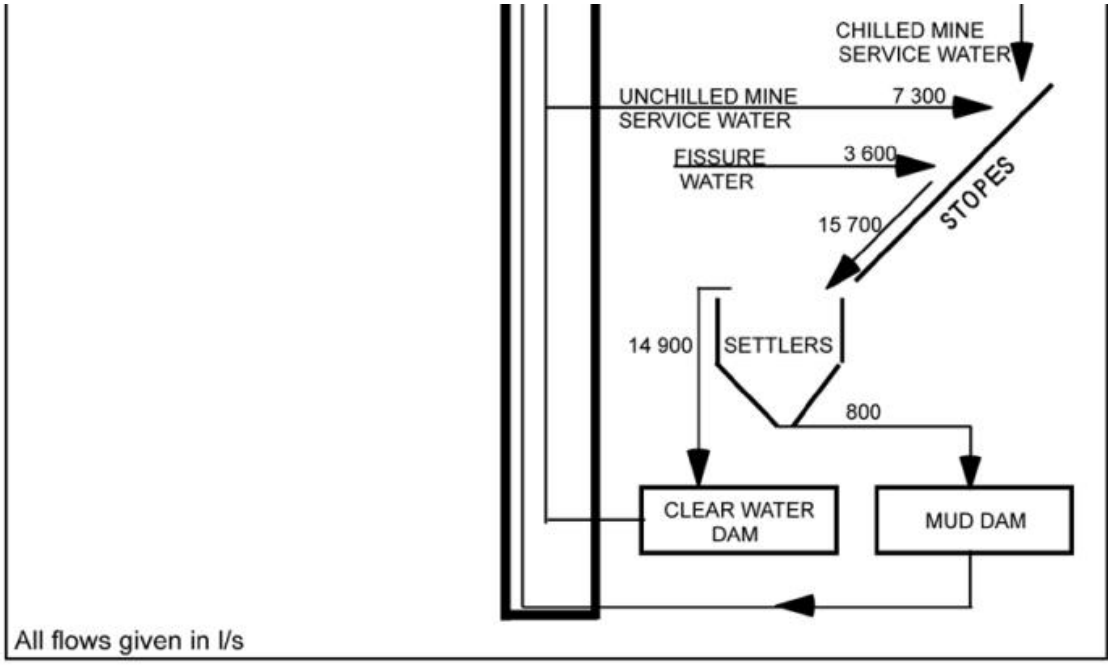

Figure 59: Diagrammatic representation of the water purification process underground [56]

Mine water can contain between 100 mg/L and 400 mg/L of suspended solids, which could cause the following issues [47]:

- Clear water dams filling up with silt.
- Erosive wear on dewatering equipment such as pumps and pipes.
- Fouling of heat exchanger tubes and subsequent efficiency loss.
- Ineffective water disinfection, which could lead to health risks.

This process of purification improves the service life of the equipment and general health and safety in the mine.

A.6. Water dams

A water dam, in terms of the study, is defined as a void that has the capacity to store water and is used for that purpose. Therefore, clear water dams and emergency dams are the only two applicable water dams since mud dams are not used for water storage, while shaft bottom is not intended to store water albeit being a void capable of doing so.

- Clear water dams store purified (cleaner) water before being pumped to surface via the dewatering system.
- Some mines have emergency dams that are used as additional storage capacities during an emergency. These dams are usually kept as empty as possible to ensure the entire capacity is available when need be.

A.7. Dewatering pumps

Figure 60 shows a 1.1 MW mine dewatering pump. As with the spindle pump, dewatering pumps are available in a range of models that are supplied accordingly to meet the defined requirements. However, most deep-level mines use multistage, high-pressure centrifugal pumps. These pumps are capable of pumping a head as much as 1 000 m [47].

Figure 60: An 11 MW mine dewatering pump

Appendix B: Detailed Underground Audit

Underground audits are extremely time-consuming and should be carried out efficiently to avoid wasting time on unnecessary actions. Regarding the study, the components identified in Section 2.2.2 and defined above need to be investigated, which requires the following equipment:

- Camera – to keep record of the observations made.
- Notepad and pen – to document all the observations made and note important information.
- Tape measure – to measure small distances (< 2 m), elevations, and pipe diameters.
- Laser distance meter – to measure larger distances (> 2 m).
- A flotation device – to measure water flow in drains.
- Empty vessel – to measure flow from leaks/holes in pipes, etc.
- Ultrasonic water flow meter – to measure water flow in pipes.

A drawing exchange format (DXF) document of the applicable levels can be sourced from the mine's planning department. This is used to map water flow paths, note locations of certain equipment, measure distances of paths/travelways, and measure elevation changes. Figure 61 illustrates an example of a DXF document of a mining level.

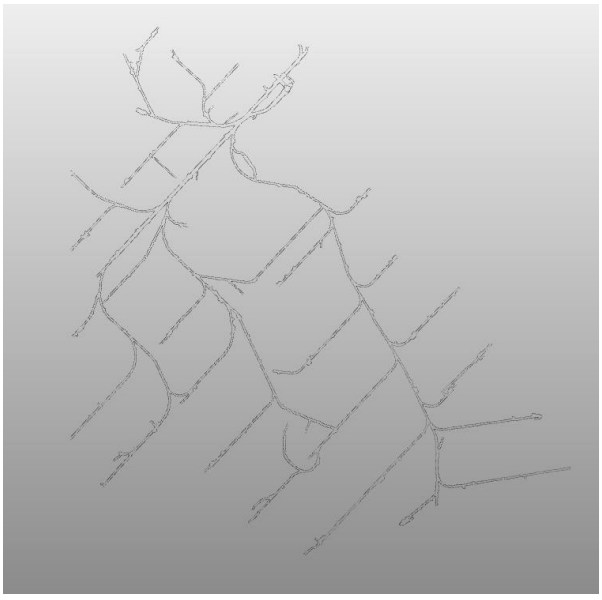

Figure 61: A DXF document of a mining level

Figure 62 shows a DXF document with notes taken during an audit of a level. Generally, multiple copies of the level are made to ensure there is enough space for notes to be taken.

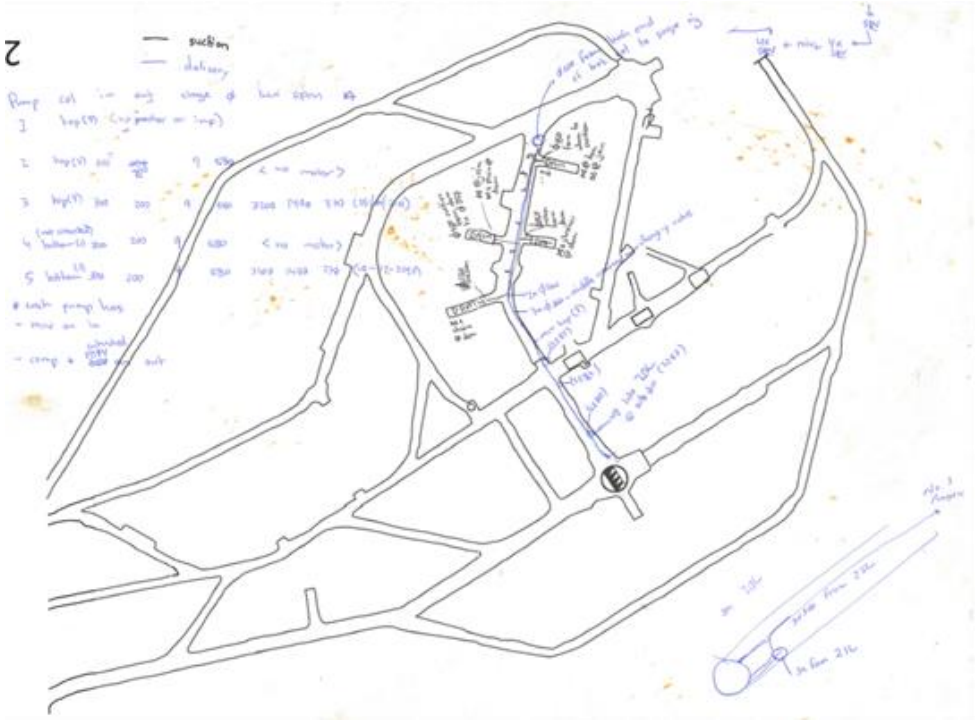

Figure 62: DXF document with notes from an audit

Figure 63 to Figure 72 show typical images taken underground during an audit. These are used to verify the design parameters (such as pipe sizes, equipment specifications, and flow paths) and ensure that the simulation accurately represents the real-life system.

Figure 63: Settler area inlet drains

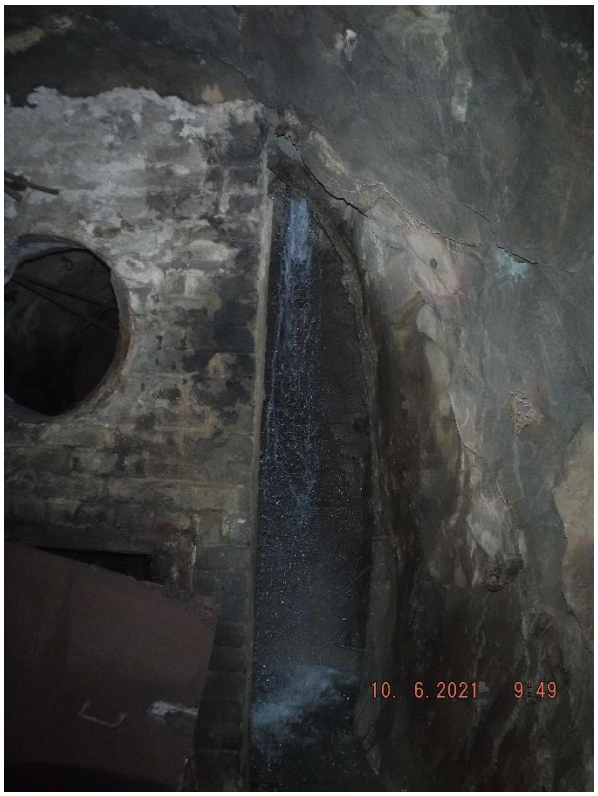

Figure 64: Annex hole that opens onto the footwall

Figure 65: Unfinished pipe with a closed butterfly valve

Figure 66: Pipe configuration with leakages and unfinished sections

Figure 67: Dewatering pump impeller and motor specification plates

Figure 68: Dewatering pump outlet pipe manifold with valves

Figure 69: Dewatering pipe configuration with valves

Figure 70: Dewatering pipe opening into a drain in the settler area

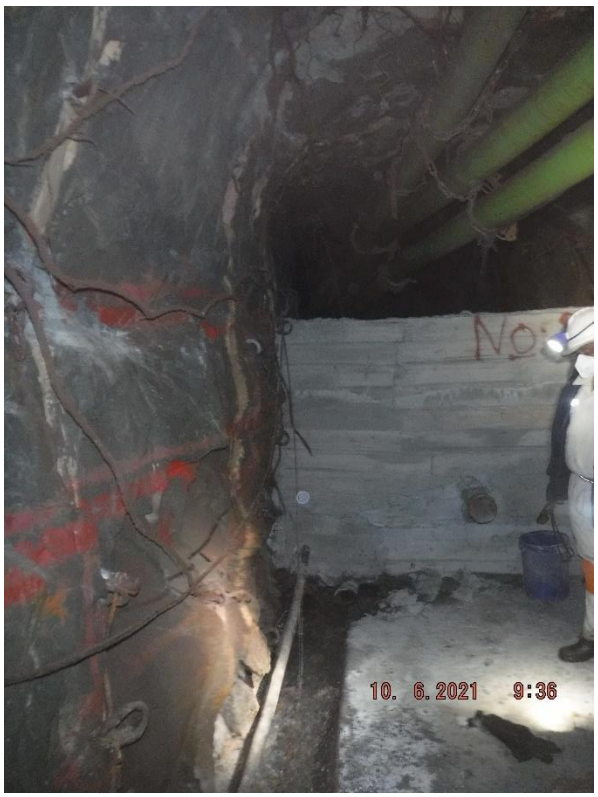

Figure 71: Emergency dam created by closing off a haulage section

Figure 72: Empty settler with a drain manifold constructed to allow water to flow past

Appendix C: SCADA Data Extraction Process

The SCADA system, as depicted in Figure 73, illustrates a system, subsystem, or section in a two-dimensional diagram. The instrumentation that records data is linked to a data tag that is accessed in the diagram window. The tags applicable to the system are visible in data boxes that can be clicked to extract historical data.

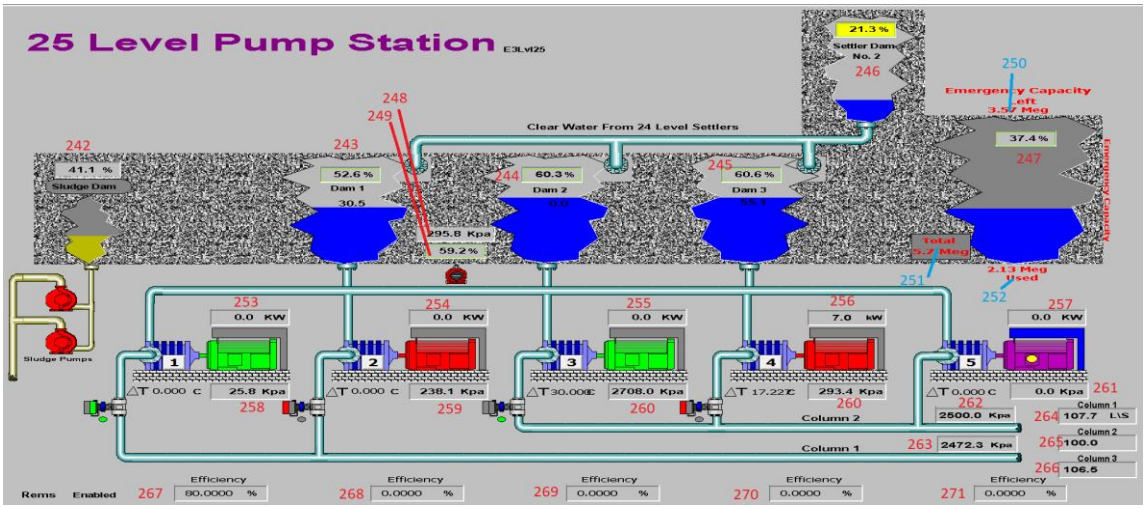

Figure 73: SCADA user interface

As tag names can sometimes be misleading, a database is usually available with tag descriptions. Table 17 defines the tag names with matching descriptions applicable to the pump station system in Figure 73. For ease of use, a tag number (labelled in red on Figure 73) was manually assigned to the matching SCADA tag on the SCADA diagram window in Figure 73.

Table 17: SCADA tag categorisation

25L Pump Chamber		
Tag No.	**SCADA Tag Name**	**Tag Description**
242	T25_LT_A5PV	PS25 25 Lvl Sludge Dam Level
243	T25_LT_A1PV	PS25 25 Lvl Clear Water Dam 1
244	T25_LT_A2PV	PS25 25 Lvl Clear Water Dam 2
245	T25_LT_A3PV	PS25 25 Lvl Clear Water Dam 3
246	T25_LIT_25SL	PS25 Settler Dam No. 2
247	T25_EME_PV	Emergency Dam Capacity level

25L Pump Chamber		
248	T25_PT_A11	PS25 Pumps Suction Press
249	T25_LT_A10PV	PS25 25 Lvl Pump Suction Column
250	T25_EME_Available /1000	#N/A
252	T25_EME_Used /1000	#N/A
253	T25_JT_A8PV	PS25 Pump 1 Motor Power
254	T25_JT_B8PV	PS25 Pump 2 Motor Power
255	T25_JT_C8PV	PS25 Pump 3 Motor Power
256	T25_JT_D8_C	#N/A
257	T25_JT_E8PV	PS25 Pump 5 Motor Power
258	T25_PI_A40	PS25 Pump 1 Delivery Press
259	T25_PI_B40	PS25 Pump 2 Delivery Press
260.1	T25_PI_C40	PS25 Pump 3 Delivery Press
260.2	T25_PI_D40	PS25 Pump 4 Delivery Press
261	T25_PI_E40	PS25 Pump 5 Delivery Press
262	T25_PI_A31	PS25 Column 2 Press
263	T25_PI_A30	PS25 Column 1 Press
264	T25_FIT_COL1PV	25 LV Column 1 Water Flow
265	T25_FIT_COL2PV	25 LV Column 2 Water Flow
266	T25_FIT_COL3PV	25 LV Column 3 Water Flow
267	T25_PUMPEFF_01	Pump 1 Efficiency Value
268	T25_PUMPEFF_02	Pump 2 Efficiency Value
269	T25_PUMPEFF_03	Pump 3 Efficiency Value
270	T25_PUMPEFF_04	Pump 4 Efficiency Value
271	T25_PUMPEFF_05	Pump 5 Efficiency Value
A15	T25_DELTA_T1	25 Lvl Pump No. 1 Delta Temp
A16	T25_DELTA_T2	25 Lvl Pump No. 2 Diff Temp
A17	T25_DELTA_T3	25 Lvl Pump No. 3 Delta Temp
A18	T25_DELTA_T4	25 Lvl Pump No. 4 Delta Temp
A19	T25_DELTA_T5	25 Lvl Pump No. 5 Delta Temp
A20	T25_LT_F1PV	PS25 25 Lvl Clear Water Dam 1
A21	T25_LT_F2PV	PS25 25 Lvl Clear Water Dam 2
A22	T25_LT_F3PV	PS25 25 Lvl Clear Water Dam 3

Once the desired tag is identified, it can be imported into PTB to ensure all the data is kept and is accessible in one place. Figure 74 illustrates PTB's SCADA function – the tag applicable to a component can be added to that component's directory. From there, data available on SCADA can be accessed through PTB in graphical form or as Excel data.

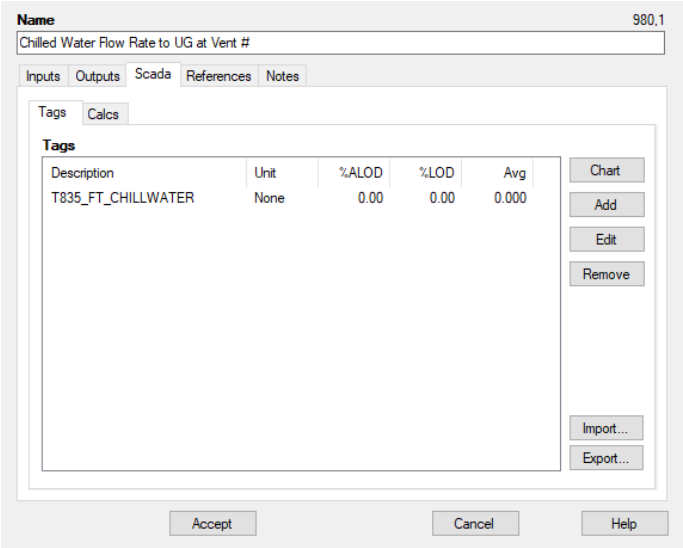

Figure 74: PTB's SCADA function

Figure 75 and Figure 76 show graphical illustrations of historical SCADA data for a water flow meter on a pipe. Figure 75 illustrates the actual data for the defined period given a one-hour interval. The data points are extracted on an hourly basis across the period.

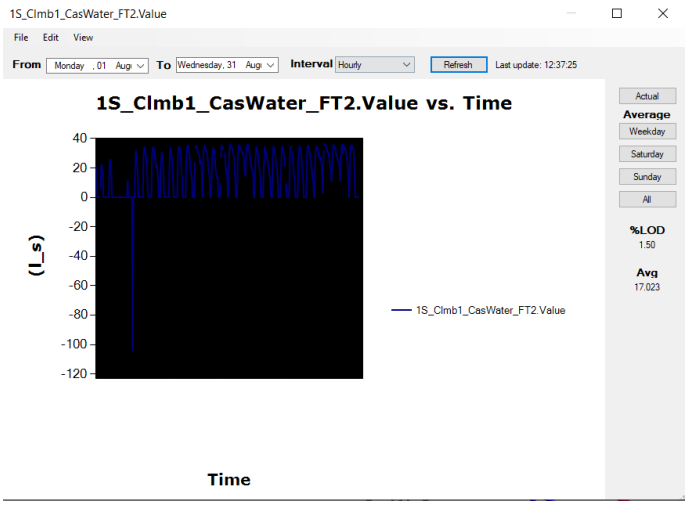

Figure 75: SCADA data for water flow rate over one month on an hourly interval

Figure 76 illustrates the same data set taken in Figure 75 but only data acquired on weekdays were considered and then averaged.

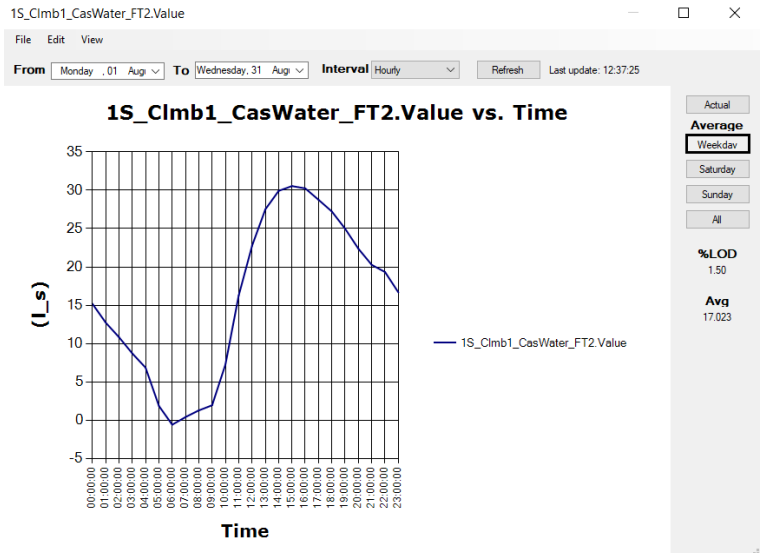

Figure 76: SCADA data for water flow rate over one month with a weekday average calculated

Figure 77 illustrates how data is exported to Excel from PTB's SCADA function. The period considered with the defined interval is located in the left-most column (column A) while the values applicable to that point in time is located in the right column (column B).

	A	B	C
1		1S_Clmb1_CasWater_FT2.Value	
2	2022/08/01 00:00	20.08661748	
3	2022/08/01 01:00	16.93068141	
4	2022/08/01 02:00	5.850726153	
5	2022/08/01 03:00	0.095467934	
6	2022/08/01 04:00	0.107461906	
7	2022/08/01 05:00	0.103429052	
8	2022/08/01 06:00	0.087831957	
9	2022/08/01 07:00	0.086108026	
10	2022/08/01 08:00	0.092310017	
11	2022/08/01 09:00	0.123345397	
12	2022/08/01 10:00	0.126521234	
13	2022/08/01 11:00	NaN	
14	2022/08/01 12:00	NaN	
15	2022/08/01 13:00	6.237139449	
16	2022/08/01 14:00	21.99143571	
17	2022/08/01 15:00	21.79748562	
18	2022/08/01 16:00	21.61515939	
19	2022/08/01 17:00	18.24008195	
20	2022/08/01 18:00	17.72682522	
21	2022/08/01 19:00	12.43265652	
22	2022/08/01 20:00	0.533343549	
23	2022/08/01 21:00	0.133807076	
24	2022/08/01 22:00	0.139956221	

Figure 77: Excel export of SCADA data from PTB

In the case of data loss, the respective data points will be exported as NaN. This ensures that these points do not affect calculations such as when averages are calculated.

Appendix D: Detailed PTB Water Component Inputs and Outputs

Water nodes are used in PTB to link other water components in the simulation environment. These nodes are required where flow paths split or a change in elevation occurs. The nodes provide the system's environmental conditions, such as temperature, pressure, and enthalpy, at specified points. Figure 78 illustrates a water node's input and output interface.

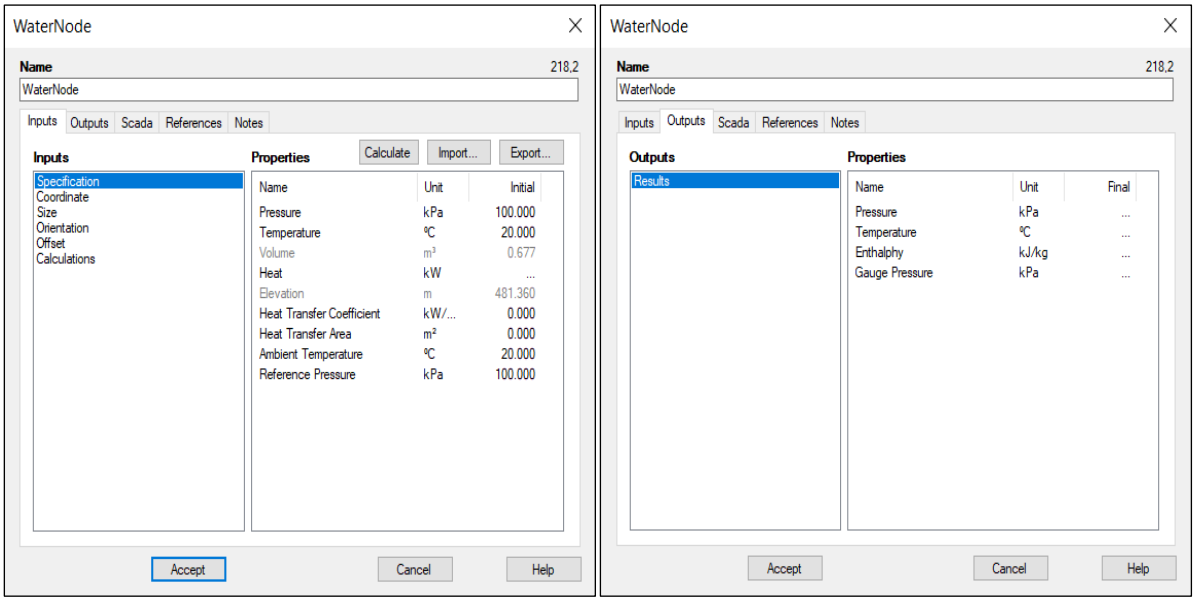

Figure 78: Water pressure node input and output interface

The outputs of a component in PTB can either be provided in a tabular or graphical format. Figure 79 illustrates both output variations for a water node's pressure output. The output data is exported to either a bitmap or Excel-compatible file for further processing.

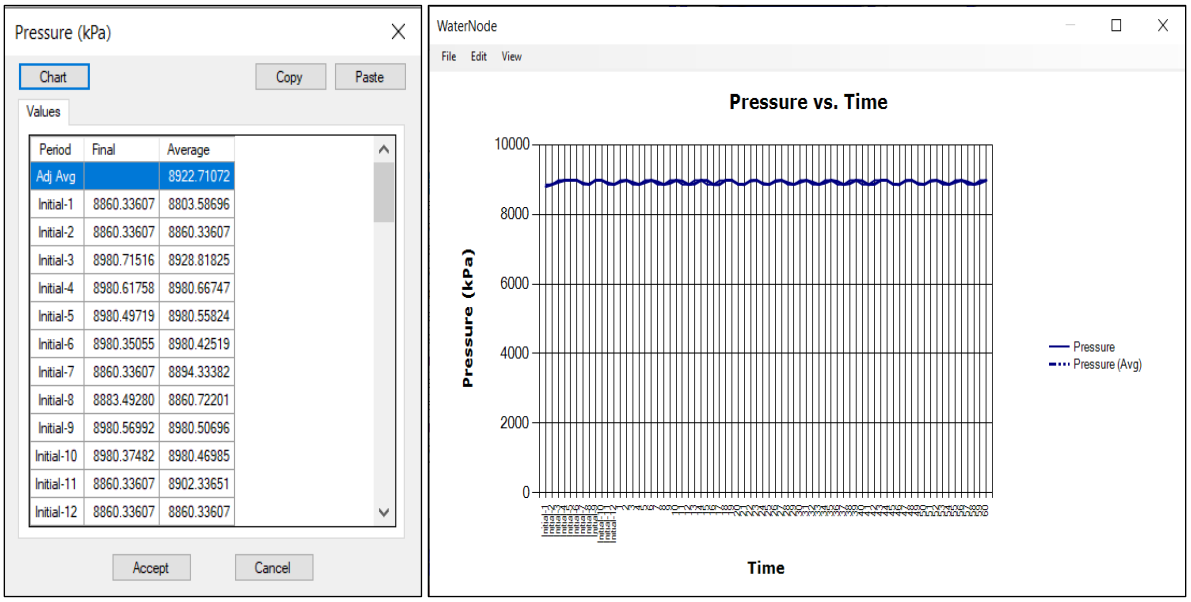

Figure 79: Tabular and graphical results of a water pressure node's pressure output

Water pipes are usually included between water nodes to represent the actual system's water flow paths. The water pipes are used to calculate the losses of the network and the convective heat transfer coefficient using the hydraulic calculate and thermo-calculate input interface, respectively. Figure 80 depicts the input parameters for each calculation that can be carried out by the water pipe component.

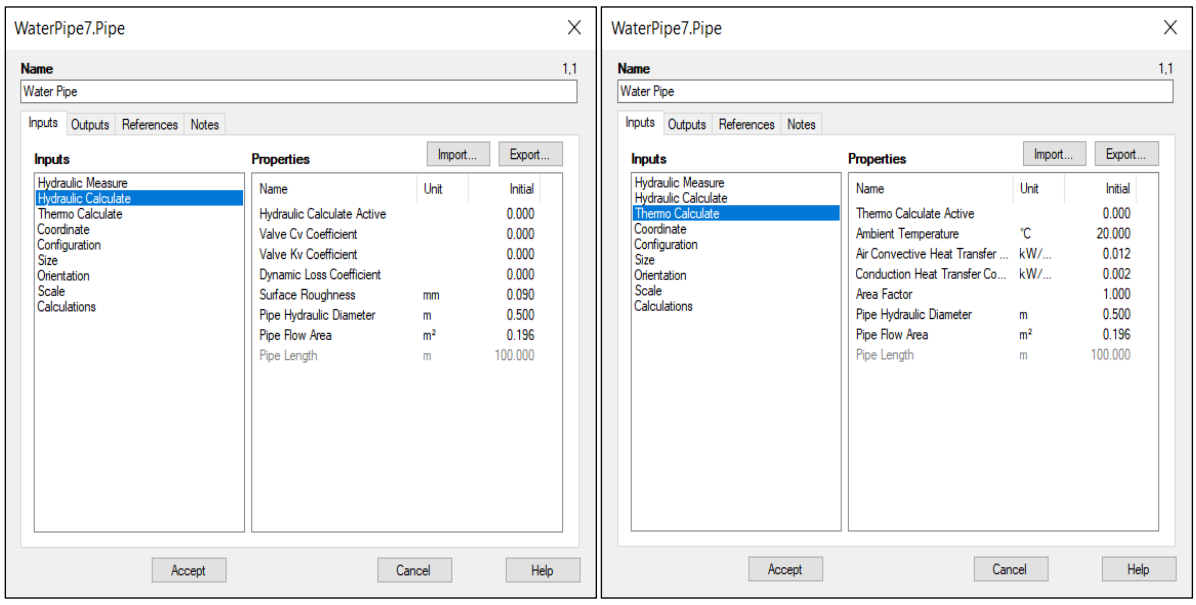

Figure 80: Water pipe hydraulic and thermodynamic input parameter interfaces

Figure 81 shows the pipe's hydraulic measure input parameters. The flow, inlet pressure, and outlet pressure are initial values that get adjusted by the simulation according to the calculations carried out on the nodes before and after the water pipe component, respectively. Important to note here is that the pipe's valve fraction can be changed. This can vary according to a profile provided to the simulation to stop, decrease, or increase flow through a pipe section.

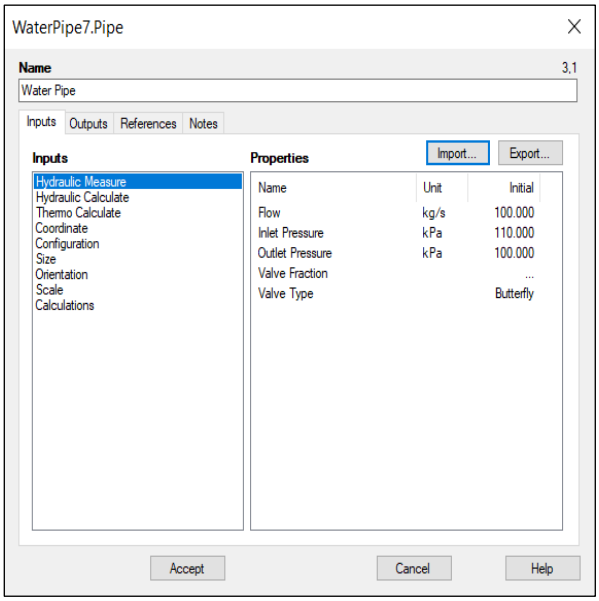

Figure 81: Water pipe hydraulic measure input parameters

PTB has a range of predetermined pipe selections commonly found in industry with pipe sizes ranging from 25 mm to 1 000 mm. The platform further has a selection of valves (gate valve, butterfly valve, check valve, and globe valve) that can be imported with the corresponding pipe size. This eases the simulation construction process as each water pipe component already has a precalculated value. Figure 82 illustrates the imported values associated with a 200 mm pipe with a butterfly valve.

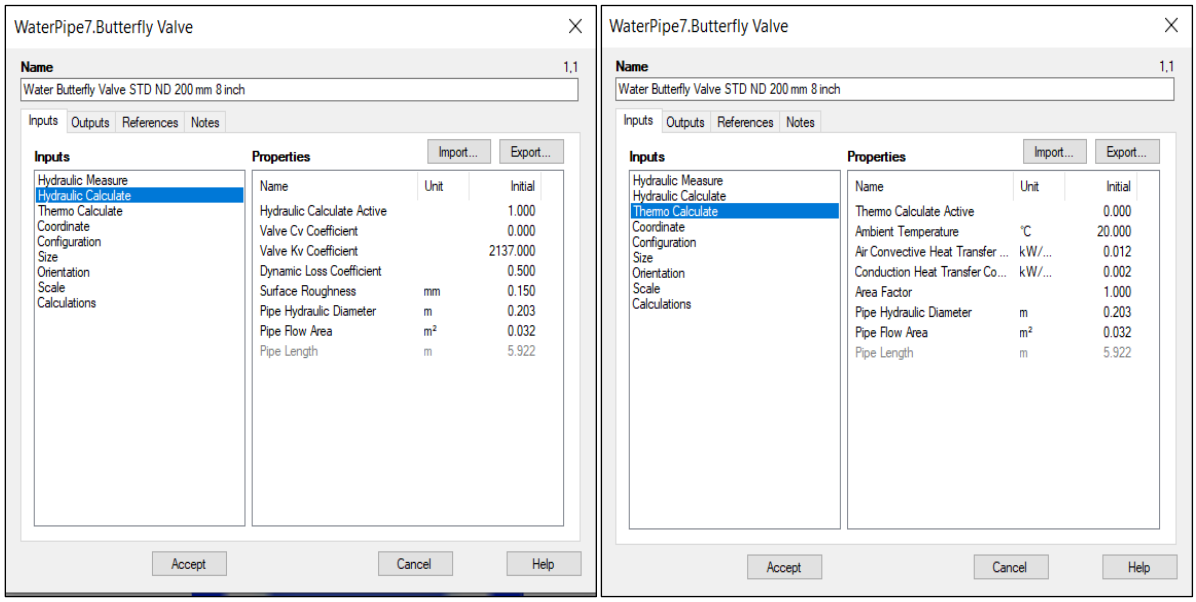

Figure 82: Hydraulic and thermodynamic properties associated with a 200 mm pipe with a butterfly valve

Each pipe has its own unique set of input values that can be adjusted to obtain the correct output values during calibration according to the measured results. The 'active' value can set to either '1' or '0' ('1' being yes, and '0' being no) to indicate whether that function should be included in the calculation.

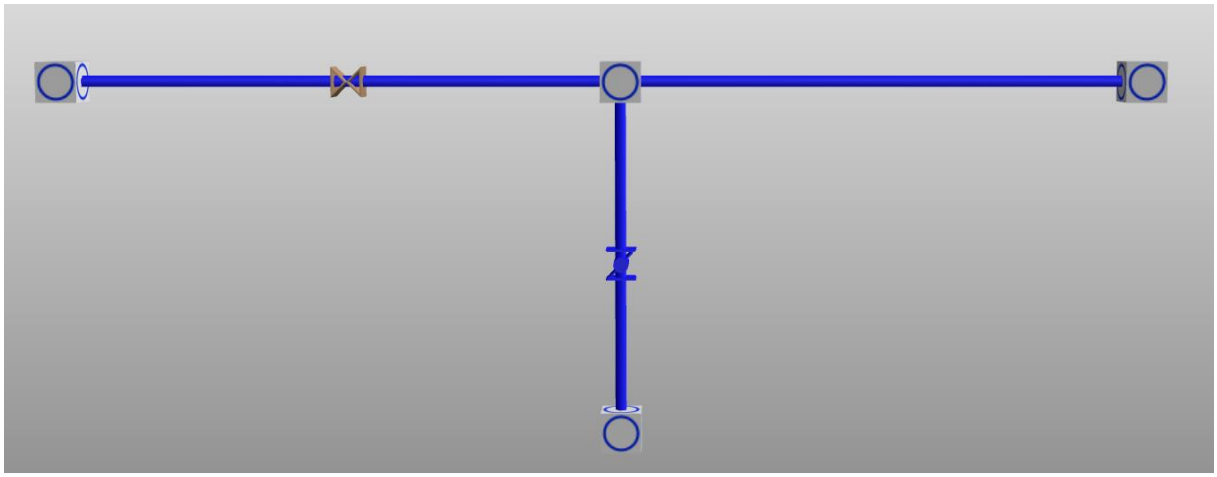

Figure 83: Basic water pipe – water node connection

As previously mentioned, changes to the pipeline, such as tie-offs, reductions/restrictions, and elevation changes, can be simulated using water nodes. Figure 83 indicates a basic water pipe to node connection with a T-split. The figure also shows PTB's illustration of the pipe's

valves. The bottom pipe includes a butterfly valve; the left split includes a check valve; and the right split pipe does not have a valve.

The pipe's hydraulic diameter and pipe flow area are the two most important input parameters. These two values must correspond with that of the real-world pipe's values to ensure the highest level of simulation accuracy. The distance of the pipe is also important for the simulation to calculate losses, but this is automatically calculated in PTB as the nodes are connected.

Figure 84 shows the output interface of a water pipe. During the simulation calculations, it is assumed that the thermal-dynamic conditions remain constant along the length of the pipe.

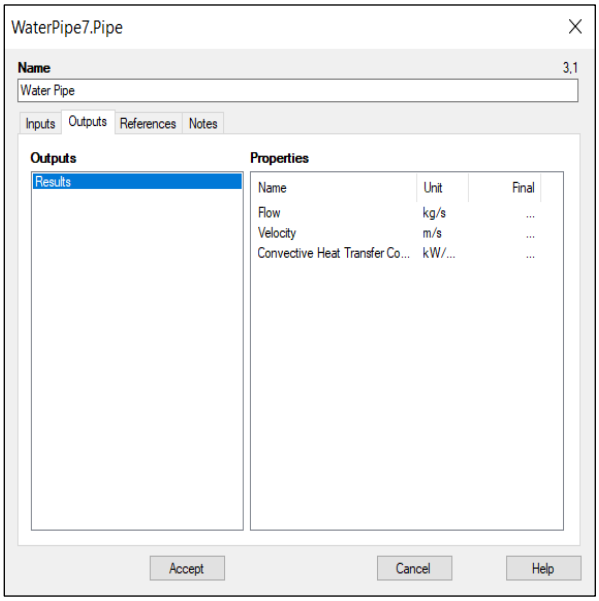

Figure 84: Water pipe output interface

The next component, following from Table 3, is the water pressure boundary. As the name suggests, this component is used to characterise the boundary conditions of the system. It maintains the user-specified pressure and temperature profiles – shown in Figure 85 – that indicate the conditions where the boundaries of the system are defined. A water pressure boundary essentially acts as an infinite source or volume that can be connected to a water pipe component to produce a flow rate or to allow water to move into.

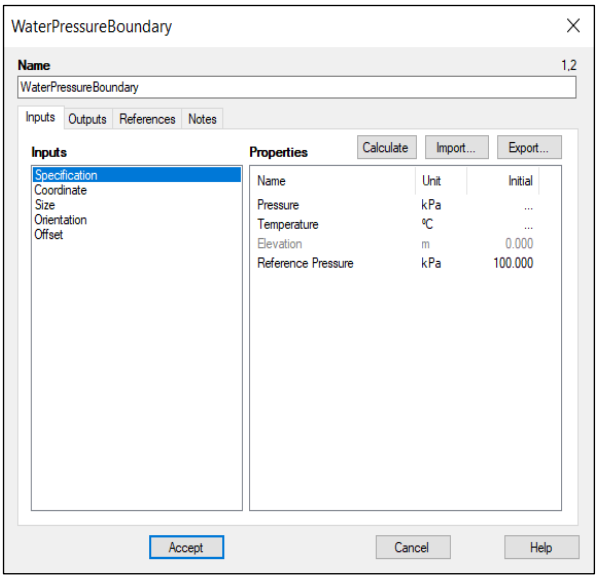

Figure 85: Water pressure boundary input interface

The next component is a water pump for simulating the operation of real-life dewatering pumps. Water pumps generate a pressure difference in the network to induce water flow. The flow that is generated is a function of the pressure difference over the water pump. The water pump component requires significant input as shown in Figure 86 – most of which can be acquired from the actual pump curve. Also shown in Figure 86 is the output interface. The water pump component acts as a specialised pipe component that can be connected between two nodes.

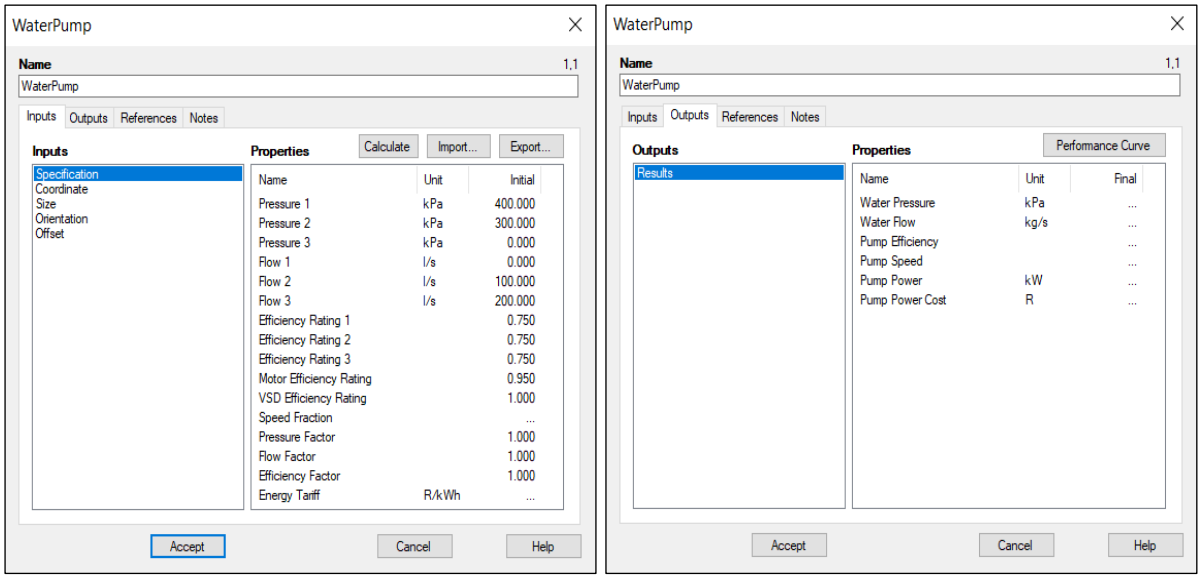

Figure 86: Water pump input and output interface

If the curve is unavailable, use the equations that follow to estimate the parameters. The required data can be obtained through the digital system or through manual measurements done during the system investigation phase.

Equation 3

$$\nu = \frac{\mu}{\rho}$$

Where:

- $\nu =$ Kinematic viscosity [mm^2/s]
- $\mu =$ Absolute viscosity [mPa·s]
- $\rho =$ Fluid density [kg/m^3]

Equation 4

$$V = \frac{Q}{A}$$

Where:

- $V =$ Velocity [m/s]
- $Q =$ Volumetric flow rate [m^3/s]
- $A =$ Area [m^2]

Equation 5

$$Re = \frac{D \times V \times \rho}{\mu}$$

Where:

- $Re =$ Reynold's number
- $D =$ Hydraulic diameter [m]
- $V =$ Velocity [m/s]
- $\rho =$ Fluid density [kg/m^3]
- $\mu =$ Absolute viscosity [Pas]

Equation 6

$$P_{ideal} = \rho \times g \times h$$

Where:

- P_{ideal} = Static pressure/head [kW]
- ρ = Fluid density [kg/m^3]
- g = Gravitational acceleration [m/s^2]
- h = Pumping height [m]

Equation 7

$$P_{required} = \frac{P_{ideal}}{\eta_{pump}}$$

Where:

- $P_{required}$ = Required pressure/head [kW]
- P_{ideal} = Static pressure/head[kW]
- η_{pump} = Pump efficiency[–]

Equation 8

$$P_{motor} = \frac{P_{required}}{\eta_{motor}}$$

Where:

- P_{motor} = Pump motor power [kW]
- $P_{required}$ = Required pressure/head [kW]
- η_{motor} = Pump motor efficiency[–]

Equation 9

$$F_p = \frac{f_d \times L \times \rho \times V^2}{2 \times D}$$

Where:

- F_p = Pipe friction loss [Pa]
- f_d = Darcy friction factor [–]
- L = Length [m]
- ρ = Fluid density [kg/m^3]
- V = Velocity [m/s]
- D = Hydraulic diameter [m]

Equation 10

$$f_d = \frac{64}{Re}$$

Where:

- f_d = Darcy friction factor [–]
- Re = Reynold's number [–]

A water dam is the final water system component. This can either be configured as a round dam or a square dam as depicted in Figure 87. Figure 88 indicates the water dam's input and output interface. The water dam component acts as a specialised node component that is connected between two pipes.

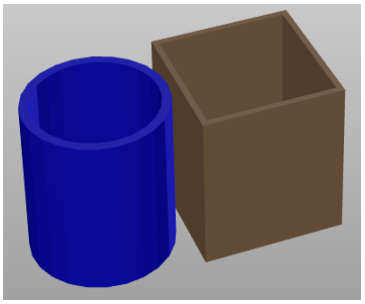

Figure 87: Water dam configurations

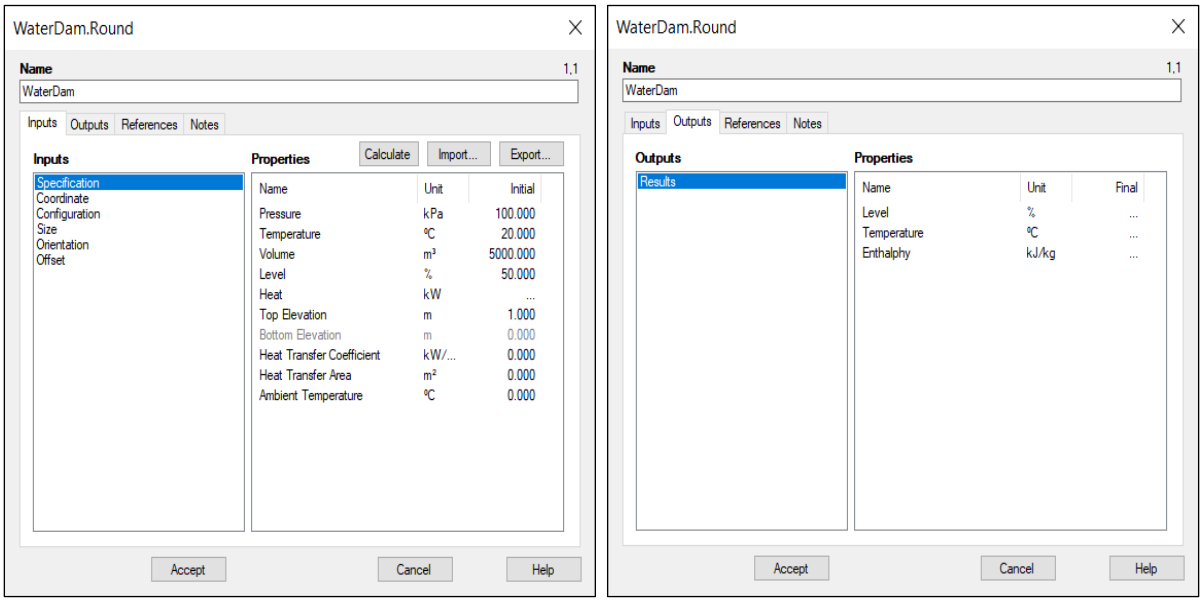

Figure 88: Water dam input and output interface

The water dam's bottom elevation corresponds to its coordinate value, but the top elevation needs to be defined along with the volume according to its size. These inputs ensure that the dam level outputs respond accordingly to the size of the actual dam.

The five components listed above are used to construct the dewatering system in the simulation platform. Each component is defined according to the parameters of the physical component they represent. However, controllers need to be included in order to control the system as it would be controlled in reality. PTB has two controllers, namely a PI controller and a step controller, that can be of good use.

A PI controller delivers an output of between 0 and 1 to control the component according to the user-defined schedule. A step controller, on the other hand, delivers an output of either 0 or 1. Figure 89 and Figure 90 provide the input and output interfaces of the PI controller and the step controller, respectively.

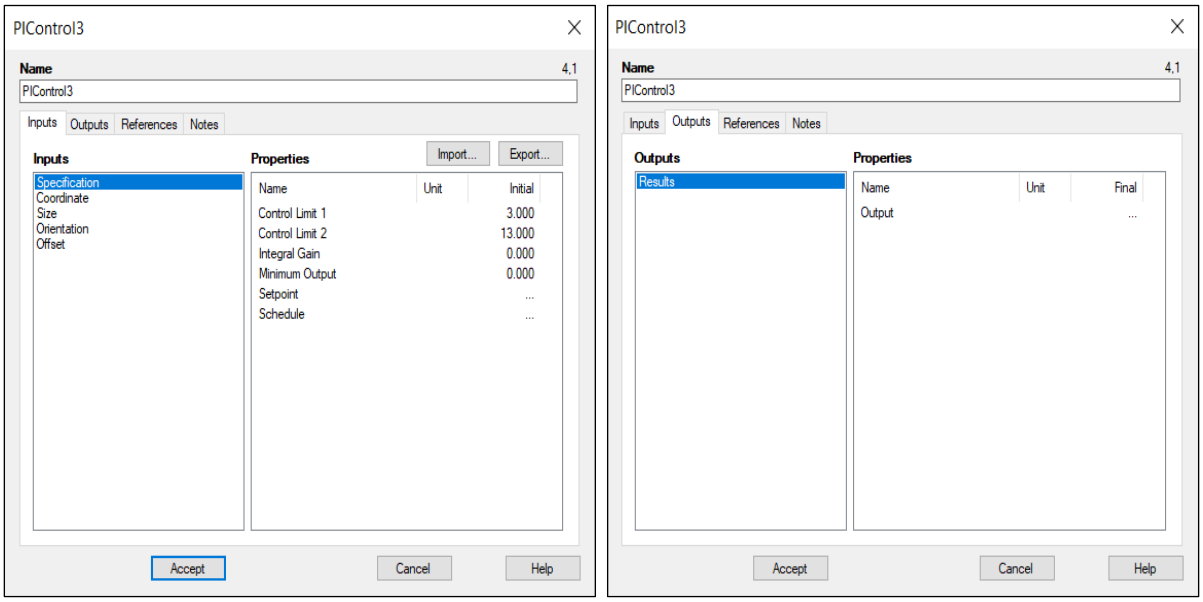

Figure 89: PI controller's input and output interface

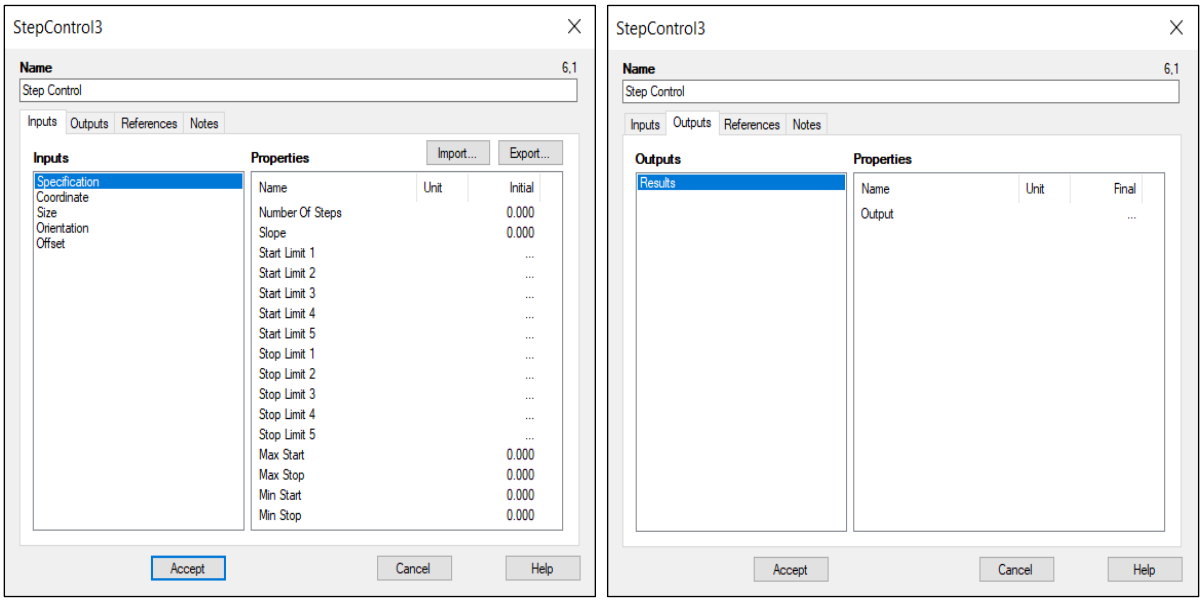

Figure 90: PI controller's input and output interface

Both controllers use the output value of a component as the initial value. If the initial value does not match the defined schedule value, the controller alters the connected component's input value until the desired value is obtained. The only difference is that the step controller can only use a stop/go or open/close function while a PI controller can vary the output function. For example, if the controllers are connected to a dam and a pump that is scheduled to control the pump's flow rate based on the dam's level:

- The PI controller acts as a variable speed drive and alters the pump's performance until the dam level reaches equilibrium on the set point.
- The step controller switches the pump on and off to keep the dam level as close to the set point as possible.

Figure 91 illustrates a control philosophy on a basic water system. The water pressure boundary's pressure and temperature are defined according to the chosen boundary conditions at that point. This provides a water flow through a pipe and into a dam. A PI controller is used to define the water flow through the pipeline. The controller throttles the valve through the valve fraction input of the water pipe to achieve the desired flow. A step controller is used to control the level of the dam between 40% and 60%. The step controller's start limit 1 is set to 60 and the stop limit 1 is set to 40. This ensures that the pump starts pumping at 60% and stops pumping at 40%. The water is pumped to the water boundary exit, which is defined according to the conditions at that point.

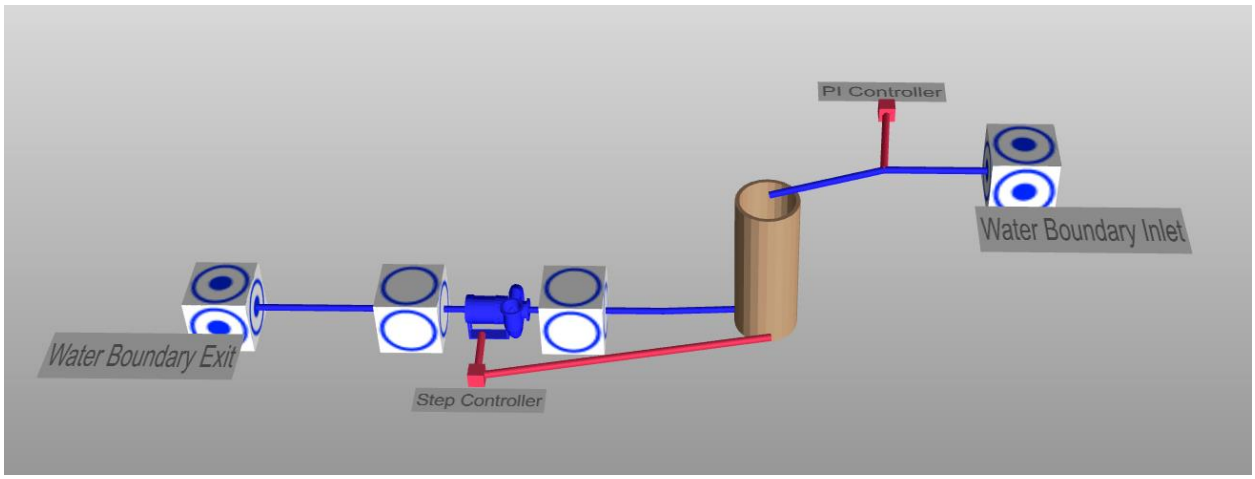

Figure 91: Basic control system

Figure 92 depicts the output of the PI controller with the corresponding water flow rate for the defined input parameters. Figure 93 depicts the pump flow rate and dam levels that correspond to the output of the step controller.

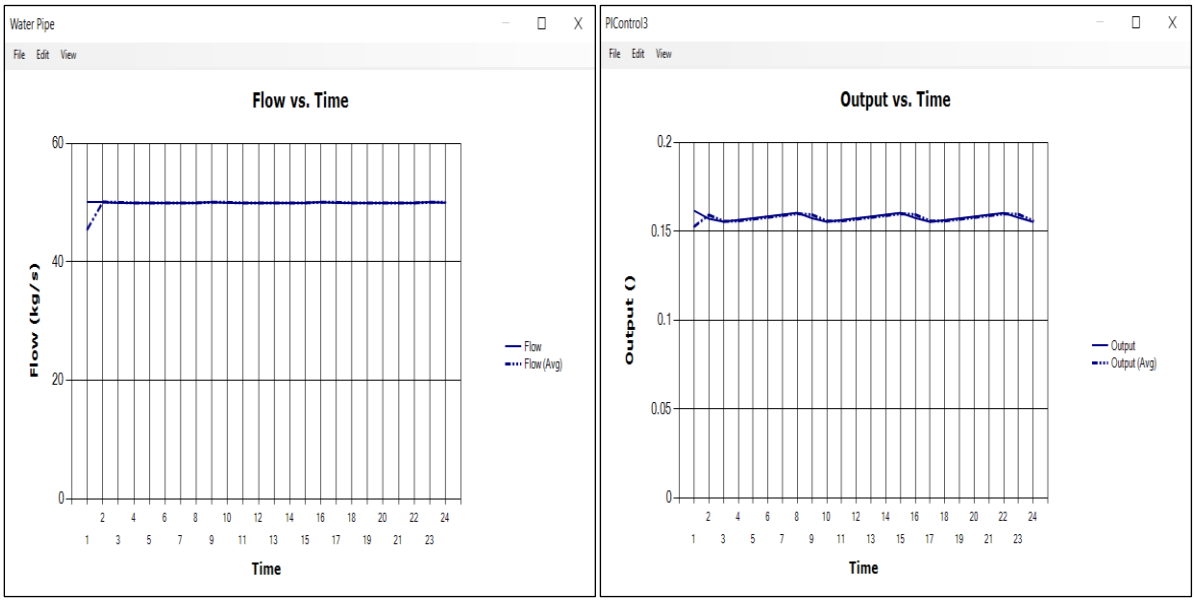

Figure 92: PI controller outputs and corresponding water pipe flow rate

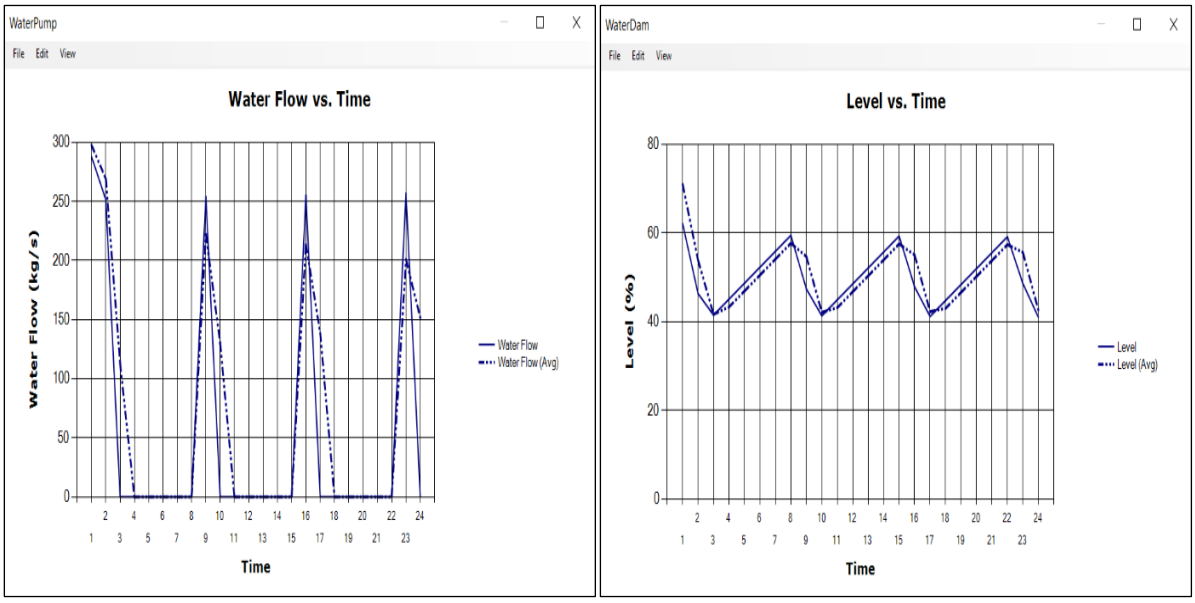

Figure 93: Pump flow rate and dam levels corresponding to the step controller outputs

The final function to note on the PTB simulation platform is the simulation properties as defined in Figure 94. The simulation time period can be adjusted to the requirements; in this instance, a 24-hour simulation period is selected. The component output provides the values calculated at the end of each time period. The time steps correspond to the number of calculations done within each time period. For example: in a 24-hour time period, if there are 60 time steps, 60 calculations will be done in one hour, therefore providing a calculation for

each minute of the 24 hours. The size of the time step corresponds to the breakdown of the time period; therefore, 3 600 indicates the number of seconds in one hour.

If the output is required in half-hourly increments of a 24-hour period, the time period is adjusted to 48 (48 half-hour periods); the time steps can be changed to 30 (30 calculations per time period – 30 minutes per half hour); and the size changed to 1 800 (1 800 seconds per half hour).

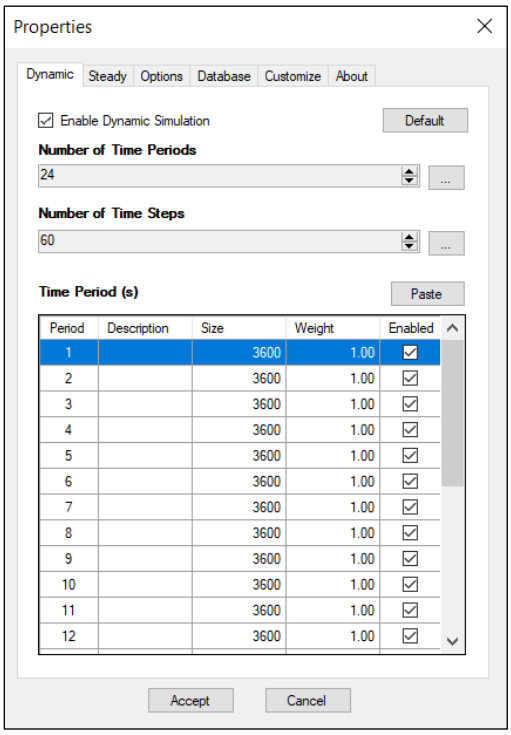

Figure 94: Simulation properties

Lastly, on the simulation properties, it is evident that PTB can simulate steady-state or dynamic environments. Due to the mining environment being a proven dynamic system, the 'enable dynamic simulation' will always be selected.

Appendix E: Simulation Results of Mine B and Mine C

This section is aimed at applying the research method to two other mines (Mine B and Mine C) to test the method's generic applicability. Mine B and Mine C are situated in South Africa and are both single-shaft, medium- to deep-level mining complexes. A 48-hour total power failure emergency requirement also applies to both shafts as stipulated by their managing structures.

Mine B

After thorough and detailed system investigation iterations specifying the system parameters, physical and digital investigations, the following information was obtained on Mine B:

- Potable water is supplied by the local municipality. Most potable water is wasted and is, therefore, considered in the dewatering system.
- Service water is supplied by a surface refrigeration system and supplied in the form of cascade and hydropower water.
- Fissure water is located at different points in the shaft.
- There is only one dewatering level, namely 27L. The water is pumped directly to surface from 27L. In the event of pump failure, two additional pumps can pump water from 27L to a joining shaft's dams on 16L.

Figure 95 depicts the water flow rates considered for the simulation, and Figure 96 illustrates the defined system parameters for Mine B. As previously mentioned, the system parameters are specified concurrently with the physical and digital investigations. Therefore, the information provided in Figure 96 is the culminations of a complete, iterated system investigation.

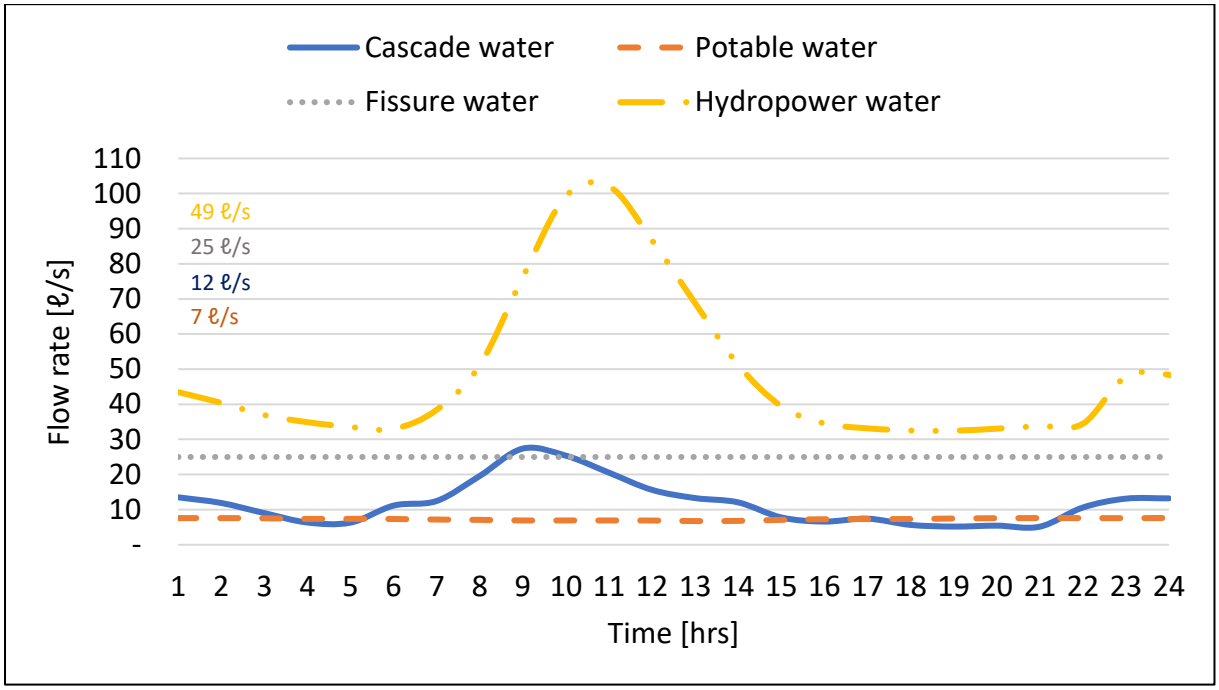

Figure 95: Water flow rates for Mine B

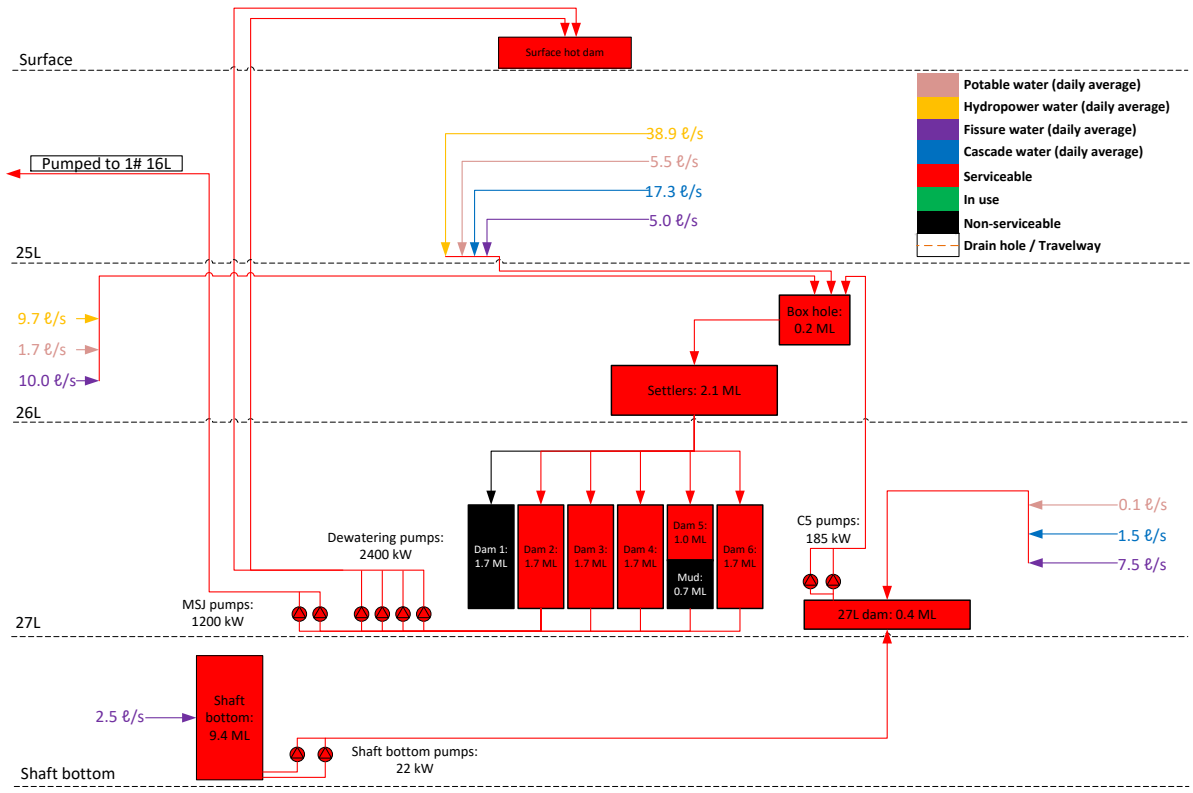

Figure 96: Mine B's defined system parameters

The baseline simulation PTB model, developed according to the information gathered in the system investigation, is depicted in Figure 97. The simulation was developed to depict the real-world environment and simulate everyday operations accurately. The components are all represented on a 1:1 scale as identified during the physical investigation while controllers were used to ensure the simulation is representative of daily operating procedures (such as flow rates, pump and schedules).

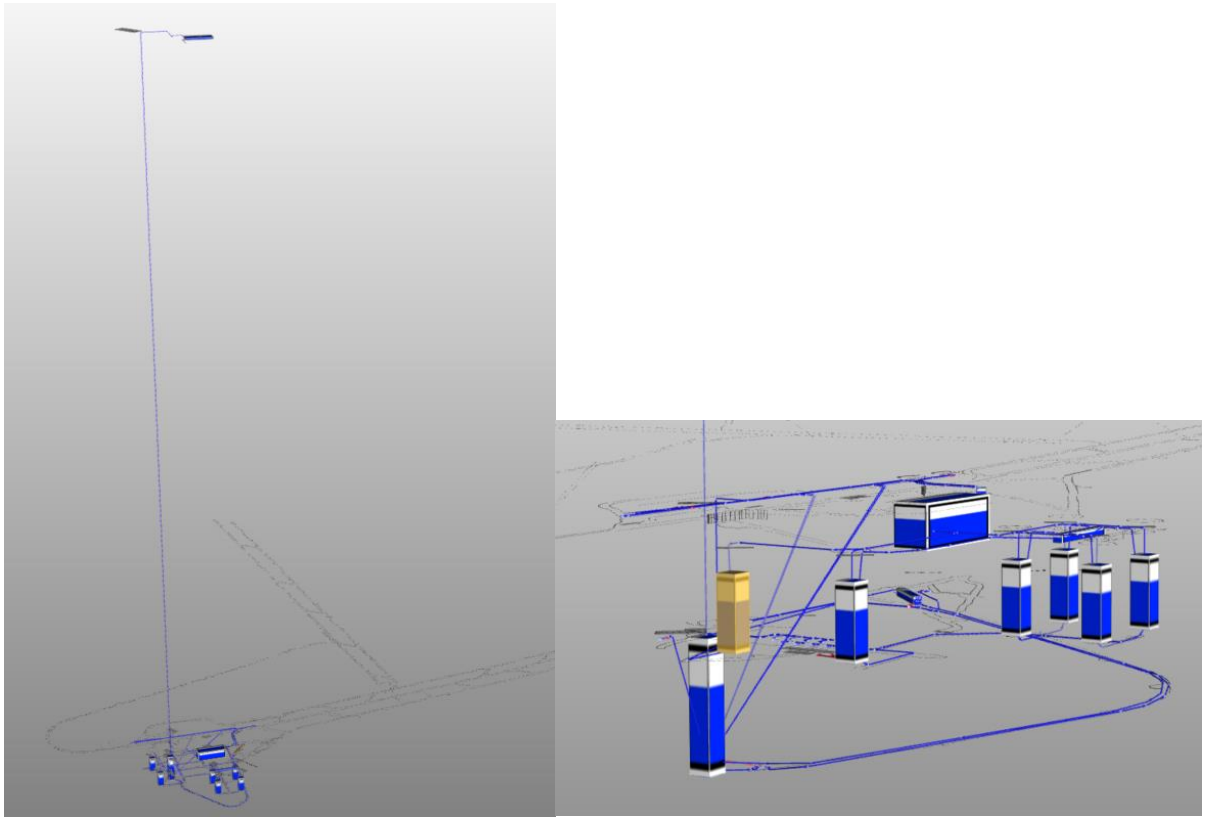

Figure 97: Baseline PTB simulation model of Mine B's dewatering system

An extensive calibration and verification cycle yielded a successful simulation model calibration as none of the components fell short of the 5% calibration requirement. Therefore, the model accurately reproduces the dewatering operating conditions of Mine B and can be used for what-if analyses.

In keeping with the research aim and objectives, the what-if analysis is conducted to determine the shaft's water storage capability during a total power failure. Table 18 summarises the shaft's available storage capacity during a total power failure according to the information gathered during the investigations.

Table 18: Mine B's available emergency capacity

Capacity	Verified capacity [Mℓ]
Spare capacity of 27L dams	5.70
Shaft bottom	9.40
Total	**15.10**

The following was identified through the physical investigation:

- During a total power failure, the hydropower supply will immediately be cut off as hydropower requires electricity to operate.
- During a power failure, the spindle pumps on each level will not be operational.
    - The water on each level will not be pumped to the required drain holes.
    - The water will flow along the drains, channel through the tips, and flow into shaft bottom.

Figure 98 illustrates the flow profiles for the water sources in Mine B during a total power failure, and Figure 99 illustrates the storage capacity levels during the total power failure.

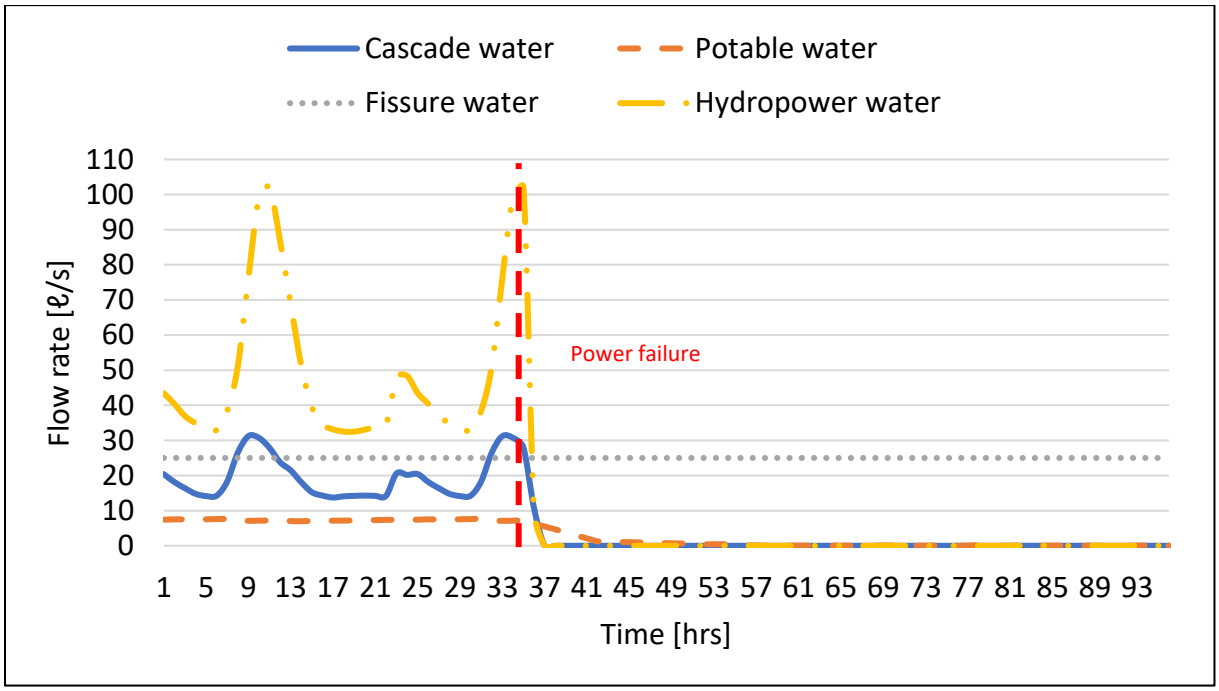

Figure 98: Mine B's total power failure water flow rates

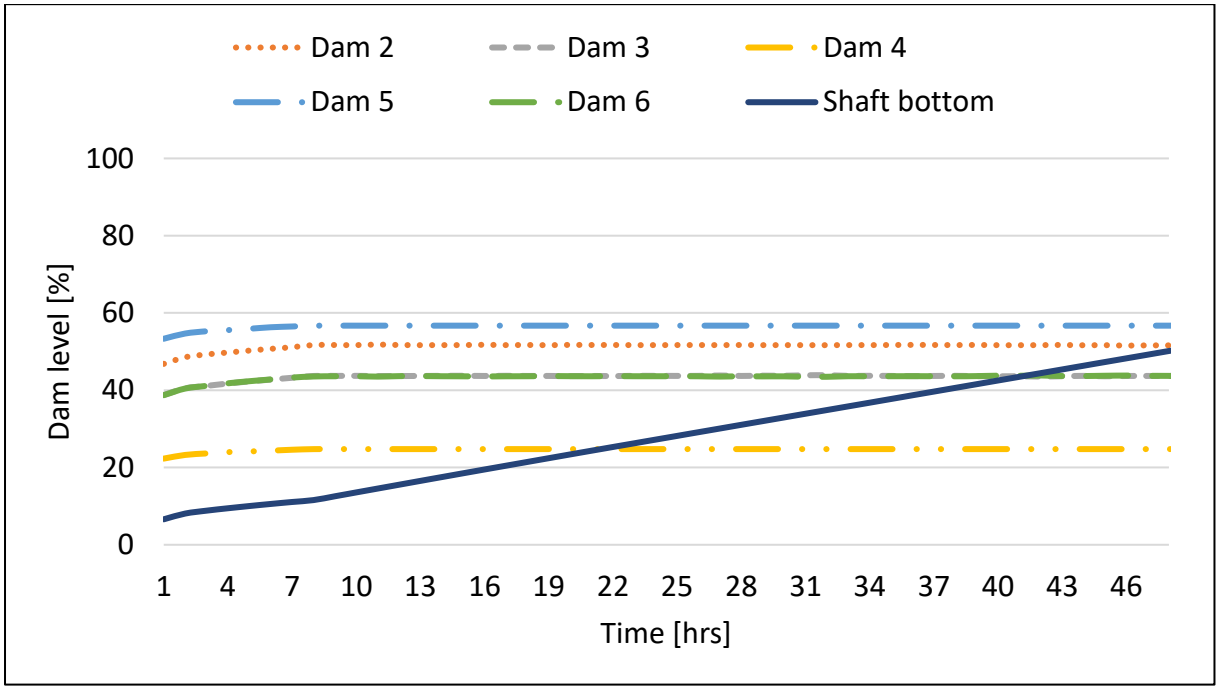

Figure 99: Mine B's total power failure capacity results

Mine B's emergency storage capacity adhered to the stipulated 48-hour requirement and did not require any scenario simulations to be run or upgrades to infrastructure made. Table 19 summarises the results for Mine B's flood time.

Table 19: Summary of results for Mine B's flood time

No.	Description	Total hours
0	Industry method	138
1	Simulated existing configuration	> 48

Mine C

After thorough and detailed system investigation iterations specifying the system parameters, physical and digital investigations, the following information was obtained on Mine C:

- Potable water is supplied by the local municipality.
- Service water is supplied by a surface refrigeration system in the form of a cascade.
- Fissure water is located at different points in the shaft.

- There is only one dewatering level, namely MPS, located below 16L. The water is pumped directly to surface from MPS.
- The shaft receives a fissure water from a joining shaft (i.e., Shaft 2, known as 2#).
    - Most fissure water is piped and gravity-fed to the settler area.
    - The remainder of the fissure water is pumped at certain times throughout the day and varies over a 24-hour profile.
- The shaft is able to receive water from another joining shaft (1#) at times, but this is a rare occurrence.

Figure 100 depicts the water flow rates considered for the simulation, and Figure 101 illustrates the defined system parameters for Mine B. As previously mentioned, the system parameters were specified concurrently with the physical and digital investigations. Therefore, the information provided in Figure 101 is the culmination of a complete, iterated system investigation.

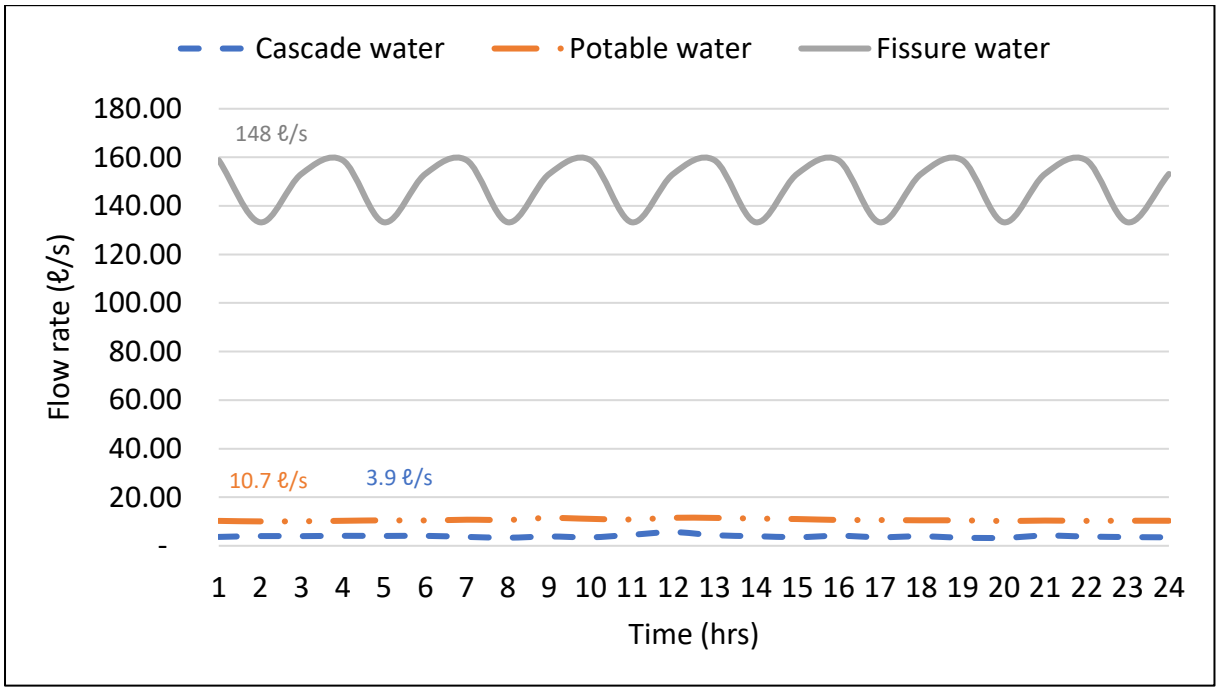

Figure 100: Water flow rates for Mine C

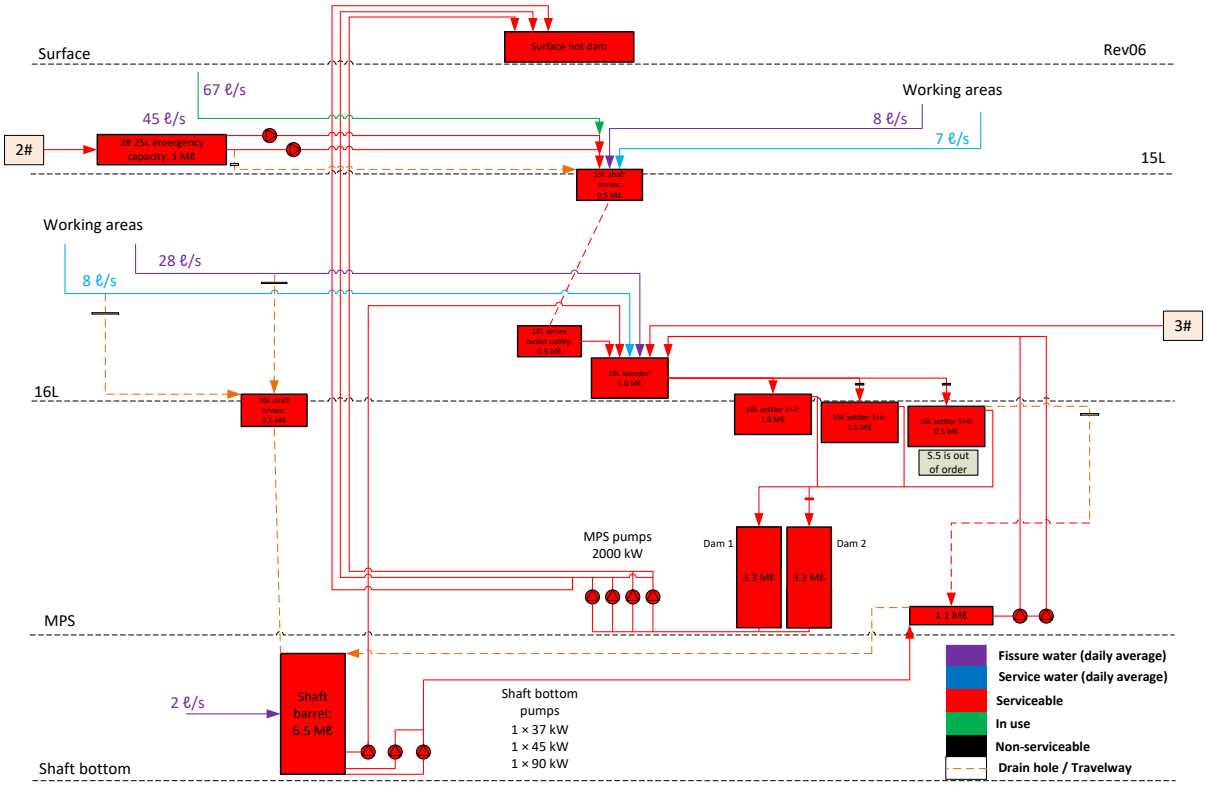

Figure 101: Mine C's defined system parameters

The baseline simulation PTB model, developed according to the information gathered in the system investigation, is shown in Figure 102. The simulation was developed to depict the real-world environment and accurately simulate everyday operations. The components are all represented on a 1:1 scale as identified during the physical investigation while controllers were used to ensure the simulation is representative of daily operating procedures (such as flow rates, pump and schedules).

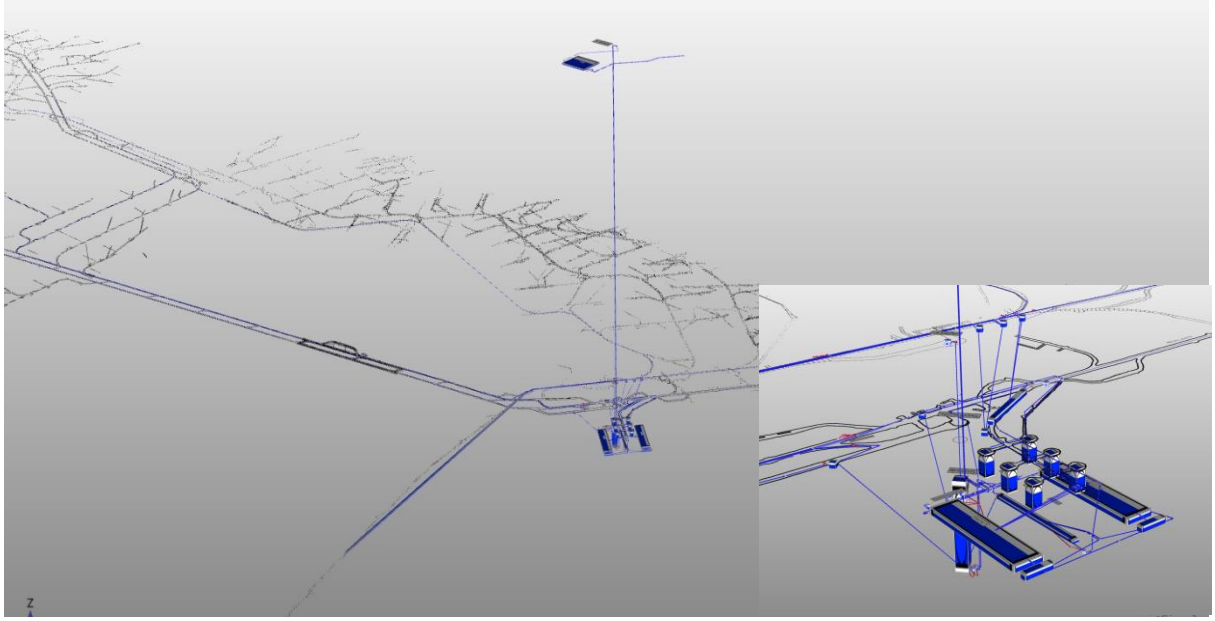

Figure 102: Baseline PTB simulation model of Mine C's dewatering system

An extensive calibration and verification cycle yielded a successful simulation model calibration as none of the components fell short of the 5% calibration requirement. The model accurately reproduces the dewatering operating conditions of Mine C and be used for what-if analyses.

In keeping with the research aim and objectives, the what-if analysis was conducted to determine the shaft's water storage capability during a total power failure. Table 20 summarises the shaft's available storage capacity during a total power failure according to the information gathered during the investigations.

Table 20: Mine C's available emergency capacity

Capacity	Verified capacity [Mℓ]
Spare capacity of MPS dams	2.50
Shaft bottom	6.50
Spare capacity of settlers	1.50
Total	**10.50**

The following was identified through the physical investigation:

- The MPS dams are horizontal dams; therefore, the blasted areas down to the dams were included in the capacities.
- There is no means of stopping the water from 2# during a total power failure.

Figure 103 illustrates the storage capacity levels during a total power failure.

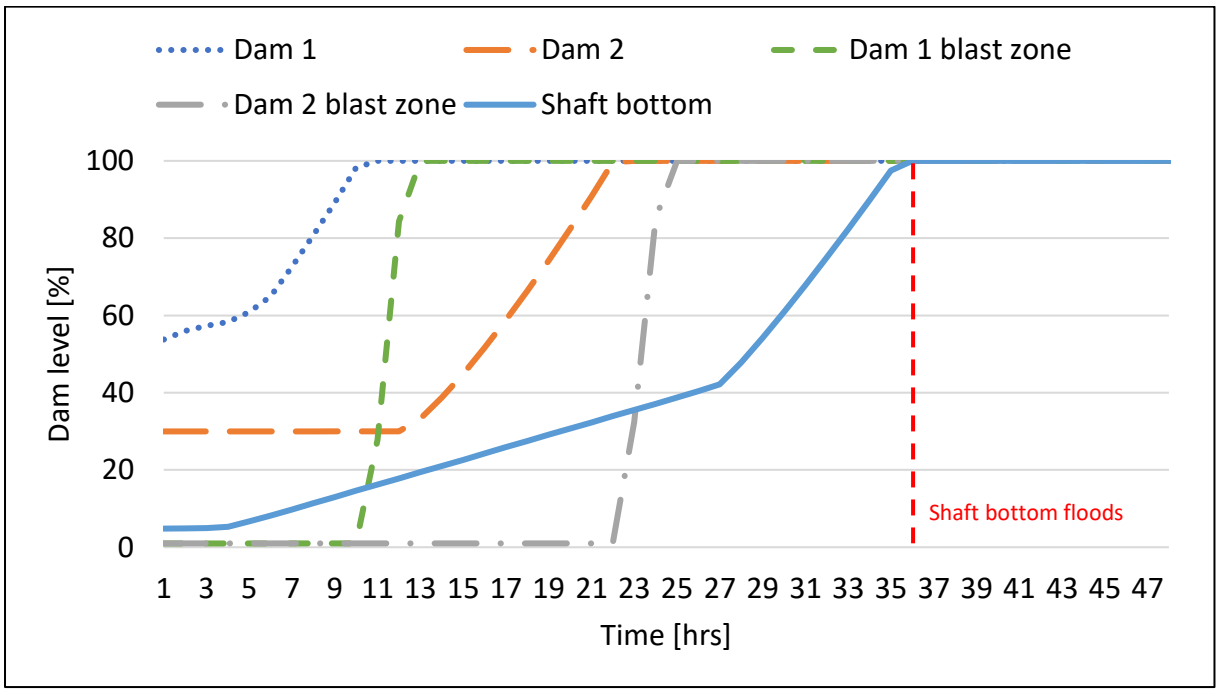

Figure 103: Mine C's total power failure capacity results

Mine C's emergency storage capacity did not adhere to the stipulated 48-hour requirement; therefore, scenario simulations were required.

Scenario 1: fix settler 5

Scenario 1's aim was to ensure that all the settlers could be used during an emergency. If water enters Settler 5, it will flow out the bottom and start flooding the MPS level. The results are depicted in Figure 104.

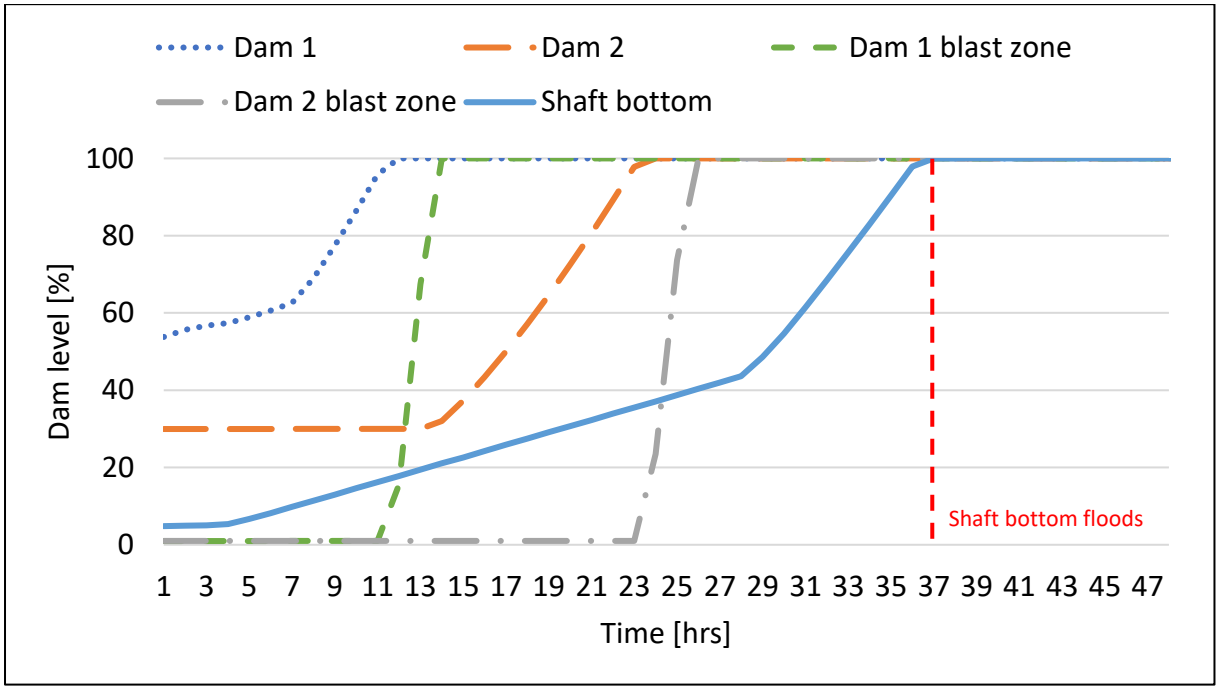

Figure 104: Mine C's emergency capacity results from Scenario 1

Only one hour was gained from the proposed change. Although this may seem insignificant, it provides much needed safety in the settler area and MPS if the settler area begins to flood.

Scenario 2: install a water door

After much deliberation with shaft engineers and supervisors, the consensus was that the water from 2# was the biggest issue. Equation 11 was used to show that shaft bottom could handle the water in the shaft:

Equation 11

$$t = \frac{Volume}{Q}$$

Where:

- t = flood time [s]
- $Volume$ = water storage capacity [L]
- Q = water flow rate [ℓ/s]

Therefore, Scenario 2 was aimed at proposing a solution to store the fissure water from 2# during a total power failure. The proposed changes (illustrated in Figure 105) are as follows:

- Construct a water door in the travelway towards 2#.
- Install a valve on the pipe from 2# that gravity-feeds fissure water to the shaft.
- Install a tie-off pipe with a valve on the pipe that gravity-feeds fissure water to the shaft to divert water behind the water door in an emergency.

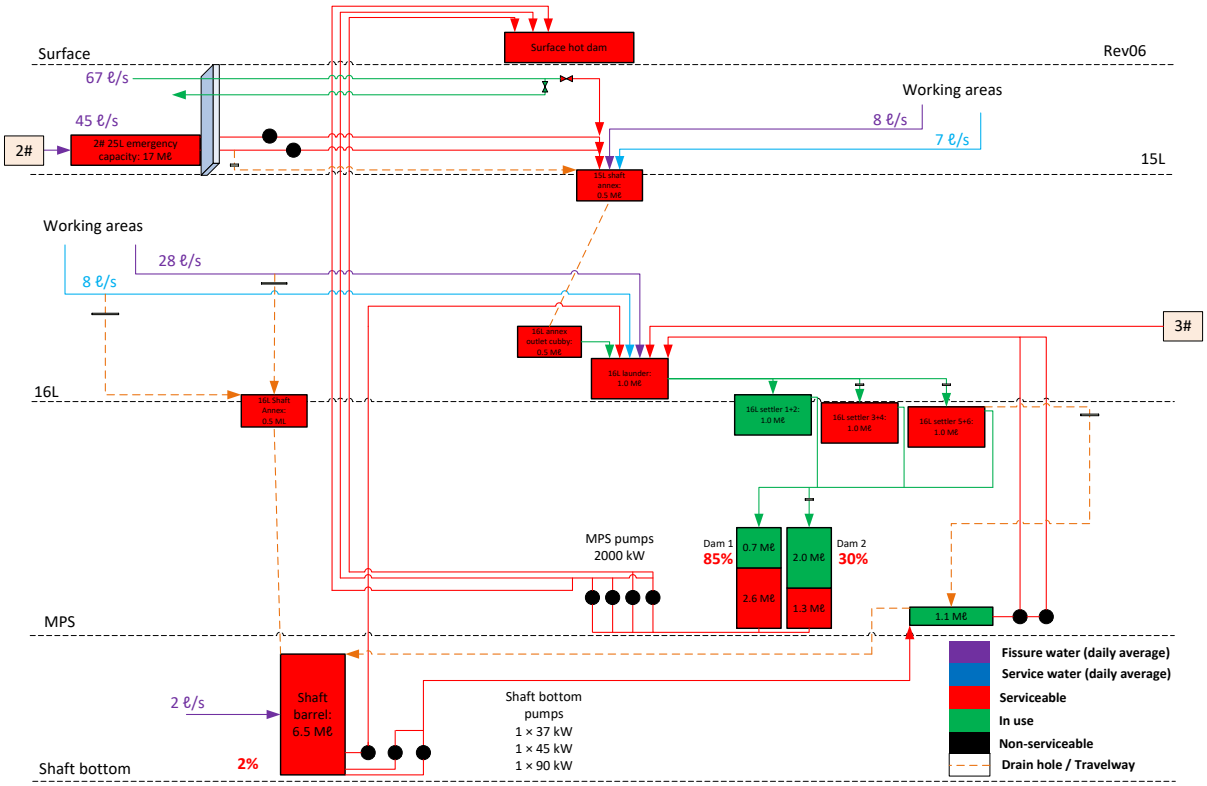

Figure 105: Proposed changes to Mine C for Scenario 2

Figure 106 illustrates the simulation results for Mine C and scenario 2's proposed changes.

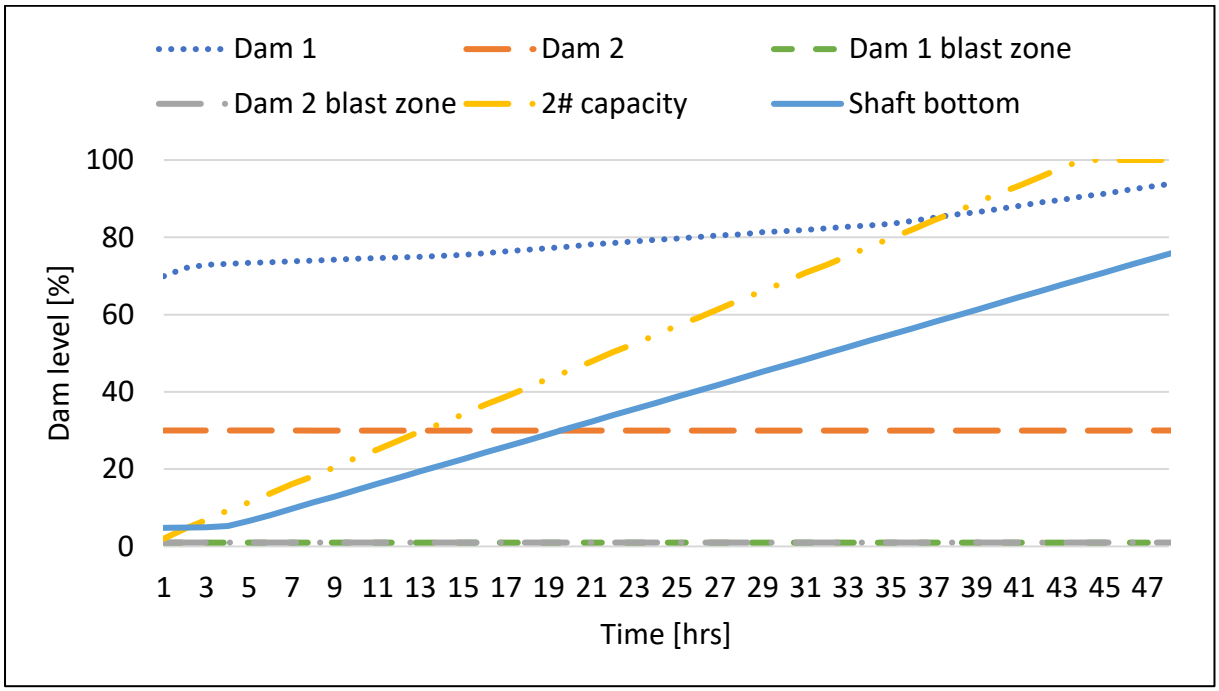

Figure 106: Mine C's emergency capacity results from Scenario 2

Table 21 summarises the scenario results for Mine C.

Table 21: Mine C's simulation summary

No.	Description	Total hours
0	Industry method	55
1	Current configuration	36
2	Fix settler 5	37
4	2# water door	63